Successful Routes to Triosmium Decacarbonyl Bisethoxide and Analysis of Reactivity with Benzamide and 4-Nitrobenzamide

A Thesis in Chemistry by Bridget Willson

Examining Committee:

Mary-Ann Pearsall, Thesis Advisor

Chemistry

Kimberly Choquette, Member

Chemistry

Marc Boglioli, Member

Anthropology

MAY 2025

Table of Contents

Abstract

The triosmium dibridged decacarbonyl complex, $Os_3(CO)_{10}(\mu^2\text{-}OEt)_2$ is of interest as bridging ethoxides activate ligand exchange with several organic groups at the axial carbonyl and ethoxide locations. Addition of various ligands may result in antitumor activity, as suggested by literature. Synthesis of $Os_3(CO)_{10}(\mu^2\text{-}OEt)_2$, bisethoxide, utilizes reactions of halide intermediates of Cl, I, and Br with $Os_3(CO)_{12}$. In this work, reactions using iodide intermediates have been optimized, and a greener approach with chlorine intermediates has been developed.

Reactions of $Os_3(CO)_{10}(OEt)_2$ with amides ($RCONH_2$) generate the binuclear product, $Os_2(CO)_6(RCONH)_2$ (R = Ph, Ph-NO_2) where the amide is bidentate. This compound can have two isomers head-to-head and head-to-tail, with respect to the amide ligand, which differ in overall polarity. This study analyzes the isomer ratios at two temperatures (110°C and room temperature), and the kinetics of the equilibrium reaction over time. Prolonged heating of these complexes, however, results in overreaction into a polymer, which is difficult to revert once formed, and additional work was done with $CO_{(g)}$ to attempt to revert the polymer to the monomer and stabilize the monomer under reflux.

Introduction

Osmium, a transition metal, forms organometallic clusters where the metal-carbon bonds enable unique reactivity. Compounds formed by the reactions of bisethoxide and amides are of interest as similar organometallic clusters have been proven to contain biological activity.

Amides are bidentate ligands, meaning each can coordinate in two positions to the transition metal cluster, figure 1.

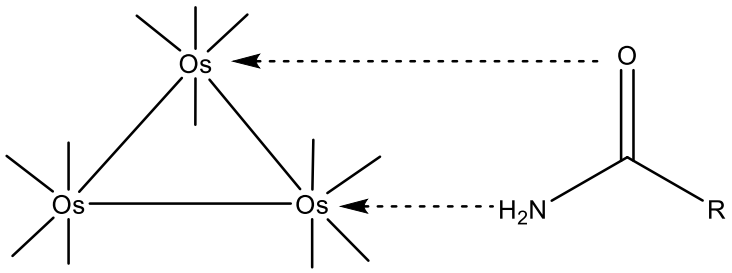

Figure 1: highlighting the bidentate property of amides. Electron density can be donated from both the oxygen and nitrogen.

When bisethoxide reacts with an amide, one of bisethoxide's osmium-osmium covalent bond can break, resulting in the diosmium complex, $Os_2(CO)_6(RCONH)_2$ (R = Ph, Ph-NO_2) seen in figure 2. These products exist as two possible isomers differing in polarity due to the positioning of the NH groups, head-to-head (H,H) or head-to-tail (H,T) which have been found to interconvert, figure 2.

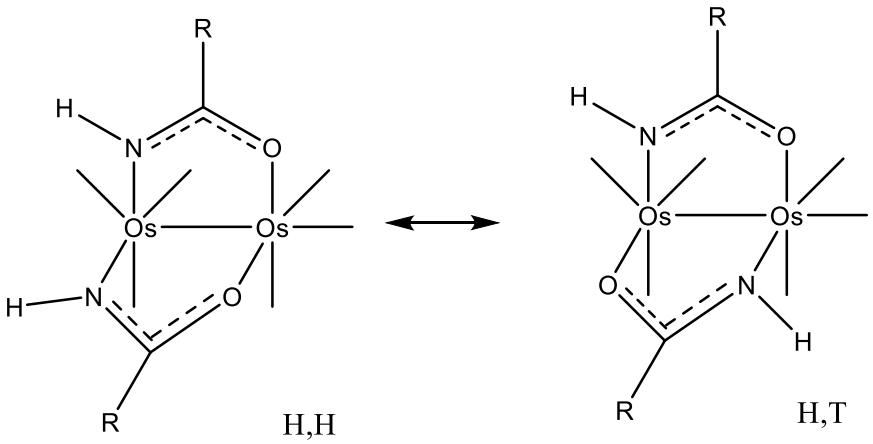

Figure 2: Isomers of diosmium diamide complexes (R=Ph, Ph-NO_2)

The ratio of these isomers over time has been investigated. The initial ratio is assumed equivalent to reaction ratio at reaction temperature, 110°C, and the ratio is then analyzed as it comes to equilibrium under room temperature.

For this research, the $Os_2(CO)_6(RCONH)_2$ (R=Ph, Ph-NO_2) isomers were synthesized, and the change in isomer ratios at different temperatures over time was analyzed using ^{1}HNMR integrations of the N-H peak. This studies two effects: thermodynamic and kinetic. The former is analyzed through the final isomer ratio, and the latter studies the rate of the reaction coming to equilibrium, gathering information about the isomer interconversion mechanism.

Importance of Transition Metal Research

Transition metals are a field of chemistry that is constantly evolving as their behavior differs from main group metals or nonmetals, including biochemical involvement. In the body, transition metals are present as components in certain proteins. Cowan's analysis of Mg(II) amine derivatives on the enzyme topoisomerase I, describes it mimics the hydrogen bonding that naturally occurs in the body, figure 3.[1]

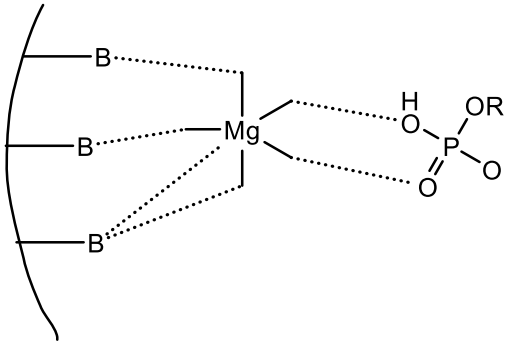

Figure 3: "B" symbolizing hydrogen bond donors that stabilize the Mg-phosphate complex within the protein structure such as amino acid side chains or backbones, highlighting the ability for transition metal centers to interact with the body with the coordination of a phosphate.

Further, transition metals also work as components of enzymes and electron transport proteins.[2] This is seen in zinc finger motifs, a protein domain folded over a zinc ion. This allows structure and stability of DNA binding domains. This is possible because transition metals are versatile with multiple oxidation states and bonding modes. New drugs are being developed that utilize biological properties of transition metals, but, without fundamental understanding of transition metal behavior, work cannot be done invivo.

Transition Metal Complexes and Clusters

Transition metals are unique as they have partially filled d orbital electrons playing a crucial role in bonding. Interactions with the transition metal's d orbital results in a variation in its oxidation state. This is the basis of transition metal complexes, in which the metal center can have ions or molecules, ligands, interact with the d orbital electrons.

There are three categories of ligands that can occur in a metal complex: pi-donor, pi-acceptor, and sigma-donor, figure 4.

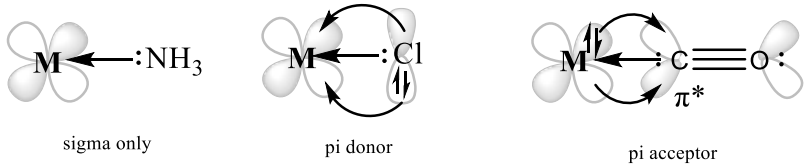

Figure 4: ligand bonding highlighting NH_3 as a sigma-donor, Cl^- as a pi-donor, and CO as a pi-acceptor

Sigma-donor ligands have only a simple sigma interaction between the ligand and metal. Pi-donor ligands have a filled pi type orbital that contributes electron density to the metal's empty d orbital. Pi-acceptor occurs when the ligands have an available pi type antibonding orbital, accepting electron density from metal's filled d orbital. It is important to note that pi-acceptor and pi-donor also have sigma interactions, and all three of these interactions work to stabilize the ligand and overall cluster, seen in figure 4.

Depending on oxidation state, the metal can have a vacant or partially filled orbital. An increase in oxidation state can result in a vacant orbital on the transition metal, available to accept electron density from the ligand; essentially, the transition metal acts as a lewis acid, its vacant orbital accepting electron density from the Lewis base, the ligand. If this donation leaves the d orbital partially filled, the transition metal can then exhibit lewis base-like activity, donating this electron density to the ligand, known as back donation, figure 5.

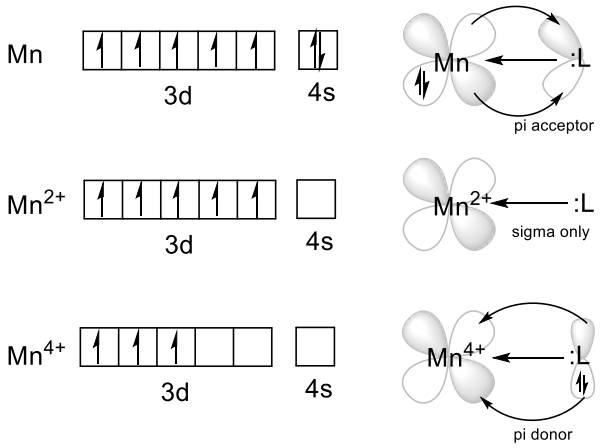

Figure 5: showing different oxidation states (electrons in the d orbital) resulting in different ligand interactions

When at least one of these ligands contains a carbon donating electron density to the metal, an organometallic complex is formed. A common example of this is carbonyl ligands, shown above in figure 2. In contrast to simple complexes, organometallic complexes have a variety of coordination modes and oxidation states due to valence electrons in the nd orbitals where bonding behavior follows the 18 electron rule. Similarly to the octet rule, in which main group elements have 8 electrons occupying 4 bonding orbitals, the 18 electron rule describes 18 electrons surrounding the metal will occupy the 9 bonding valence orbitals of 5(3d)+1(4s)+3(4p).

An example of this relationship is seen with the complex $Fe(CO)_5$. Iron has the electron configuration [Ar] $3d^6\ 4s^2$, and so it contributes 8 valence electrons. There are 2 electrons in each Fe-CO bond, 10 total. Thus, 18 electrons surround the iron in this complex, count below in figure 6.

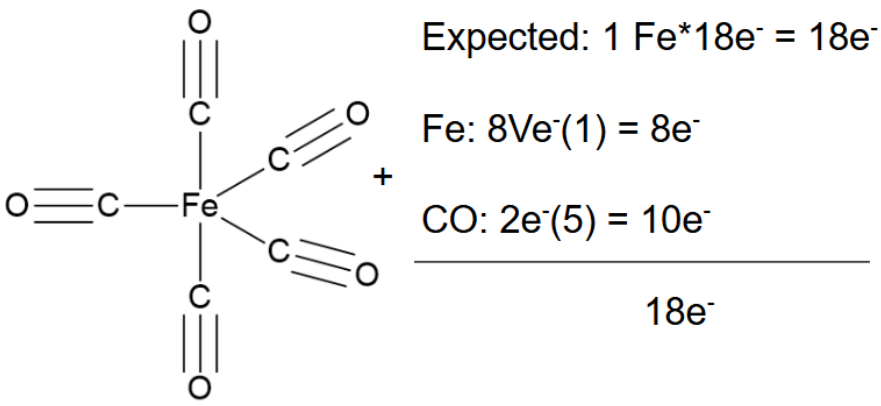

Figure 6: electron count for $Fe(CO)_5$ highlighting the 18 electron rule

An important note for this organometallic complex is that the oxidation state surrounding the iron is zero. A change in this oxidation state would affect the number of valence electrons and the overall stability of the complex.

Additionally, metal metal bonds are possible and can be favored. This is true of the transition metal studied in the Pearsall lab, osmium, where $Os(CO)_5$ is unstable. Os is in the same group as Fe but two periods below, and so it has the electron configuration [Xe] $(4f^{14})$ $5d^6$ $6s^2$. The 8 valence electrons + the 10 from Os-CO bonds show 18 electrons, but it is important to realize that the 4f electrons are not involved in bonding as they have a poor shielding effect due to the lanthanide contraction.[3] This leads to very strong Os-CO and Os-Os bonds as it has been found that the complex $Os_3(CO)_{12}$ is preferred to $Os(CO)_5$. Complying with the 18 electron rule, the expected amount of electrons surrounding each osmium would be 18, and so, theoretically, there should be 54 total electrons contributing to bonding. However, only $48e^-$ are contributed by the osmiums' valence and carbonyl electrons, so the difference is made up by the formation of 3 Os-Os bonds, figure 7.

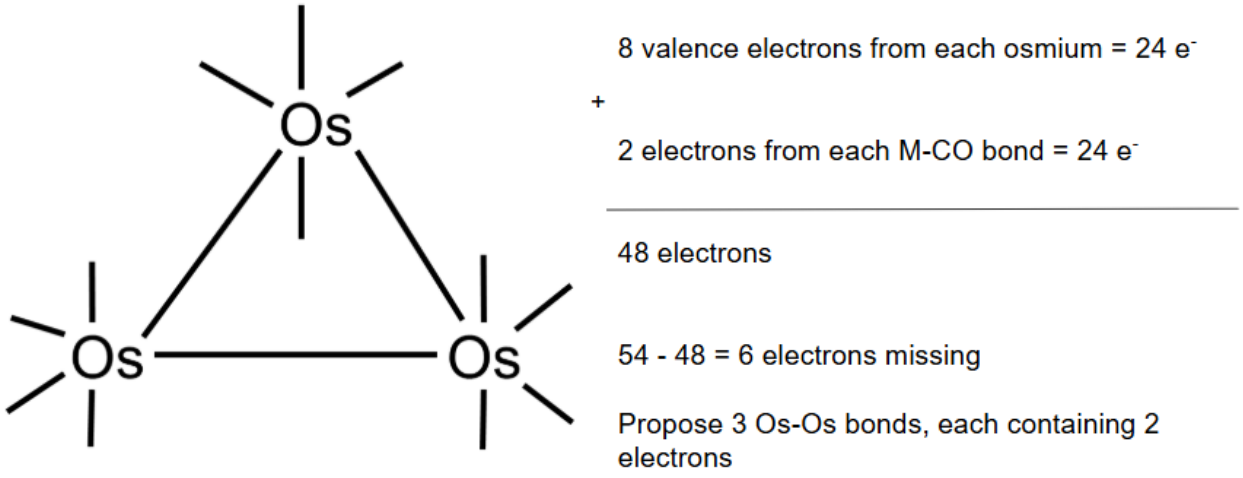

Figure 7: electron count for $Os_3(CO)_{12}$ using the 18 electron rule, providing evidence for the 3 Os-Os covalent bonds

In evaluation of the carbonyl ligands associated with the organometallic cluster $Os_3(CO)_{12}$, the commercially available starting material for research in the Pearsall lab, it can be found that they are acting as pi-acceptor ligands. Thus, the carbon can accept electron density from osmium's d orbital, resulting in a stable and unreactive compound.

An example of the lack of reactivity can be seen in reactions of $Os_3(CO)_{12}$ with benzoic acid. Pyper et. al. found the reaction required the use of microwave radiation at 300W and 190°C to obtain the $Os_3(CO)_{10}(\mu\text{-H})(\mu\text{-benzoate})$ as the major product in 50.3% yield in addition to an unidentifiable minor product.[4] These extreme reaction conditions, poor yield, and lack of specificity highlight the stability of the $Os_3(CO)_{12}$ complex.

Reactivity of the $Os_3(CO)_{12}$ starting material can be enhanced by adding bridging ligands. Similarly to the above reaction with acetic acid, the Pearsall lab utilizes the

microwave to attach two iodide ligands to the complex, resulting in the osmium retaining its trinuclear shape and the iodide attaching as bridging ligands, figure 8.

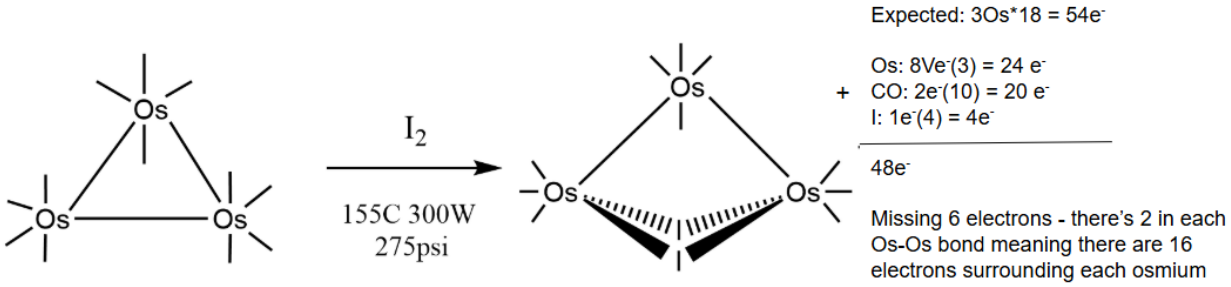

Figure 8: reaction scheme of microwave reaction with $Os_3(CO)_{12}$ and I_2 and electron count

Once these bridging ligands are added, the M-M bond is weakened, and the surrounding carbonyls are activated towards substitution. Reactivity can occur through substitution at the bridging ligands, a common reaction to produce the Pearsall lab's starting material $Os_3(CO)_{10}(OEt)_2$, bisethoxide. Ashish Shah was one of the first researchers of the Pearsall lab to obtain bisethoxide through the chlorine intermediate in low yield (35%), and this procedure was optimized through the use of the solid base, alumina, to neutralize the solution and remove the competing hydrogen chlorine byproduct, 79%.[5,6] Due to the toxicity of chlorine gas, I_2 and Br_2 intermediates were tested and found to provide similar reactivity.[5]

$Os_3(CO)_{10}(\mu_2\text{-}I)_2$ provides a safer conversion than the $Os_3(CO)_{10}(Cl)_2$ and higher yield than $Os_3(CO)_{10}(\mu_2\text{-}Br)_2$, and so it was favored moving forward. The conversion from diiodide intermediate to bisethoxide, figure 9, occurs at a low temperature, 78°C, highlighting that this is a controlled reaction that results in a single product; if heated at a high temperature, such as 200°C, multiple products form.

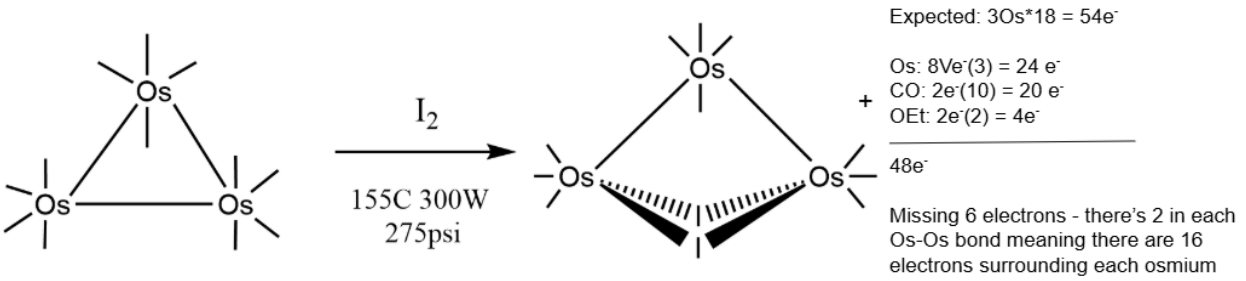

Figure 9: reaction scheme of conversion of $Os_3(CO)_{10}(I)_2$ to $Os_3(CO)_{10}(OEt)_2$, bisethoxide and electron count

The ethoxide ligands are more electron donating than the I_2, resulting in stronger bonds between the osmium and bridging ligands, while retaining a reactive complex.

Alternatively, reactivity can occur through substitution at the carbonyl trans to the metal-metal bond. Timothy Barnum and Cristabella Fortna studied the mechanism of axial carbonyl substitution through the reaction of $Os_3(CO)_{10}(X)_2$ and $P(OMe)_3$ where X=Cl, Br, I to give $Os_3(CO)_8(P(MeO)_3)_2(X)_2$.[7,8] It should be noted that both X and OR bridging ligands activate the triosmium cluster towards substitution, and so, in this case, Fornta synthesized X dibridged clusters as the reaction is simpler and requires less time. This reaction occurs at a relatively low temperature compared to other reflux temperature, indicating the bridging halides create an overall more reactive cluster, activating the trans carbonyl towards substitution, figure 10.

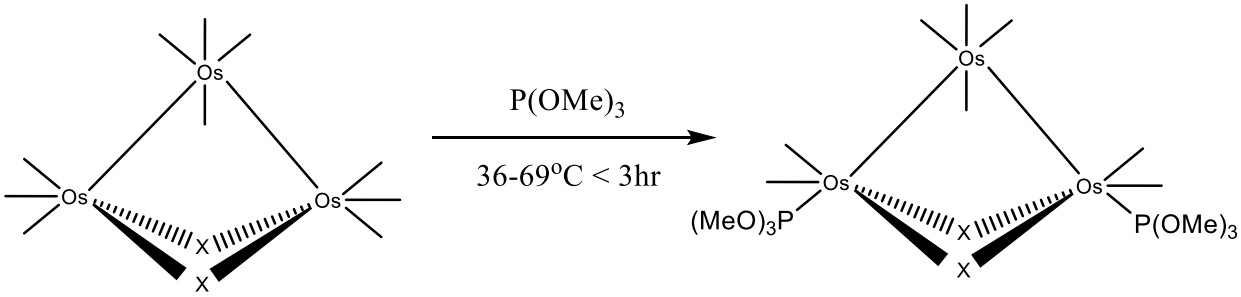

Figure 10: reaction scheme of reaction with $Os_3(CO)_{12}(X)_2$ where X = Cl, Br, I and $P(OMe)_3$

The mechanism by Fortna proposed for this reaction is that there exists an equilibrium where the Os-Os bonds break and CO bridges the osmiums. As the $P(OR)_3$ donates electron density into the osmium, a CO is forced into a bridging ligand between two osmiums. These delocalized Os-CO bonds are easier to break, resulting in an intermediate, $Os_3(CO)_9(P(OR)_3)$. This process then will occur a second time at the other trans carbonyl, figure 11.

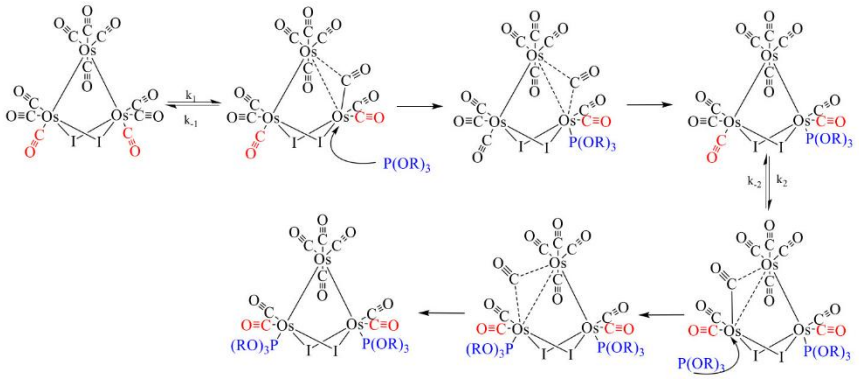

Figure 11: proposed mechanism of axial carbonyl substitution with $P(OMe)_3$. Produced by Fortna.[7]

<u>Reaction of Osmium Clusters and Carboxylates</u>

The replacing of bridging ligands can also occur with a change in nuclearity. This is seen with anionic bidentate ligands, such as amides and carboxylates, which each can coordinate in two positions to the cluster. The kinetics in the synthesis of bisethoxide and carboxylate products was previously studied in 2013 by Lynn Schmitt.[9] Schmitt's work confirmed that monosubstituted triosmium clusters are intermediates in the overall reaction of bisethoxide with carboxylic acids and this monosubstituted product can only be isolated when reacting carboxylic acids with small R groups. Further, when the monosubstituted product is formed, A is much more prevalent than B, figure 12.

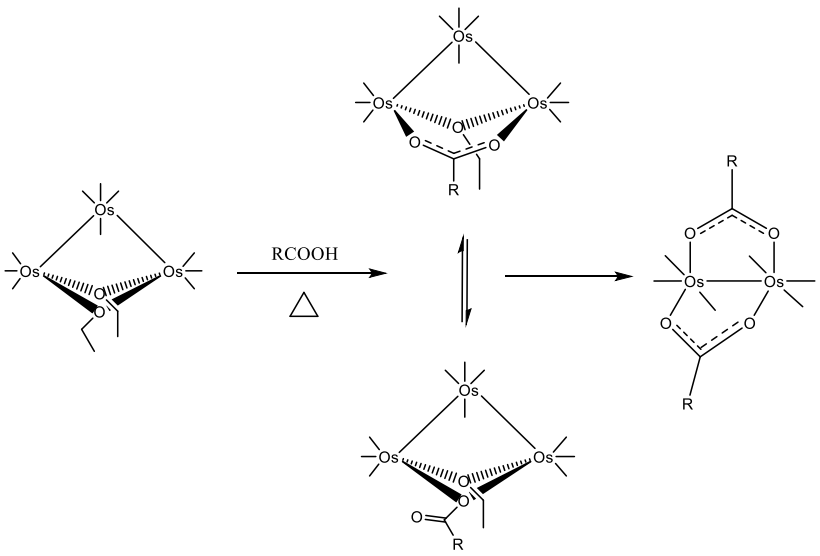

Figure 12: intermediate and products of bisethoxide reaction with carboxylate, investigated by Schmitt (R=CH_3, $CH2CH_3$, $CH(CH_3)_3$, $CH(CH_3)_3$, Ph, CF_3, p-(Ph)-CF3)

This is as B has octahedral geometry about a strained osmium with the R group pointing towards terminal carbonyl ligands. Comparatively, the bidentate coordination mode results in R pointing away from the carbonyls. In carboxylates with large R groups, the second substitution occurs much more rapidly, as the second substitution donates electron density to the cluster to provide for the loss of the metal-metal bond, and so the intermediate is rarely seen.

In 1969, a study analyzed reactions between $M_3(CO)_{12}$ (M = Os, Ru) and acetic acid.[10] They found that these metals have identical reactivity, and produced the dinuclear product discussed above, confirmed through IR and NMR spectroscopy. Crooks et al discovered that, in a solvent with the presence of a stoichiometrically significant amount of acid, the tetrahydro-derivative, $H_4M_3(CO)_{12}$ forms (M=Os,Ru). When reacted with a carboxylate, the reaction is catalyzed to result in a high yield of

infinite polymers through bridging carboxylate groups by displacing CO ligands trans to the M-M, figure 13.

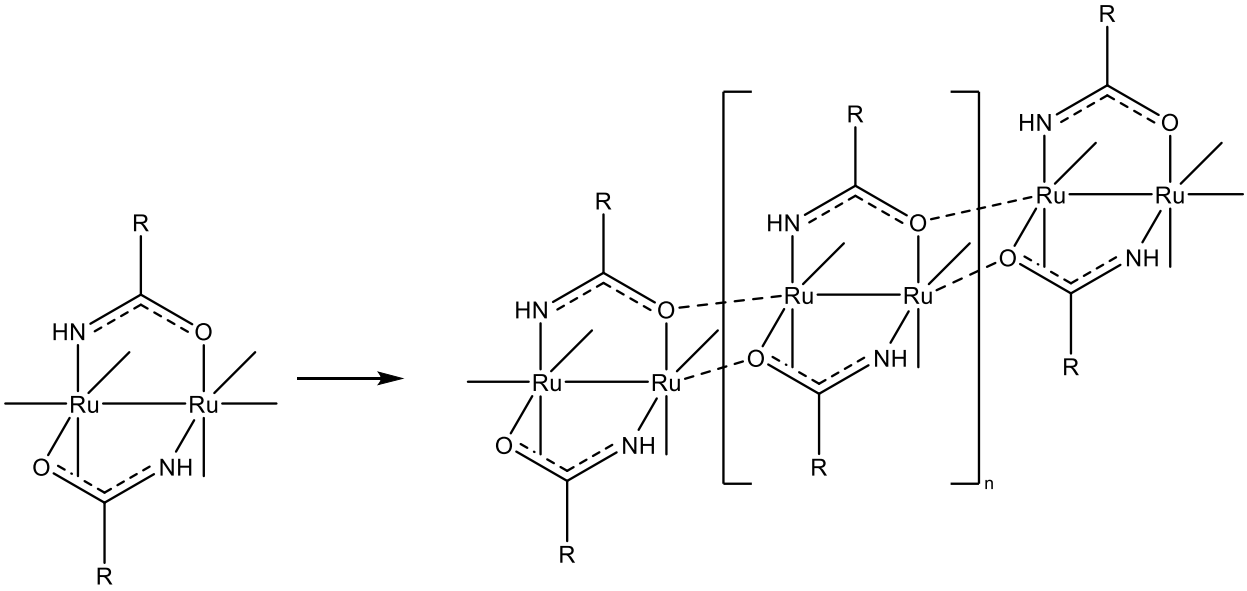

Figure 13: polymerization of $H_4Ru_3(CO)_{12}$ with carboxylic acid

Additionally, Crook's et al found that the $Ru(CO)_2(MeCO_2)_n$ polymer, when reacted with CO gas will revert to form the monomer $Ru_2(CO)_6(MeCO_2)_2$ as it will break apart the Ru-O bonds, and a CO ligand can attach. This is stated to be comparable in reactivity to $Os_2(CO)_6(RCO_2)_2$ (R=Me,Et), and gives insight into polymer formation and reversal in the Pearsall lab.

Previous Amide Research in the Pearsall Lab

The reactions of $Os_3(CO)_{12}$ with amides were analyzed by Katie Marak and Sarah Costa. Reactivity similar to carboxylic acids has been seen in reactions with amides, and the mechanism likely follows the proposed carboxylate mechanism Lynn Schmitt developed in 2013. When reacted with bisethoxide, a bridging ethoxide will be substituted for the amide, the nitrogen donating its electron density. This results in a monosubstituted trinuclear intermediate. The bond between one of the osmiums and

the oxygen will then break, and the oxygen will fill the vacant site as the bidentate coordination experiences less steric clash between the R group and terminal carbonyls. The dinuclear product has only been seen thus far in the Pearsall lab, indicating that the second substitution occurs rapidly, consistent with Schmitt's findings.[9,11,12] The addition of bridging ligands donating electron density allows for breaking of the Os-Os bond, forming the final product, $Os_2(CO)_6(RCONH)_2$ (R = Ph, Ph-NO_2), figure 14.

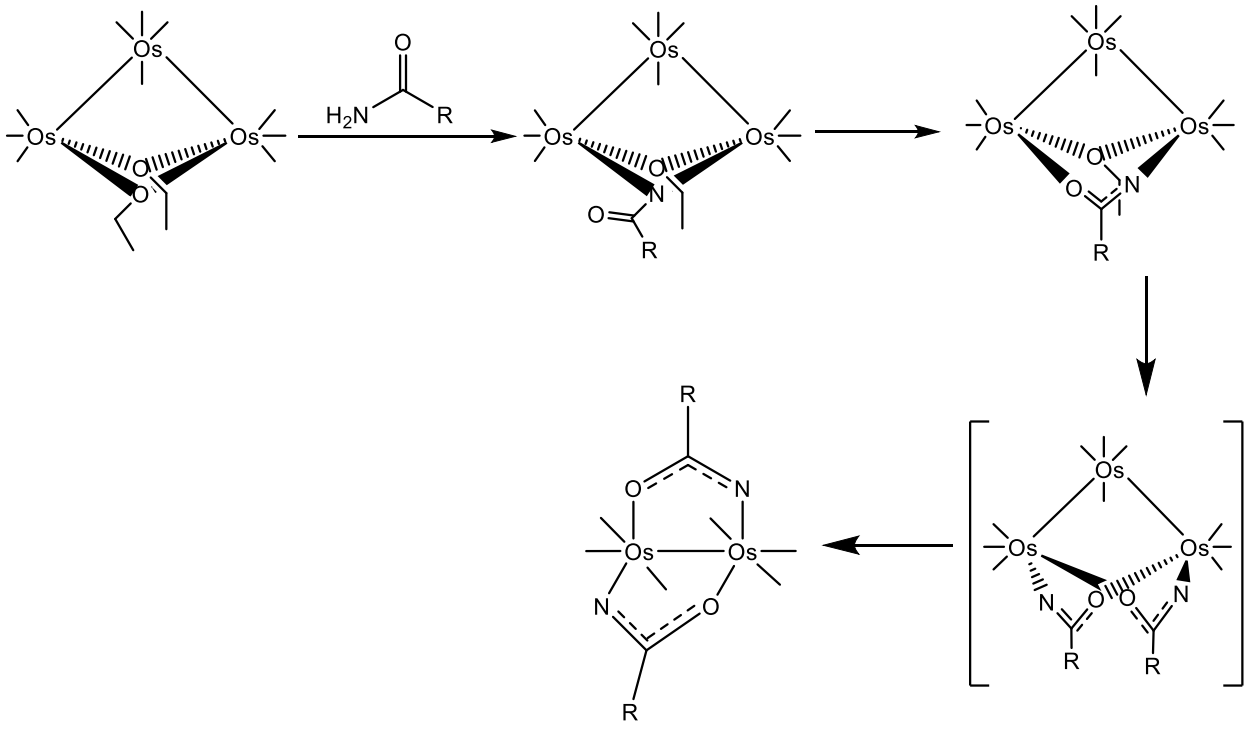

Figure 14: likely reaction mechanism of amide ligand substitution with bisethoxide, following Schmitt's mechanism with carboxylic acids[9]

Differing from the carboxylic acids, osmium cluster reactions with amides result in isomers, labeled as head-to-tail (H,T) and head-to-head (H,H), figure 15.

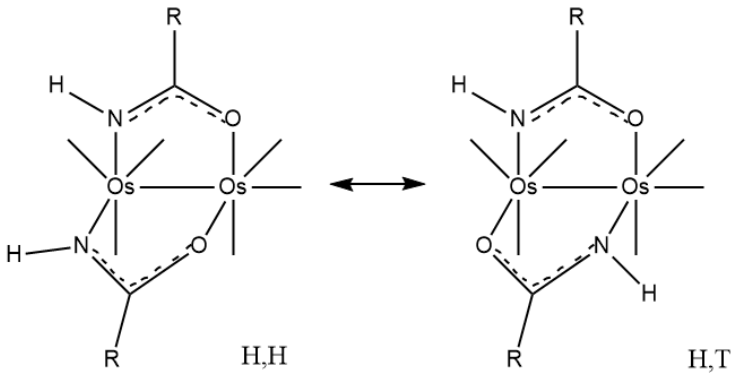

Figure 15: two possible isomers of $Os_2(CO)_6(RCONH)_2$. Head-to-head (H,H) and head-to-tail (H,T)

The equilibrium isomer ratios of benzamide, acetamide, and 4-nitrobenzamide were previously obtained at 110°C in the Pearsall lab by Katie Marak in 2017.[11] Marak isolated the isomers of benzamide through PrepTLC, and these two solutions, as well as the crude mixtures of acetamide, were analyzed through HNMR integrations in $CDCl_3$, resulting in inconsistent patterns. Marak observed benzamide isomers interconvert over time as the reaction came to equilibrium at room temperature, favoring the head-to-tail isomer with a H,H:H,T ratio of 39:61. However, Marak found acetamide had a H,H: H,T ratio of 52:48, minorly favoring the H,H isomer; her results are outlined below in table 1.

Table 1: reaction summaries of bisethoxide and bidentate ligands (A) and further information on benzamide isomer interconversion post TLC seperation (B) as studied by Katie Marak in 2017.

1A:

Bidentate ligand	**Solvent and temperature**	**Ratio (H,H:H,T)**	**Interconversion over one month**
CH_3CONH_2	Toluene 110°C	52:48	D_2O exchange is slow and H,T is exchanging at faster rate than H,H
$PhCONH_2$	Toluene 110°C	39:61	Isomers interconvert in solution

1B:

	Solution A		Solution B	
	H,H	**H,T**	**H,H**	**H,T**
Initial (110°C)	3	97	95	5
Week 3 (RT)	12	88	43	57

Table 1A highlights that there is an almost equivalent amount of H,T vs H,H isomers in acetamide at reaction temperature 110°C, and that, over time, it can slowly exchange protons with D_2O, and the H,T isomer exchanges faster. This reactivity differs from benzamide, which favors the H,T at reaction temperature. Table 1B provides more information on the isomer interconversion, proving that the H,T, exchanges faster, similarly to acetamide. This raises the question of whether similar behavior occurs with other amide ligands and how different environments can affect this reactivity.

Additionally, Sarah Costa analyzed the thermodynamic effect on isomer interconversion.[12] Costa studied a crude mixture of the acetamide and bisethoxide

monomer $Os_2(CO)_6(CH_3CONH)_2$ with HNMR at 110°C (the initial reaction mixture), and then over three temperatures: 303K, 308K, and 313K, graph 1.

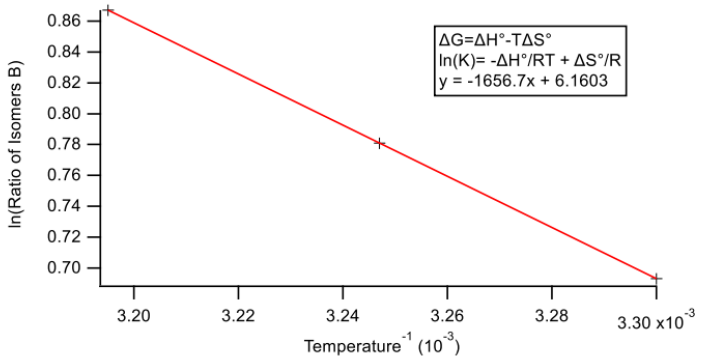

Graph 1: natural log of proportion of H,T to H,H vs 1/temperature. Initial isomer ratio at 110°C (48:52) and then held at RT and taken NMR until consistent ratio was seen (equilibrium, slope of ratio/time = ~0). Temperature increased to 303K, 308K, and 313K. Determines ΔH, ΔS, and thermodynamic product (H,T peak increases as temperature increases).

Costa concluded that there is a higher rate of conversion to the head-to-tail isomer at higher temperatures, and obtained ΔH = -1.650 kJ and ΔS =+6.14 J/mol. Thus proving that this interconversion favoring the head-to-tail at higher temperatures is spontaneous and favorable.

Polymers were believed to be formed in the Pearsall lab with acetamide, acetic acid, benzamide, and nitrobenzamide, with comparable reactivity to Crooks et al's polymerization with carboxylic acids.[10,12] The polymer can be identified as it is only partially soluble, and the infrared spectrum differs from the monomer as there are different patterns of carbonyls and symmetry in the molecule. Additionally, Costa, in 2019, synthesized an acetamide polymer, and found one of the most indicative signs to be the formation of a semi soluble precipitate.[12,13] Costa, also found this polymerization

was reversible for the acetamide reaction by keeping it under $CO_{(g)}$ at room temperature, figure 16.

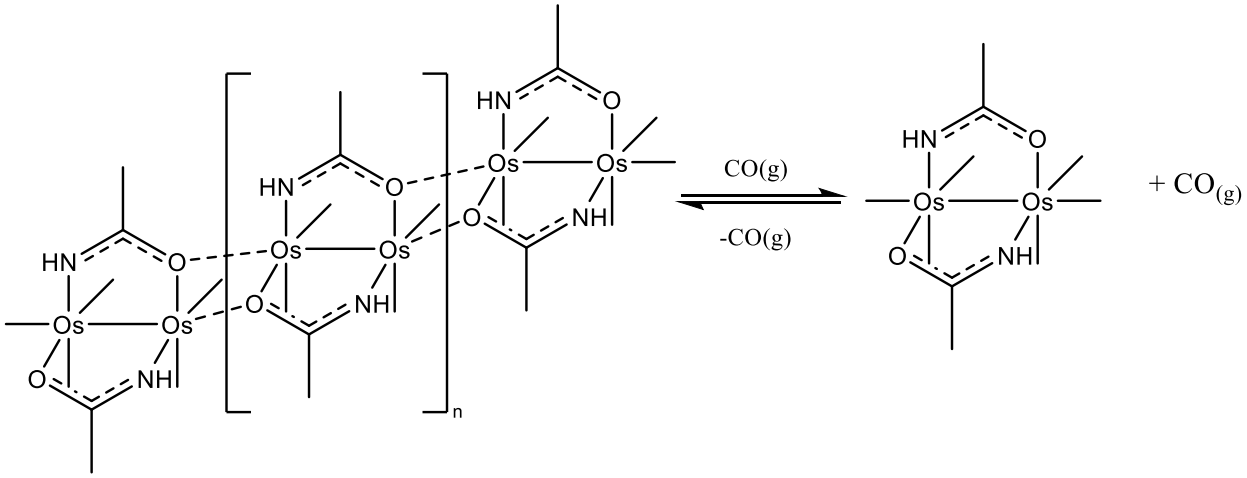

Figure 16: Sarah Costa conversion to monomer with $CO_{(g)}$ and reversal to polymer with the removal of $CO_{(g)}$

This behavior is possible due to the cluster's bonding properties. The more the complex polymerizes, the less effective the reversal is, proven experimentally in this work. The oxygen has one fully available lone pair for donation to the Os, and so Os-CO bonds would theoretically be favored, but the real driving force of this polymerization is the bulkiness of the polymer. There reaches a point in which $CO_{(g)}$ cannot insert into the complex. However, if the reversal process is begun quickly, Costa found it to be very successful. Further, it is worth noting that Costa found this successful only with the least bulky amide, acetamide, thus adding to the hypothesis that bulkiness of the polymer is what dictates reversal success, which is what this work further explores.

The major difference between this acetamide polymer and Crook's carboxylate polymer is that Crook's polymer is less stable than the monomer, proven by it being reversible at room temperature while the acetamide polymer requires the addition of $CO_{(g)}$.[10,12]

However, it appears that the polymers of benzamide and nitrobenzamide complexes are extremely difficult to revert once completely formed with no previous successful research repeated in the Pearsall lab. This makes it difficult to analyze isomers If a procedure can be accomplished in which the polymer does not form, then kinetic and thermodynamic isomer ratios can be determined. Additionally, it is important to note that there is a current hypothesis of the H,T monomer polymerizing as opposed to the H,H as the H,T orientation provides more stability, so the Os-O bonds can be easily displaced during the process of polymer formation when in the presence of excess ligand.[12,14]

Studying Diosmium-Diamide Complexes

Due to the success of Pt-derivatives, much research has been done on transition metals complexes and antitumor properties. A research group from Ohio State University synthesized di-rhodium di-amide derivatives from the H,T isomer of $Rh_2(HNOCCH_3)_4$ which can form DNA crosslinks.[13] Ligands were attached through reaction with light and water. Rhodium cluster, cis-$[Rh_2(HNOCCH_3)_2$-$(CH_3CN)_2$, was found to produce two isomers, which were successfully separated through column chromatography as they found the H,H isomer to be insoluble in the CH_3CN/CH_2Cl_2 solvent system used for separation due to the H,H isomer being a polar molecule and the solvent having more nonpolar properties. They found the equatorial ligands can exchange with water during photolysis, figure 17.

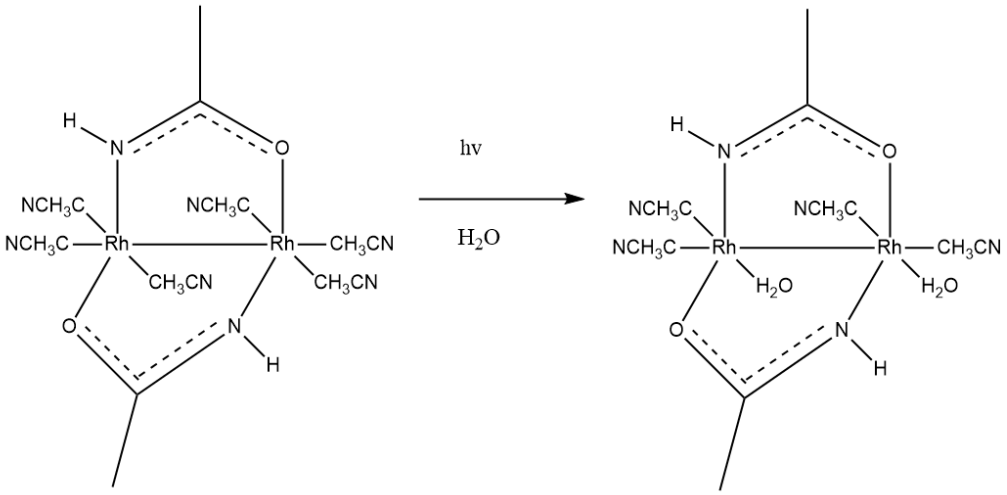

Figure 17: head-to-tail isomer of cis-$[Rh_2(OCCH_3NH)_2(CH_3CN)_6]^{2+}$ and its product when reacted with light

The group performed DNA mobility shift assays, showing the H,T isomer can bind to linearized DNA when irradiated with low energy light, resulting in a potential use in photochemotherapy.

Comparatively to the osmium-amide products in figure 15, the structures and behaviors are very similar, leading to a conclusion that there are more possibilities for biologically active transition metal clusters. Thus, it is suggested the osmium-amide complexes are worthy of future study.

Pathways to $Os_3(CO)_{10}(\mu^2\text{-}OEt)_2$ "bisethoxide"

In 2007, the Pearsall lab at Drew University found that $Os_3(CO)_{10}(\mu^2\text{-}OEt)_2$, bisethoxide was a byproduct in the formation of $Os_3(CO)_{12}$, formed in a 3-5% yield.[15] $Os_3(CO)_{12}$ is a very stable molecule, and so it does not undergo the intended substitution when introduced to ligands. Thus, bisethoxide became a desirable product as the ethoxide bridging ligands activate the cluster to substitution.

Robert Sommerhalter studied effective synthetic approaches to bisethoxide, analyzing three different halogens, chlorine, bromine, and iodine, to catalyze the breaking of the strong osmium-osmium bond.[5] Chlorine, bromine, and iodine react with $Os_3(CO)_{12}$ under heat to form a linear product of $Os_3(CO)_{12}X_2$ where X=Cl,I,Br, figure 18A. Upon further reflux in toluene, the linear complex undergoes nucleophilic substitution in which the carbonyl in the axial position breaks off and the complex closes. Baum and Cavalier attributed variation in rate constants of these intermediates (Cl>Br>I) to a steric effect occurring only trans to the Os-Os bond, resulting in a disubstituted $Os_3(CO)_{10}(X)_2$ product (X=Cl,I,Br), figure 18B.[16,17]

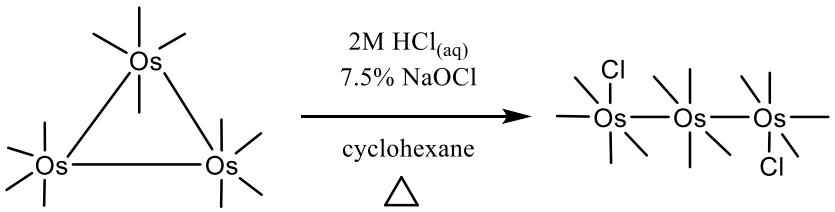

18A

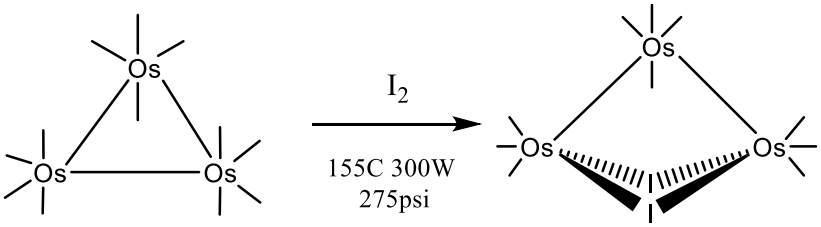

18B

Figure 18: halide products of $Os_3(CO)_{12}$ where 18A shows the linear product $Os_3(CO)_{12}X_2$ and 18B shows the dibridged product $Os_3(CO)_{10}(X)_2$ (X=Cl,I,Br).

In this work, chlorine and iodine reactions are analyzed as Sommerhalter found bromine produces a lower yield, resulting in iodine and chlorine being the standard halides in the Pearsall lab.[5]

Bisethoxide is then produced from a reflux of the halide products in alumina and ethanol. Research on this reaction has been accomplished through the understanding of bridging ligands in $Os_3(CO)_{10}(\mu^2\text{-}OH)_2$, activating the carbonyls towards substitution by Stephanie Schlect, Brian Baum, and Shari Uldrich at Drew University. Further, $Os_3(CO)_{10}(\mu^2\text{-}OEt)_2$ has similar properties to $Os_3(CO)_{10}(\mu^2\text{-}OH)_2$, but Vinnie Cavelierie found bisethoxide reacts at a faster rate and lower temperature, and so it is the standard starting material of the Pearsall lab. Cavelierie also hypothesized that the reason chlorine ligands produce the best yield may be as bromine and chlorine are larger, and so steric hindrance may be a factor.[17] Later studies of these halide intermediates provide more information of how these reactions occur, so that more precise procedures can be achieved.

$Os_3(CO)_{12}Cl_2$ generation

In the Pearsall lab, generation of the $Os_3(CO)_{12}Cl_2$ intermediate previously relied on bubbling chlorine gas into a solution of $Os_3(CO)_{12}$ at reflux.[9] While this resulted in higher yields of the desired bisethoxide product than the use of other halides, it is dangerous environmentally, to the scientist using it, and the school storing the gas. Green chlorination methods have been used in different settings; Faukuyama et. al studied a rapid and in situ chlorination of cyclic alkanes in which the combination of aqueous HCl and NaOCl resulted in chlorine gas. When done in a closed container and bubbled through to a reaction mixture, it was found that this wet gas reacted well with their cyclic alkanes.[18] Additionally, if added with NaOCl in excess, an aqueous water layer will form, neutralizing the product and making it safer to work with as studied by Wright and Hallstorm, two organic chemists from Pfizer, studying green chlorination of

organic materials.[19] Wright and Hallstorm's procedure was completed in dichloromethane, which allows the reaction to occur at room temperature.

These papers are of interest as they describe green chlorination procedures that can be applied to the reaction with $Os_3(CO)_{12}$. The isolation of the chloride product would be more difficult as it is soluble in this solvent. If the $Os_3(CO)_{12}$ was contained in a cyclohexane, the $Os_3(CO)_{12}Cl_2$ product would form and crash out, thus over chlorination and nucleophilic substitution would not occur, resulting in a linear shape with two chlorine ligands in an axial position.

$Os_3(CO)_{10}(\mu^2\text{-}I)_2$ generation

The $Os_3(CO)_{10}(\mu^2\text{-}I)_2$ intermediate was more standard in recent research in the Pearsall lab as it is less dangerous to work with when compared to chlorine gas. This reaction can occur in a two-reflux process in which $Os_3(CO)_{12}$ is refluxed in cyclohexane, and iodine in cyclohexane is dropped into the reflux through a separatory funnel until a 1:1 molar equivalence is added, forming the linear molecule. This compound is then reacted in toluene to undergo nucleophilic substitution to form the dibridged osmium compound of $Os_3(CO)_{10}(\mu^2\text{-}I)_2$.[7,20]

Comparatively, the use of the microwave allows for a one step reaction. Iodine is added in a 1:1 molar ratio of $Os_3(CO)_{12}$ and I_2 in cyclohexane under temperatures of 275 psi, 300 W, and 150˚C, forming the $Os_3(CO)_{10}(\mu^2\text{-}I)_2$ product.[20] However, the overall bisethoxide yields using this intermediate are lower than when the chlorine gas procedure was used. Cristabella Fortna worked on a procedure to increase the yield and purity of this product as well. It was found that if the reaction mixture was concentrated by half its initial volume and stored overnight at -20°C, the product would crystallize

and result in a very pure product.[7] This would then be put through a column with silica gel and hexanes, resulting in Fortna's conversion of 75.3%. This is a greater yield of the iodine product historically. In this work, research was conducted to experimentally determine if optimizing conditions could increase these yields of $Os3(CO)_{10}(\mu^2\text{-}I)_2$.

$Os_3(CO)_{10}(\mu^2\text{-}Br)_2$ generation

In 1970, Lewis et al found that bromine undergoes oxidative addition of two Br atoms attaching to a linear structure, resulting in $Os_3(CO)_{12}Br_2$.[21] This reactivity was studied by Vinnie Cavelier in 2006 who found reactivity is dominated by ion size, and so reaction rate is Cl<Br<I.[17] The linear product undergoes nucleophilic substitution under further reflux in a hydrocarbon solvent, resulting in the dibridged product, which can be reacted with alumina and ethanol to produce bisethoxide. The bromine halide, however, is not used in the Pearsall lab, due to its comparably low yield.

Identifying $Os_3(CO)_{12}$ and halide intermediates

Infrared spectroscopy, IR, is used to monitor these reactions as it identifies the stretching motions of carbonyl ligands within the molecule. In the Pearsall lab, IR is used to determine carbonyl patterns in molecules, plotting in absorbance over wavenumber. Differences arise from symmetry of the compound; less symmetry results in an increased amount of bands shown on the spectrum. Completion of reactions can thus be followed through this spectroscopy as well since different stretching patterns are observed. For example, $Os_3(CO)_{12}$ has four characteristic bands: 2068cm^{-1}, 2035cm^{-1}, 2014cm^{-1}, and 2002cm^{-1} while $Os_3,(CO)_{10}I_2$ has five characteristic bands: 1988cm^{-1}, 2104cm^{-1}, 2013cm^{-1}, 2051cm^{-1}, and 2068cm^{-1}. The structural differences between these two osmium clusters correspond to the infrared spectrum as the number of carbonyls

differs, the symmetry of the molecule changes, and new combinations of stretches and dipoles are introduced.

Thin layer chromatography and nuclear magnetic resonance are also used in identifying these molecules and monitoring their reaction progress. In the Pearsall lab, spot TLC is used alongside IR throughout the reaction, taken with a reference spot of starting material to minor progress and analyze polarity. Prep-TLC is used to purify compounds as it has shown more precise separation in prior experiments. ^{1}HNMR is then used to further identify these compounds. By identifying the characteristic NH signals of the amide in the H,T vs H,H, and comparing integrations each day over time as the reaction comes to equilibrium.

Methods

Infrared spectroscopy

Infrared spectroscopy, or IR, is used to identify functional groups in molecules. This is done through infrared light being shot through a solution of the molecule. The resulting spectrum is a representation of the stretching and bending vibrations of the carbonyls which are characteristic of the transition metal cluster's symmetry. In the studied osmium clusters, carbonyl frequencies come between 2000-2200cm^{-1}. This is a higher wavenumber than the functional group's typical literature value of 1700cm^{-1} due to the extreme stabilization of the Os-CO back donation.

In addition to different wavenumbers, the patterns of IR peaks will also differ. As seen in the $Os_3(CO)_{12}$ spectrum, figure 19, there are four peaks with intensities of strong, strong, weak, weak. In the chloride product, the peak intensity pattern is medium, weak, strong, medium. These band patterns correspond directly to the geometry of the compound, and so $Os_3(CO)_{10}(X)_2$ (X=Cl,Br,I,OEt,OMe) will all have the same band pattern regardless of the ligand although wavenumber will still differ based on the ligand as discussed previously.

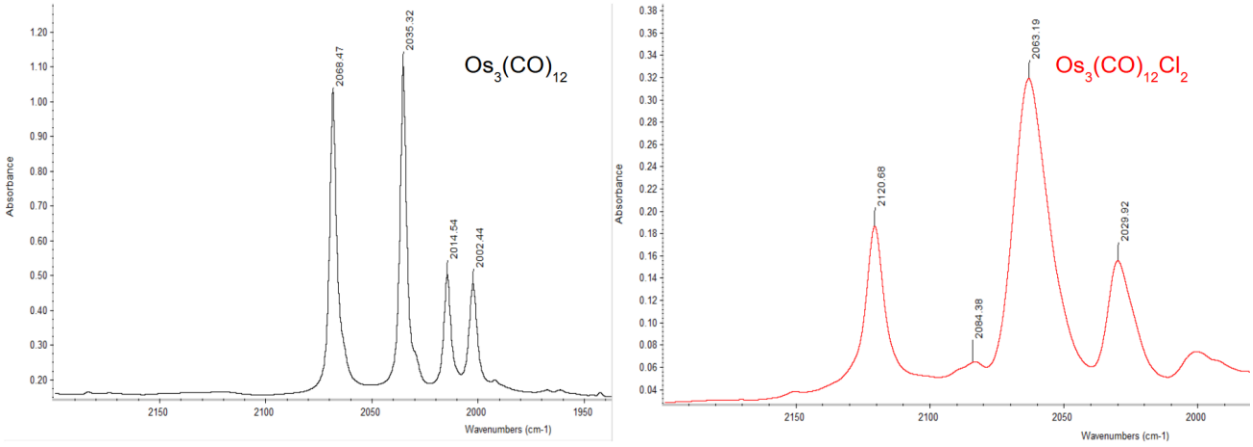

Figure 19: IRs of $Os_3(CO)_{12}$ compared to $Os_3(CO)_{12}Cl_2$. Both spectra have four peaks, but pattern and wavenumber differ (bw030).

In this research, the number of osmiums differ from the previously analyzed compounds, and so patterns will differ. This compound's carbonyl pattern is medium, strong, strong, weak, figure 19, and the IR is more complex as there is lower symmetry. Further, symmetrical carbonyls vibrate together, and so isomers of these complexes are relatively indistinguishable through IR, figure 20. Amides are seen in the 1400-1600 region, and so have the potential to be analyzed, but, with water also seen in this region, it is difficult to distinguish peaks of interest.

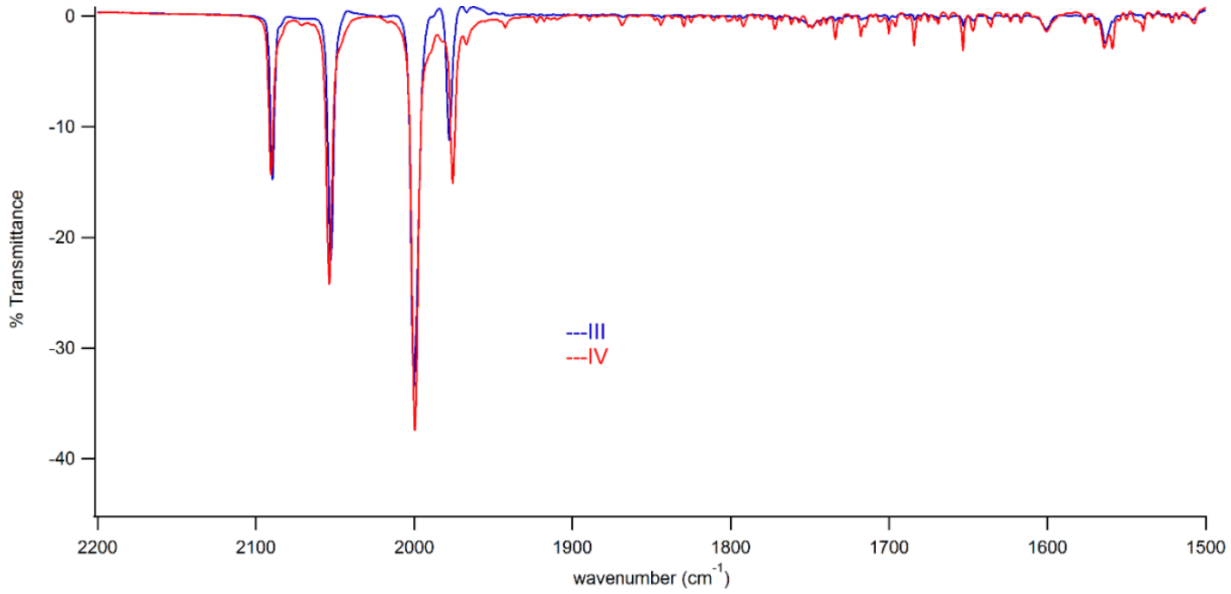

Figure 20: Overlaid IR of isomers of $Os_2(CO)_6(\mu^2\text{-}PhCONH)_2$ III H,T and IV H,H. Separation and IR done by Katie Marak 2017 proving they are indistinguishable.[11]

Thin Layer Chromatography

This method relies on intramolecular forces of a compound. In this research, spot thin layer chromatography, TLC, is used to monitor reactions, and preparatory TLC is used to separate products. TLC relies on polarity, a plate covered in silica gel is the polar

stationary phase. This plate rests in a solvent system made up of a less polar and a nonpolar organic solvent. Based on the polarity of the compound, the compound will run up the plate a specific amount with the solvent. The full distance the solvent travels is considered the mobile phase. The compound can be analyzed by its Rf value, equation one. Different ratios of the polar and nonpolar solvents are used to achieve the best separation of reaction mixture, or largest difference in Rf value.

$$R_f = \frac{distance\ compound\ traveled}{distance\ the\ solvent\ (mobile\ phase) traveled}$$

Equation one: calculating Rf value

An example of spot TLC can be seen below, figure 21. A filter paper is laid against the plate so that the solvent system remains in the environment of the plate, and the solvent does not evaporate before the compound has completed the mobile phase.

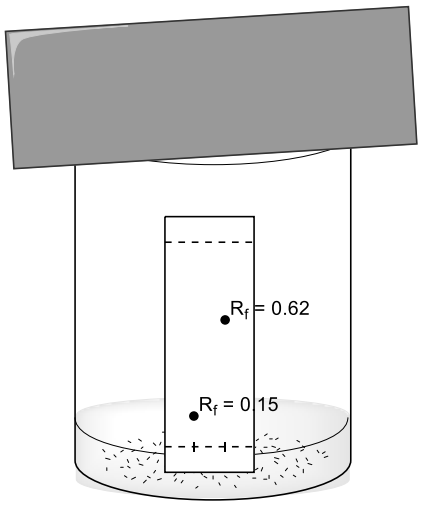

Figure 21: example of spot TLC in solvent system with Rf values

Preparative TLC is conceptually the same process. It is on a magnified scale, and uses a thicker piece of glass and silica compared to spot TLC. Contrastingly, however, this method is used to isolate pure compounds. Once the plate has been eluted, bands will appear on the plate, which can be scraped off. The silica containing compound is put

through a vacuum filtration with ethyl acetate, a polar solvent which will pull the compound off the silica. This work is done to isolate and purify the products, figure 22.

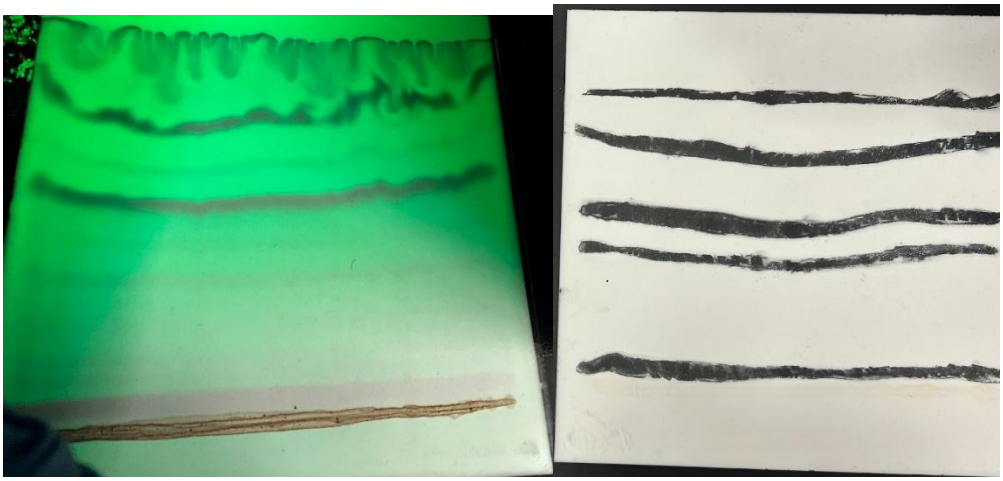

Figure 22: two preparatory TLC plate of $Os_2(CO)_6(Ph\text{-}NO_2CONH)_2$ after being run through 30% ethyl acetate 70% hexane solvent system. Right: before removal of silica under UV. Left: after removal of compound by scraping silica.

Nuclear Magnetic Resonance Spectroscopy

Nuclear Magnetic Resonance Spectroscopy, NMR, allows for compounds to be identified and analyzed. NMR creates a magnetic field around the sample, aligning the nuclear spins of the hydrogens. This allows for identifying the environment around hydrogens, providing information on the sample's structure. ^{1}HNMR is used in this research.

The spectrum provides information on chemical shift, in ppm; higher in chemical shift is also referred to as downfield or downshifted. The cause of a proton signal being more downfield is related to its environment; electron withdrawing groups deshield these protons, shifting them downfield, and so polarity can therefore be used in this spectrum.

Chemical equivalence between hydrogens can also be understood through NMR data. Integration numbers are found by the peak area under the signal, which is representative of chemically equivalent hydrogens. Unknown peaks integrations can be compared to known peak integrations to analyze the number of hydrogens represented.

Surrounding hydrogens affect the hydrogen of interest's signal in the NMR by "splitting" the peak. If a chemically unique hydrogen has no hydrogen "neighbors" then its peak will be a singlet (s), if it has one hydrogen neighbor the signal will be split into a doublet (d), if it has two hydrogen neighbors, the signal will be split into a triplet (t), if it has three hydrogen neighbors, the signal will be split into a quartet (q). There is also a possibility that the peak will be split into a multiplet (m) which is caused by complex splitting such as being split by multiple chemically nonequivalent hydrogens, or for a signal from multiple chemical equivalent hydrogens with each of their own hydrogen neighbors.

The NHs in the molecule are distinguishable through NMR, allowing for identification of each isomer, figure 23. The H,T isomer's NH is seen more downfield as it is opposite an oxygen, deshielding the hydrogen of interest. Through peak integration, information is gained on the isomer ratio.

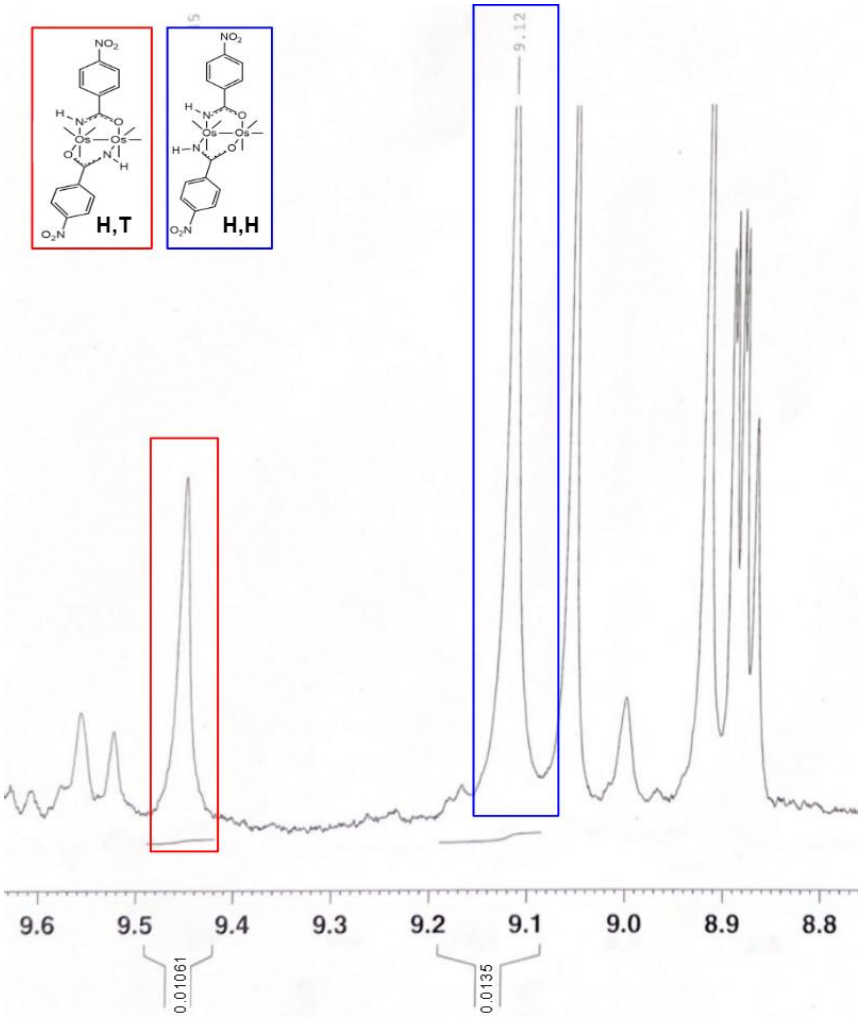

Figure 23: HNMR of crude nitrobenzamide product, showing the distinction of both isomers through chemical shift

Thus, the crude reaction mixture of the amide products can be studied in NMR using d-DMSO, with the peak area providing insight into isomer ratio. This can be studied over time, making sure that integrations are by the same chemical shifts each day. The known water peak is calibrated to 3.33ppm, and integrated from 3.4-3.26ppm. The H,H NH is integrated from 9.49-9.42ppm. And the H,T is integrated from 9.19-9.0852ppm.

Experimental

Synthetic Approaches to $Os_2(CO)_6(PhCONH)_2$

Synthesis of $Os_2(CO)_6(PhCONH)_2$ + separation with preparative TLC

Toluene was distilled over sodium in parafilm, and the reaction was carried out with 52mg of bisethoxide (0.0526mmol) and 125mg of benzamide (1.0113mmol) in 25mL of dry toluene. At 240 minutes, there was no further change in IR, and product peaks were formed, so heat was pulled off and solvent was removed with a rotavapor. A silica plug was run with the product in a 50:50 solvent system and then rinsed with Ethyl Acetate to remove any excess benzamide. An IR of the pale yellow solid in CH_2Cl_2 showed peaks at 2087, 2068, 2051, 2034, 2014, 1997, 1974, figure 24. From this, it was concluded that the product was formed and benzamide was separated.

The best solvent system to monitor this reaction was determined to be 20:80 ethyl acetate: hexanes as it showed the cleanest separation between isomers, figure 25, and so prepTLC was completed to isolate the isomers. Three bands, excluding the baseline, were isolated from the prepTLC. From least to most polar, they were labeled band A, B, C. IR was taken of products A, B, and C: figures 26, 27, 28, respectively.

Synthesis of $[Os_2(CO)_4(PhCONH)_2]_n$ (wet solvent)

This reaction was carried out in molar equivalence, and with toluene that had been distilled the previous year and was continuously opened under nitrogen. 20mg of bisethoxide (0.0202mmol) and 8mg of benzamide (0.066mmol) was added to 10mL of toluene. At 45 minutes, no product peaks had formed, and 2021cm^{-1} was growing in. After 80 minutes, heat was removed, and IR showed overwhelmingly the polymer with an intense peak at 2019cm^{-1}, figure 29.

Solvent was removed from the product by rotevapor, and further analysis required ^{1}HNMR. NMR was taken in d-DMSO, showing signals in the aromatic region, and a strong signal at 5.7ppm, figure 30. Further, NMR was repeated each day for 7 days, and no change was observed in any of these signal's integrations.

Synthesis of $Os_2(CO)_6(PhCONH)_2$, using intermittent addition of $CO_{(g)}$

Work was done to test if carbon monoxide gas could reverse the polymer formation once it began. 20.0 mg of bisethoxide (0.02121mmol) and 8.0 mg of benzamide (0.066039) was refluxed in 10mL of toluene for 45 minutes. In benzamide polymer formation, the polymer peak begins to appear as a shoulder on 2012, and develops into its own intense peak. Once this was seen in this reaction, carbon monoxide was set up to flow into one neck of a three neck flask, continuing to keep the solution under nitrogen and at reflux, figure 31. The carbon monoxide could be easily removed from the reaction. As highlighted below, $CO_{(g)}$ was added in four rounds, and relative intensities of unique carbonyl peaks were monitored with IR, watching for peaks 2069 (bisethoxide), 2087 and 2050 (product) and 2019 (polymer); table 2, table 3, and figure 32 highlights the rounds of $CO_{(g)}$ added.

Table 2: $CO_{(g)}$ added to crude benzamide reaction mixture

Time (min)	$CO_{(g)}$
0-25	on
25-35	off
35-45	on
45-55	off
55-65	on

65-75	off
75-85	on

Synthesis of $Os_2(CO)_6(PhCONH)_2$ and isomer interconversion

Work was done to follow up on Katie Marak's analysis of benzamide isomer interconversion. 20.0 mg of bisethoxide (0.0212mmol) and 9.9 mg of benzamide (0.0817mmol) was refluxed in 10mL of toluene for 15 minutes. A similar $CO_{(g)}$ cycle as seen in table 2 was performed for 185 minutes total until IR stopped . The resulting IR had peaks of 2102, 2088, 2067, 2051,2024, and 2014, figure 33.

HNMR in d-DMSO was obtained for 1024 scans over 112 hours, 6 days. The product was fully dissolved in DMSO, and so isomer conversion analysis was performed immediately. NH signals at 9.00ppm and 9.10ppm were used for monitoring, and calibrated with water peaks to 3.33ppm and integration of 500, figure 34. The isomer ratio was followed over six days, table 4, graph 3.

Table 4: H,T and H,H $Os_2(CO)_6(PhCONH)_2$ isomer NMR integrations over 112 hours

Time (hours)	H,T integration (9.1ppm)	H,H integration (9.0ppm)	H,H:H,T
0	0.0569	0.0074	88.5:11.5
16	0.044	0.0093	82.6:17.4
42	0.0347	0.0122	74.1:25.9
63	0.0197	0.0152	56.5:43.5
85	0.0159	0.0166	49:51
112	0.0156	0.0199	43.7:56.3

Synthetic Approaches to $Os_2(CO)_6(NO\text{-}PhCONH)_2$

Synthesis of $Os_2(CO)_6(NO_2\text{-}PhCONH)_2$ and polymer formation

50mg bisethoxide (0.0506mmol) and 25mg nitrobenzamide (0.1503mmol) was added to 25mL of freshly distilled toluene. The reaction was monitored with IR and spot TLC in a 30:70 solvent system.

After 360 minutes, IR of the crude reaction mixture showed peaks at: 2113.43, 2091.41, 2068.19, 2055.83, 2020.58, 1998.28, and 1979.49cm^{-1} and so the solution was removed from heat, figure 35. The spot TLC had three spots excluding the baseline: Rf =0.257 and Rf = 0.537, and a bisethoxide spot, figure 36.

PrepTLC was completed in the same 30:70 solvent system with eight plates. Four bands resembling spot TLC appeared, although the Rf values differed as solvent ran over. Bands were labeled product A, B, and C from most polar to least polar. Each band was scraped off, and extracted through vacuum filtration with ethyl acetate to isolate the product. Product B was of interest with IR showing carbonyl peaks at 2091.18, 2055.06, 1998.23, 1979.83cm^{-1} and amide peaks at 1579.38, 1529.12cm^{-1}, figure 37. Product C was also of interest, showing carbonyl peaks at 2090.90, 2069.06,2054.79, 2023.67, 1997.57, 1979.26cm^{-1}, figure 38. ^{1}HNMR of products B and C were obtained with 1054 scans in d-DMSO. ^{1}HNMR of band B had a signal of interest at 9.47ppm, figure 37. ^{1}HNMR of band C had a signal of interest at 9.15ppm, figure 38.

Synthesis of $Os_2(CO)_6(NO_2\text{-}PhCONH)_2$ and isomer interconversion

A second trial was run to determine if isomer ratios could be found through ^{1}HNMR of the crude reaction mixture. 51mg of bisethoxide and 25mg of nitrobenzamide was added to 25mL of toluene and reacted for 310 minutes until a large peak at 2021cm^{-1} was seen which has been identified as the polymer. IR showed peaks at 2091.26, 2067.92, 2055.38, 2021.92, 1997.92, 1979.55, and spot TLC was observed with two spots

in 20:80 ethyl acetate to hexanes, figure 39. The product was left in the freezer overnight, and then pumped on with $N_{2(g)}$ in a vacuum. ^{1}HNMR was taken in D-DMSO each day for 14 days, figure 43. Each integration from day 1-9 was recorded, table 5.

Table 5: HNMR data collected over nine days of crude nitrobenzamide product

Time (hours)	H,H integration	H,T integration	H,H:H,T	Total peak area
19	0.0135	0.0056	70.7:29.3	0.0191
42	0.0148	0.0046	76.3:25.7	0.0194
67	0.0159	0.0041	79.5:20.5	0.0200
86	0.0155	0.0036	81.2:18.8	0.0191
116	0.0149	0.0031	82.8:17.2	0.0180
160	0.0145	0.0024	85.8:14.2	0.0169
187	0.0146	0.0023	86.4:13.6	0.0169
213	0.0144	0.0021	87.3:12.7	0.0165

Through peak area analysis, decomposition is seen at 9 days, and the isomer ratio is no longer valid. It must be noted that day 0 ratio was not reliable as not all of the H,T isomer dissolved in DMSO. This was identified by dissolving the solid left in the RBF, and obtaining an NMR in the same settings, resulting in one peak seen at 9.45ppm, figure 41.

This was plotted over time, graph 4. It can be concluded that there is interconversion between the isomers, favoring the head-to-head isomer, which remains consistent with Marak's data from 2017.[11]

$Os_3(CO)_{12}I_2$ calibration curve

Five 10mL volumetric flasks (numbered 2-6) and one 25mL flask (number 1) were collected. 25.00mg of previously obtained $Os_3(CO)_{12}I_2$ was added to flask one with 25.00mL of dichloromethane. Parallel dilution was used, where a set amount of stock solution was added into a 10mL volumetric flask and then diluted to 10mL with dichloromethane, resulting in concentrations of 0.000862M, 0.000690M, 0.0005172M, 0.0003448M, 0.0001724M, 0.0000862M, figure 42.

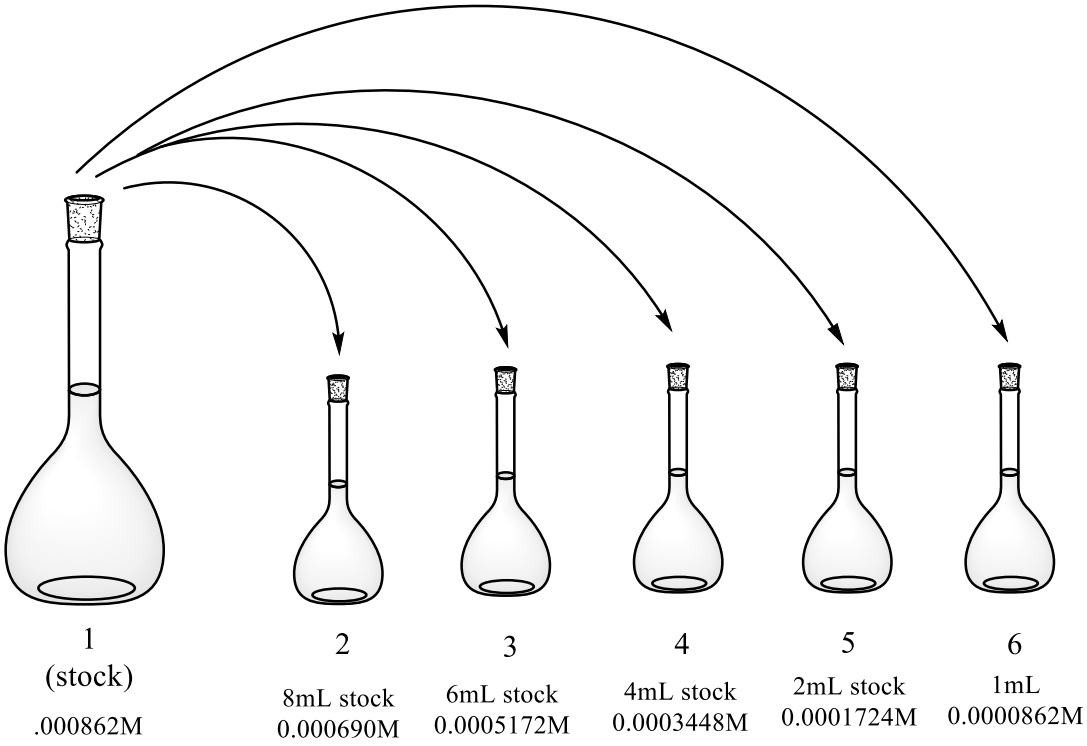

Figure 42: Parallel dilution of $Os_3(CO)_{12}I_2$

IR of each solution was taken with a dedicated calibration curve specific NaCl IR cell to analyze the distinguishing 2114 peak region, table 6, to produce the calibration curve, graph 5.

Synthesis of $Os_3(CO)_{12}$ and I_2 with Microwave Reactor

51.7mg of $Os_3(CO)_{12}$ (0.0570mmol) and 14.6mg of I_2 crystals (0.0575mmol) were added to 3.5mL cyclohexane and placed in a microwave tube. Standard procedure operated with conditions 150°C, 274 psi and 300W at max spin for 13 minutes, with an additional 30-45 minutes to cool to room temperature, figure 46. This method was repeated three additional times, varying the temperature each trial, table 7.

Table 7: amount of reactants added each temperature for $Os_3(CO)_{10}I_2$ microwave synthesis

Temperature	$Os_3(CO)_{12}$ added	I_2 added
155	51.7mg (0.0570mmol)	14.6mg (0.0575mmol)
160	51.4mg (0.0567mmol)	14.2mg (0.0560mmol)
165	51.9mg (0.0572mmol)	14.7mg (0.0579mmol)

The other conditions remained the same as the standard procedure: 300W, 275psi, 13 minutes.

After running through the microwave and cooling to room temperature, each solution was decanted into separate 100mL RBF, and the cyclohexane was evaporated from solution by Rotavaptor. Dichloromethane was added to a small amount (not measured) each solid, and an infrared spectrum was collected for each solution. The IR ratio of 2110:2069cm^{-1} highlighted the relationship between converted $Os_3(CO)_{10}(I)_2$ to starting material $Os_3(CO)_{12}$, respectively, table 8. This was compared to a reaction in previous standard temperature at 150°C, figure 43.[22] It was determined that 160°C produced the best conversion. Thus, final procedure is as follows: microwave at 160°C and leave solution to crystallize at -20°C overnight.[7]

Green Chlorination of $Os_3(CO)_{12}$ to form $Os_3(CO)_{12}Cl_2$

Method 1: dichloromethane as a solvent

22.00mg of $Os_3(CO)_{12}$ (0.02426mmol) was added to 10.00mL of dichloromethane in a three neck flask. Initial IR showed peaks at 2068, 2034, 2013, 1999cm^{-1}. 2.22mL of 2M HCl (0.0221mmol) was added using a 5mL syringe, and kept under nitrogen. The reaction was left stirring for fifteen minutes and IR of the $Os_3(CO)_{12}$ solution, the bottom layer, confirmed no reaction had taken place. A syringe containing 2.189mL of 7.5% NaOCl (0.0221mmol), was added dropwise to the solution every 20 seconds, and reaction was monitored by IR. After 1.8mL of NaOCl was added, IR confirmed complete conversion to $Os_3(CO)_{12}Cl_2$ with peaks at 2001, 2030, 2063, and 2120cm^{-1}, figure 44. The bottom layer was pipetted into a pear shaped flask and 3mL of DI water was added to wash. This process was repeated three times. The CH_2Cl_2 solution then was dried with anhydrous $CaCl_2$. Cyclohexane was added (a solvent the $Os_3(CO)_{12}Cl_2$ is insoluble in), and the CH_2Cl_2 was removed with the Rotavapor. The precipitated $Os_3(CO)_{12}Cl_2$ was left to crystallize overnight at -20^{O}C. The cyclohexane solution was decanted off to obtain $Os_3(CO)_{12}Cl_2$. Yield was not obtained.

Method 2: cyclohexane as a solvent

50.00mg of $Os_3(CO)_{12}$ (0.05514mmol) was refluxed in 25.00mL of cyclohexane in a three neck flask. There was a tube connecting the round bottom flask to a flask containing 5.50mL of 2M HCl (0.011mol). The tube into the reaction mixture had rigid glass tubing attached to bubble the gas directly into the osmium solution. A dropping funnel with a stopcock containing 5.50mL of 7.5% NaOCl (0.00554mol) was attached to the RBF containing HCl, image 1.

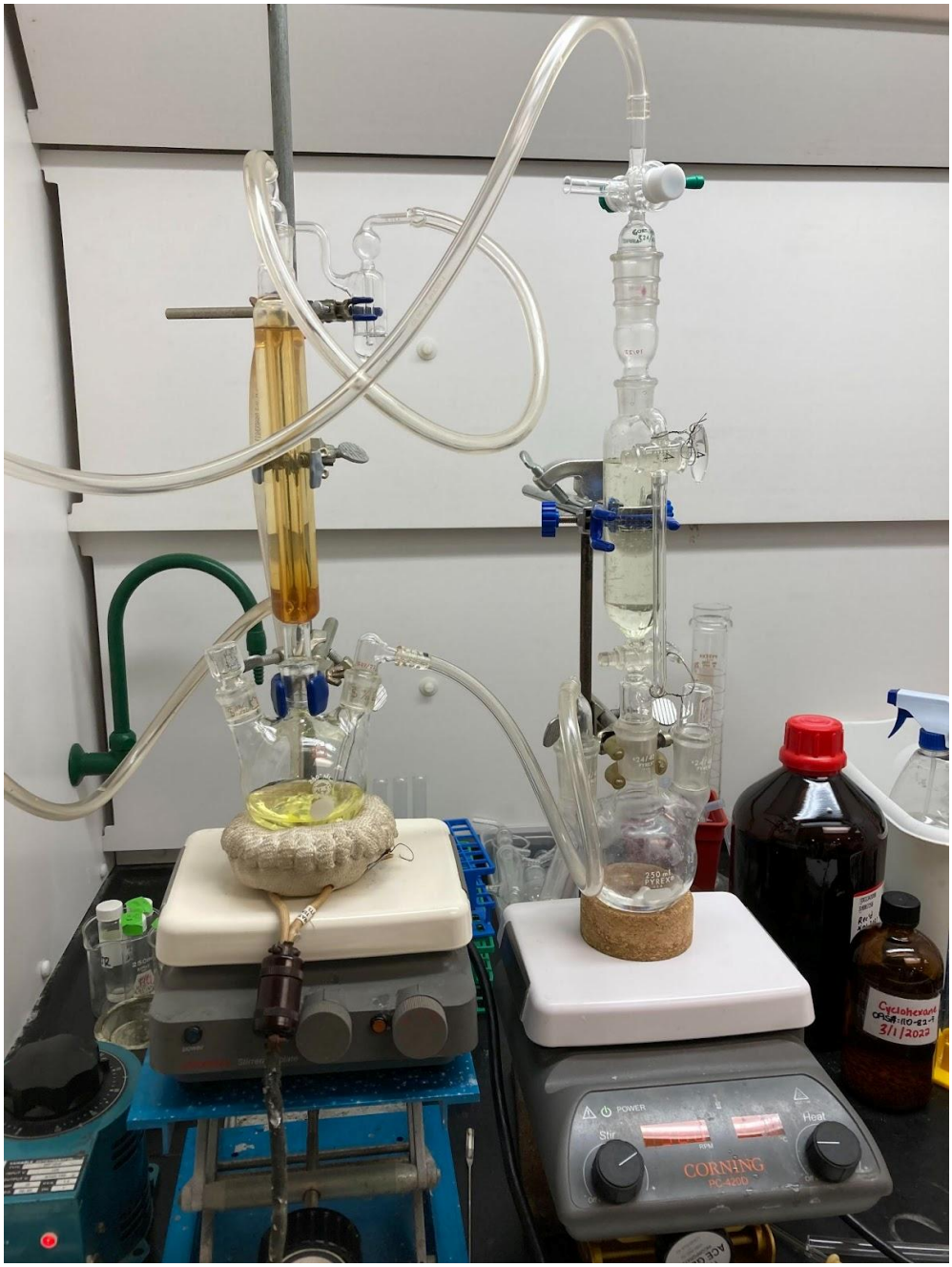

Image 1: set-up of $Os_3(CO)_{12}$ conversion to $Os_3(CO)_{12}(Cl)_2$ in cyclohexane

Bleach was added dropwise to the HCl solution, and chlorine gas was generated, as observed by bubbling in the solution. The gas traveled to the $Os_3(CO)_{12}$ solution. As the reaction proceeded, the $Os_3(CO)_{12}Cl_2$ product precipitated, and was a color change from the yellow solution to a colorless solution and yellow precipitate. The precipitated

$Os_3(CO)_{12}Cl_2$ was decanted out of the solution with a pipet, dried under nitrogen gas, and an IR in dichloromethane confirmed the product with peaks at 2120, 2084, 2063, and 2029cm^{-1}, figure 45. This procedure obtains $Os_3(CO)_{12}Cl_2$ in about a 90% yield, calculated by weight.

Results and Discussion

This work focuses on reactions of bisethoxide and benzamide/nitrobenzamide refluxing in toluene at 100°C. They both undergo the same reaction of forming a di-osmium di-amide product, figures 46 and 48. The challenges addressed in this work focus on identifying the compounds using IR and NMR spectroscopy in d-DMSO, and identifying the causes of polymer formation as well as possible reversal methods. An additional section of this work studies synthetic approaches of the Pearsall lab's starting material, bisethoxide, by analyzing past and current reactions with halide intermediates and developing a safer, green procedure of generating $Cl_{2(g)}$ in situ to efficiently produce bisethoxide in high yield.

Synthetic Approaches to $Os_2(CO)_6(PhCONH)_2$

The reaction of bisethoxide and benzamide occurs in a 2:6 molar ratio, with an Os-Os bond breaking and resulting in 3 molar equivalents of $Os_2(CO)_6(PhCONH)_2$. This forms two possible isomers: head-to-head (H,H) and head-to-tail (H,T), as pictured below in figure 46.

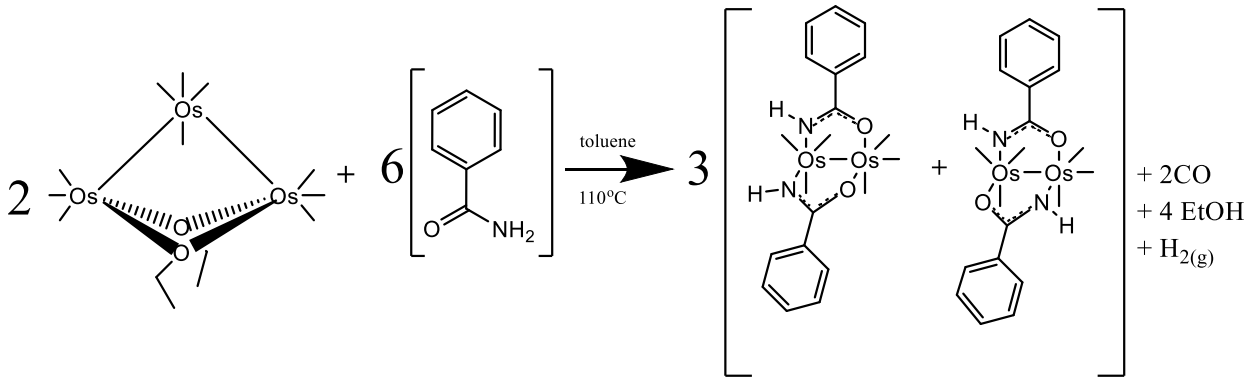

Figure 46: balanced scheme of benzamide and bisethoxide

These isomers exist in equilibrium, and the equilibrium isomer ratio of the $Os_2(CO)_6(PhCONH)_2$ isomers was previously obtained in the Pearsall lab by Katie Marak in 2017.[11] Marak isolated the isomers of benzamide through PrepTLC, and these two solutions were analyzed through ^{1}HNMR integrations in $CDCl_3$ over four weeks, resulting in initial equilibrium H,H: H,T ratio of 39:61. This reaction was initially attempted following the Marak procedure, but was unsuccessful at isolating the product; this was likely due to wet solvent and excess of benzamide. Thus, work was done to modify the experimental conditions.

Synthesis of $Os_2(CO)_6(PhCONH)_2$ + separation with preparative TLC

Preparative TLC has proven to be a successful technique to isolate the $Os_2(CO)_6(PhCONH)_2$ isomers, and so the aim of this work was to replicate this procedure.[11] Synthesis of these $Os_2(CO)_6(PhCONH)_2$ isomers is most efficient in dry solvent, as determined by previous experimentation. Thus, before beginning reaction, toluene was distilled over sodium in parafilm, and 52mg of bisethoxide (0.0526mmol) and 125mg of benzamide (1.0113mmol) were added to 25mL of dry toluene. The reaction was monitored with IR and prepTLC. Reaction to the benzamide polymer can occur quickly and with just 10 minutes of reflux past maximum product formation. It was later found that better results occurred from using a molar equivalence of benzamide to bisethoxide (benzamide is 3:1 molar ratio with bisethoxide in this reaction) instead of 7x excess as done in this trial.

Using an excess of benzamide in this reaction and freshly distilled toluene, a mixture of the coordinated amide product and polymer pattern in IR was found after 240 minutes, figure 24.

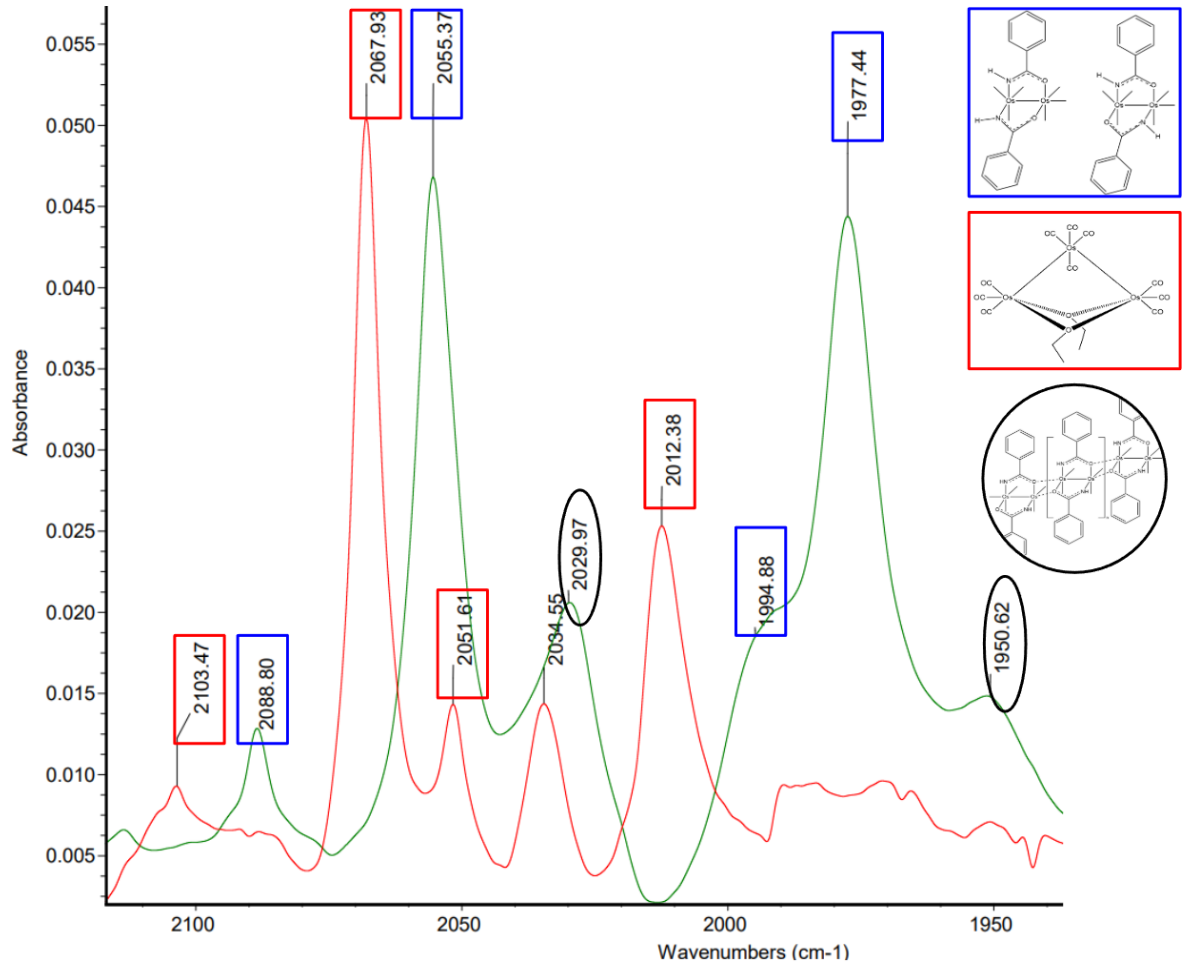

Figure 24: green spectrum = mixture of $Os_2(CO)_6(PhCONH)_2$ product (blue rectangle) in CH_2Cl_2 with slight polymer impurity (black circle) at 2029cm^{-1} (bw021) compared to red spectrum = bisethoxide starting material (red squares).

Comparison of the red spectrum (starting material) to the green spectrum (product) shows loss of 2103, 2068, 2051, and 2014cm^{-1} and the formation of 2088, 2055, 1994, and 1997cm^{-1}, which is proof of product formation. The appearance of 2029 and 1950cm^{-1} indicates the beginning formation of the polymer. We believe this is caused by continued reaction of product where two CO ligands are lost, and so the reaction should have been stopped before the appearance of this peak.[12] Since the toluene was dried, it appears that the excess of benzamide and further reaction resulted

in this polymer. PrepTLC of this reaction mixture had 3 spots, excluding the baseline. From most to least polar, Rf values were 0.478, 0.248, 0.068, figure 25.

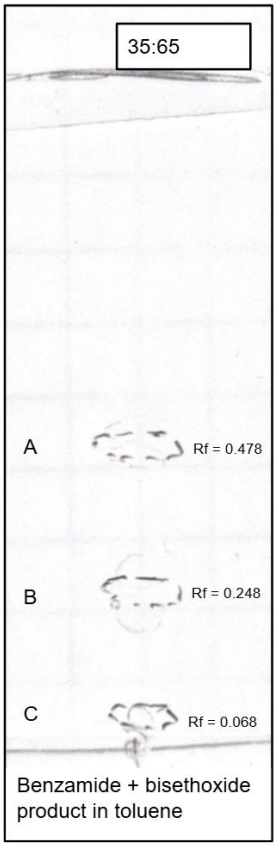

Figure 25: spot TLC in 35% ethyl acetate solvent system of $Os_2(CO)_6(PhCONH)_2$ in toluene (bw021)

PrepTLC revealed some separation; product A was a yellow solid, and an IR in CH_2Cl_2 revealed a mixture of the benzamide (starting material), monomer, and polymer, figure 26.

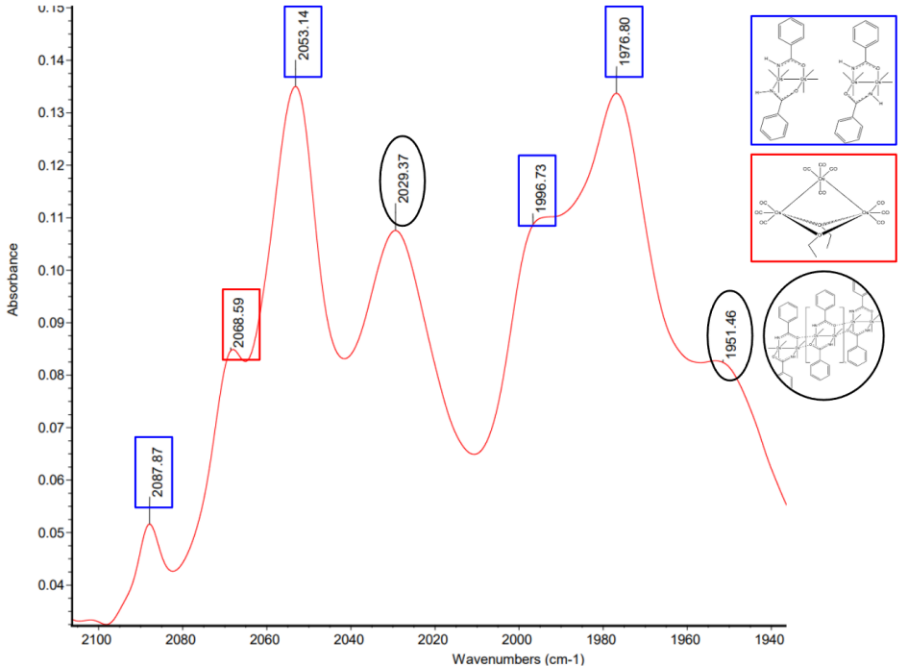

Figure 26: product A from prepTLC in $CHCl_2$, revealing polymer (black circle), starting material (red rectangle) and $Os_2(CO)_6(PhCONH)_2$ (blue rectangle) (bw021)

Product A was identified as $Os_2(CO)_6(PhCONH)_2$ and $[Os_2(CO)_4(PhCONH)_2]_n$ through monomer peaks 2088, 2053, 1997, and 1976cm^{-1} and polymer peaks 2029 and 1951cm^{-1}. Separation of product and polymer was not successful with prepTLC.

Infrared spectra of product B and C were indistinguishable and a dark yellow solid, figure 27 and 28.

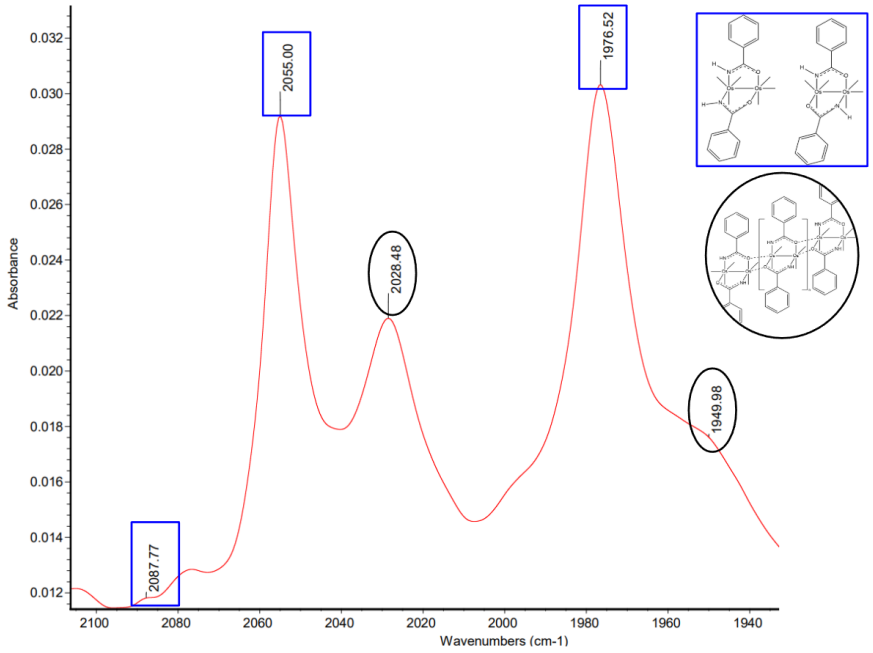

Figure 27: product B from prepTLC in $CHCl_2$, revealing polymer (black circle) and $Os_2(CO)_6(PhCONH)_2$ (blue rectangle) (bw021)

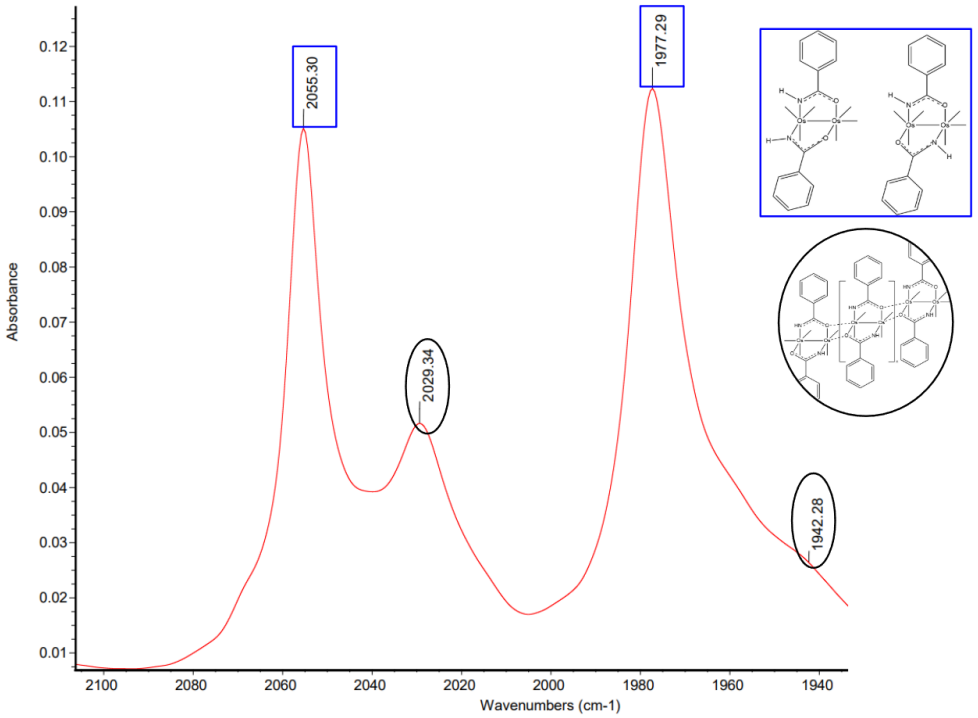

Figure 28: product C from prepTLC in $CHCl_2$, revealing polymer (black circle) and $Os_2(CO)_6(PhCONH)_2$ (blue rectangle) (bw021)

Even though 2055 and 1977cm^{-1} peaks remain in product B and C, the 2088cm^{-1} is missing which is one of the most indicative peaks of the $Os_2(CO)_6(PhCONH)_2$ product, and the pattern is different than would be expected. The pattern seems to be related to that of the polymer, and so it is unclear exactly what product B and C are. However, the IRs of products B and C being almost indistinguishable leads to the conclusion that separation was not successful, and that a different solvent system, likely a less polar one, would result in more reliable results. It was hypothesized that the excess of nitrobenzamide acts as a catalyst for polymer formation, and so future experiments were carried out with a molar equivalent of 1:3 bisethoxide to benzamide.

Synthesis of $[Os_2(CO)_4(PhCONH)_2]_n$ (wet solvent)

The aim of this experiment was to replicate the procedure described in this work by carrying out the reaction between benzamide and bisethoxide in molar equivalence and with toluene that had been distilled the previous year and was continuously opened under nitrogen.

20mg of bisethoxide (0.0202mmol) and 8mg of benzamide (0.066mmol) was added to 10mL of toluene. The reaction was monitored with IR. In addition to extended reaction time resulting in the polymer, we propose that wet solvent is a catalyst by activating carbonyls towards substitution.[6,7] This is as reactions are done on the milligram scale, and so, if 0.004% of water is in the solvent, the moles of water is comparable to the moles of reactant. It is possible the hydrogen of the water pulls electron density from the oxygen of the CO. This reduces the sigma donation by carbonyl to the metal, thus activating the carbonyl towards leaving, figure 47.

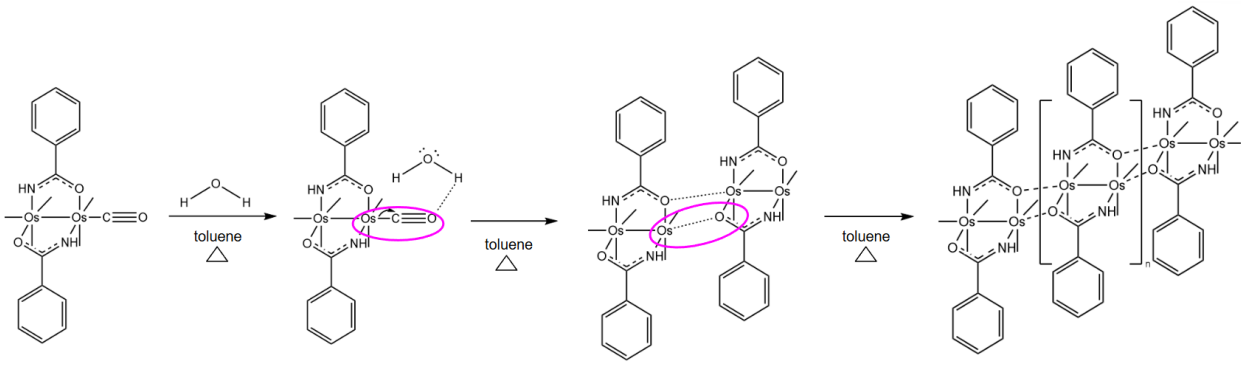

Figure 47: catalytic property of water in toluene, pulling electron density from the carbonyl's oxygen resulting in an open coordination site and polymer formation. Pink circles representing the loss of a CO ligand.

It is likely this occurred in a trial run in molar equivalence and with toluene distilled 10 days prior, figure 29.

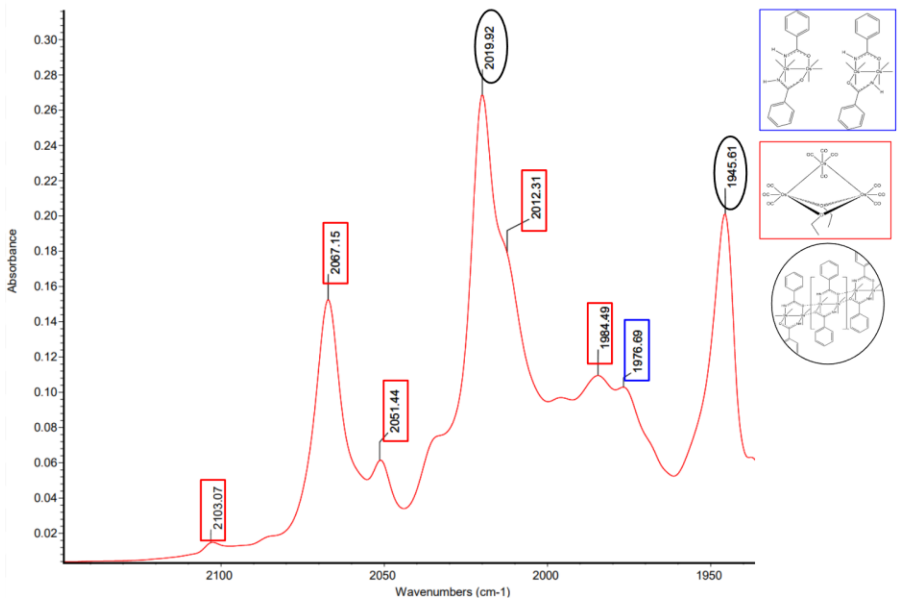

Figure 29: IR of benzamide polymer formation (black circle) catalyzed by water at 80 minutes; $Os_2(CO)_6(PhCONH)_2$ product (blue rectangle), starting material (red rectangle) (bw038)

This IR was taken 80 minutes into the reaction, which is only half of the usual reaction time. There was never significant development of the product peaks as seen by

the lack of 2088, 2055, 1994, and small 1976cm^{-1} (product peaks), and the intense 2019 and 1945cm^{-1} polymer peaks. Through this, it is clear further reaction did not occur as it had in the previous experiment, but instead that the water in the toluene favored CO substitution.

Marak completed NMRs in $CDCl_3$, but the solvent was switched for this work. The d-chloroform signal is at 7.4ppm. The H,H runs around 6.6ppm and the H,T at 7.0ppm according to Marak's work.[11] This solvent is useful for identification, but for a time trial in which it is necessary to have integrations as accurate as possible, the issue arises that the H,T runs very close to the chloroform peak. Thus, DMSO was investigated and determined to be the more useful solvent. Previous experiments proved NMR of benzamide product shows isomers at 9.1 and 9.0ppm, as seen in pages 66-67; thus, the NMR of the obtained polymer was run in DMSO with 1024 scans to further analyze it, figure 30.

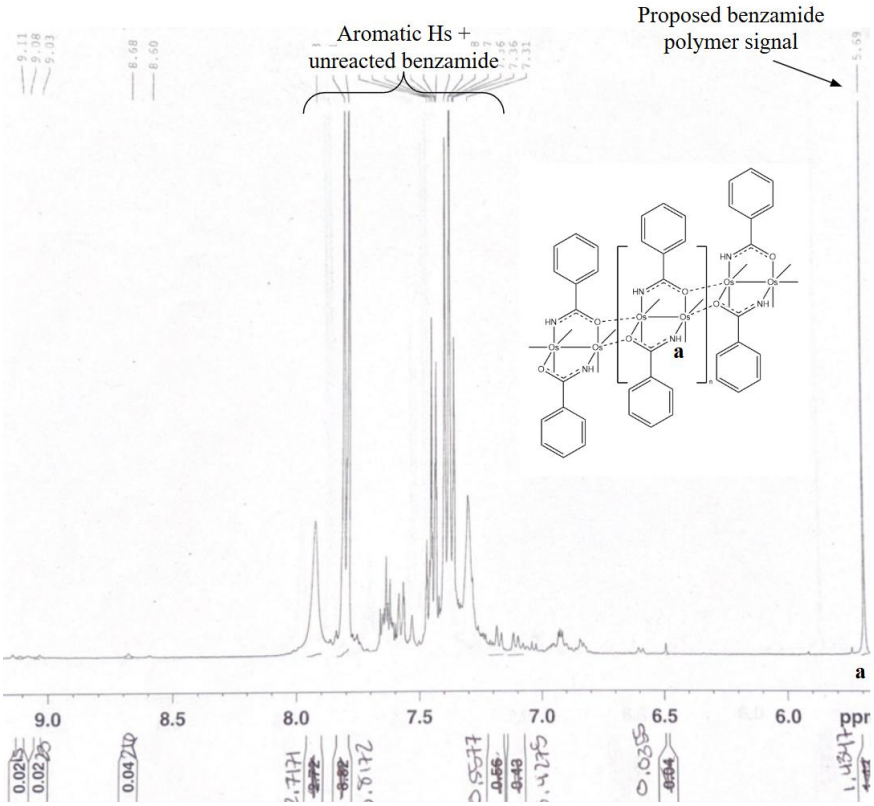

Figure 30: HNMR of benzamide polymer in DMSO (bw038)

The aromatics are seen, and the lack of signals past 8.0ppm indicates no coordinated NH of the isomers. There is a strong signal at 5.69ppm which is more upfield than the polymer signal was predicted, but this signal was strong in this spectrum. In other experiments where IR proved the product was more present than the polymer, the 5.69 signal was weak, indicating that this could possibly be the polymer signal. Further, NMRs were taken of this polymer sample over the seven day period, and there was no change in spectrum. The polymer is extremely stable over time, and so this provides further evidence this may be where the polymer appears in DMSO.[11]

Synthesis of $Os_2(CO)_6(PhCONH)_2$, using intermittent addition of $CO_{(g)}$

The polymer proved to be relatively easily formed, catalyzed by reaction with wet solvent. Thus, work was done to determine a procedure that could be utilized for

polymer reversal. Acetamide polymer reversal was studied in 2019 by Costa. The reversal was successful by bubbling carbon monoxide gas into the solution once all starting material had been consumed to break up the polymer and reattach carbonyl ligands, forming the monomers.[12] This was attempted with the benzamide polymer, but was unsuccessful, potentially due to steric clash. An alternative approach was tested, utilizing cycles of refluxing the reaction mixture and then removing heat and adding carbon monoxide.

20.0 mg of bisethoxide (0.02121mmol) and 8.0 mg of benzamide (0.066039) was refluxed in 10mL of toluene for 45 minutes. The reaction was monitored with IR. After formation of the polymer was identified through the presence of the 2019 shoulder, as seen in the red spectrum in figure 31, carbon monoxide was bubbled through solution for 10-15 minutes and then not for 10 minutes. This cycle was repeated, monitored through IR, and max product was achieved after four rounds of carbon monoxide addition through the solution, monitored by the growth of the 2088 and 2055 peaks - $Os_2(CO)_6(PhCONH)_2$, the loss of the 2019 peaks - polymer, and the loss of the 2067 peak - bisethoxide. Figure 31 below highlights the polymer formation before any carbon monoxide was added (red) and after the four rounds (orange).

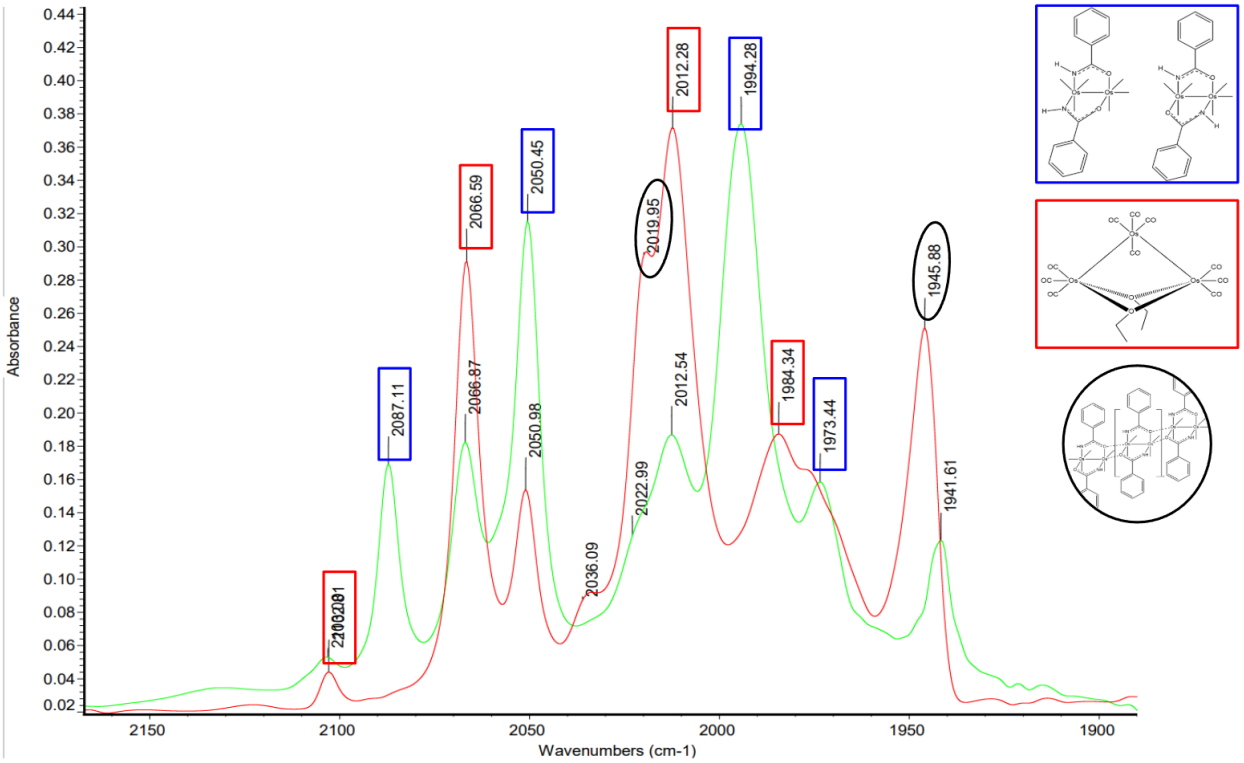

Figure 31: polymer formation (red spectrum) and $Os_2(CO)_6(PhCONH)_2$ monomer after six rounds with carbon monoxide (green spectrum); $Os_2(CO)_6(PhCONH)_2$ product (blue rectangle), starting material (red rectangle), polymer (black circle) (bw040)

After carbon monoxide was added, green spectra, the 2020 and 1945cm^{-1} peaks in the red spectra significantly decreased. These two peaks were expected as the polymer has both symmetric and antisymmetric stretching. When the carbon monoxide was off and system at reflux, there was an increase in polymer and loss of starting material, table 2 and figure 32. Thus, it is proposed that the carbon monoxide breaks apart the forming polymer, but inhibits any reaction with bisethoxide, as any carbon monoxide ligands that break off would get substituted with the CO being flowed through, reforming the starting material. This is highlighted in table 2 and graph 2 which follows the unique carbonyl peaks monitored through IR: 2069 (bisethoxide), 20187 and 2050 ($Os_2(CO)_6(PhCONH)_2$), 2019 (polymer).

Table 3: absorbance of IR peaks of crude reaction mixture as $CO_{(g)}$ is added (at RT) and removed (at 110°C)

		Approximate absorbance of peaks			
Time (min)	**Conditions**	**2069 (starting material)**	**2087 (product)**	**2050 (product)**	**2019 (polymer)**
0-25	$+CO_{(g)}$ *~26°C*	0.45	0.05	0.17	0.20 (slight shoulder)
25-35	Under $N_{2(g)}$ *~110°C*	0.32	0.05	0.13	0.47 (intense peak)
35-45	$+CO_{(g)}$ *~26°C*	0.41	0.06	0.15	0.30 (shoulder)
45-55	Under $N_{2(g)}$ *~110°C*	0.31	0.05	0.13	0.65 (intense peak)
55-65	$+CO_{(g)}$ *~26°C*	0.35	0.30	0.58	0.20 (slight shoulder)
65-75	Under $N_{2(g)}$ *~110°C*	0.50	0.15	0.30	0.52 (intense peak)
75-85	$+CO_{(g)}$ *~26°C*	0.30	0.25	0.48	0.12 (slight shoulder)

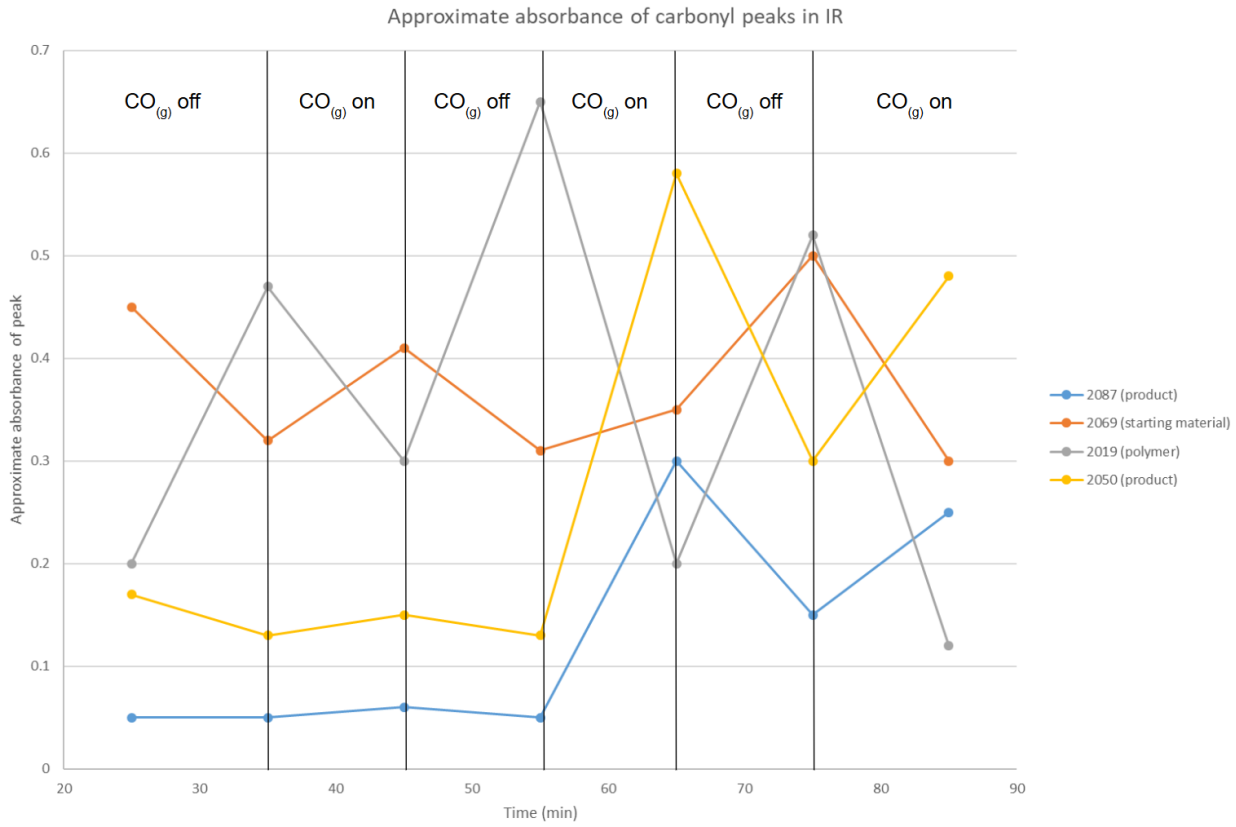

Graph 2: absorbance of IR peaks of crude reaction mixture as $CO_{(g)}$ is added at RT and removed at 110°C (blue = 2087 product peak; yellow = 2055 product peak; orange = 2069 bisethoxide peak; grey = 2019 polymer peak)

It can be seen through this data that there is a trend of decreasing polymer and starting material and increasing product when $CO_{(g)}$ is on, evidence of the reversal of the polymer. It is hypothesized that the first cycle has no major increase in product formation due to the addition of $CO_{(g)}$ driving the reverse reaction to starting material.

It is worth noting that work was done separately to see if bubbling in carbon monoxide would be successful once the polymer had fully formed, and this proved significantly less successful than cycling the gas on and off.

Synthesis of $Os_2(CO)_6(PhCONH)_2$ and isomer interconversion

The polymer consistently formed in further trials, but cycling carbon monoxide and reflux proved a successful method for reversal. Thus, work could continue to be done to analyze isomer interconversion of benzamide, by forming the product and analyzing integration of the NH peaks in HNMR. This work aimed to compare results to later nitrobenzamide trials in section page 71. and find patterns with Costa's work on acetamide and Marak's on benzamide.[11,12]

With successful $Os_2(CO)_6(PhCONH)_2$ monomer was produced using the above method and confirmed with IR and NMR, figures 33 and NMR.

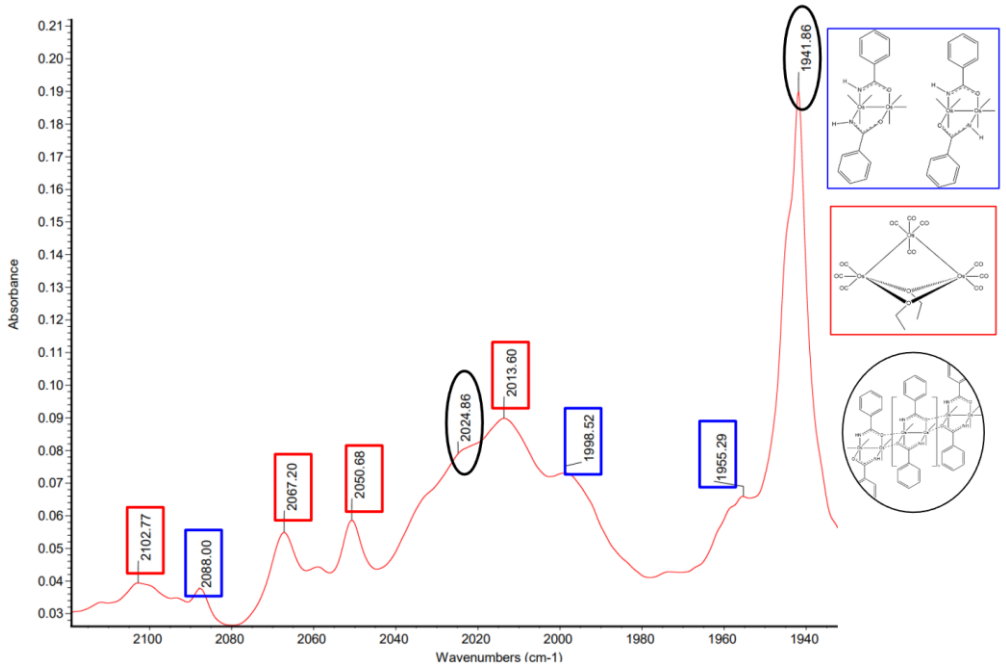

Figure 33: $Os_2(CO)_6(PhCONH)_2$ monomer in toluene after 5 rounds of $CO_{(g)}$ - $Os_2(CO)_6(PhCONH)_2$ product (blue rectangle), starting material (red rectangle), polymer (black circle) (bw044)

This spectrum exhibits poor subtraction of toluene, as indicated by the high signal to noise ratio and the intense 1945 peak. Although this is identified as a polymer peak through IR analysis in CH_2Cl_2, it is also present in toluene, so the unusually high

intensity of this 1945cm^{-1} peak is not an accurate representation of the amount of polymer present. Nonetheless, analysis was continued as the IR peaks at 2088, 1998, and 1955cm^{-1} confirm the product, and it is likely there is a 2055 present that is difficult to read due to the subtraction error. It is also clear the $CO_{(g)}$ was not fully effective at polymer reversal by the large intensity of the 2024 polymer peak compared to the product at 2088. This could be due to an accidental molar excess of benzamide added (3.9:1) or that the solvent had reached a higher concentration of water. The polymer, therefore, was still present during analysis.

The isomer signals are weak in the NMR spectra, but could be detected and integrated. NMR of crude reaction mixture shows signals at 9.0ppm (H,H) and 9.10ppm (H,T). The NMR of the mixture was then followed over five days (112 hours). At zero hours, there was barely a signal at 9.10ppm (0.0074), but one at 9.00ppm integrated for 0.0569, and at 112 hours 9.10 integration was 0.0156 and 9.0 integration was 0.0199, figure 34.

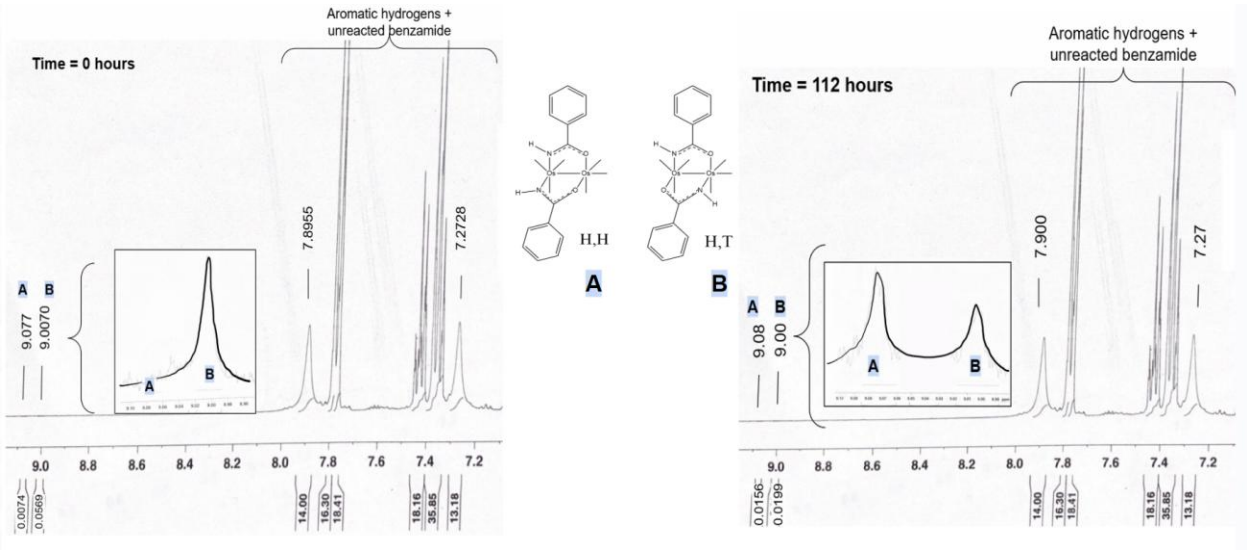

Figure 34: HNMR in DMSO of crude reaction mixture $Os_2(CO)_6(PhCONH)_2$ time 0 vs time 112 hours (bw044).

These spectra show clearly that a H,T signal grows in as the H,H begins disappearing, evidence of interconversion at RT. Over these 6 days, the isomer ratio of H,H:H,T shifts from 88.5:11.5 (110°C) to 43.7:56.3 (RT), favoring the head-to-tail isomer. The integrations were plotted onto a graph to track the trend, graph 3.

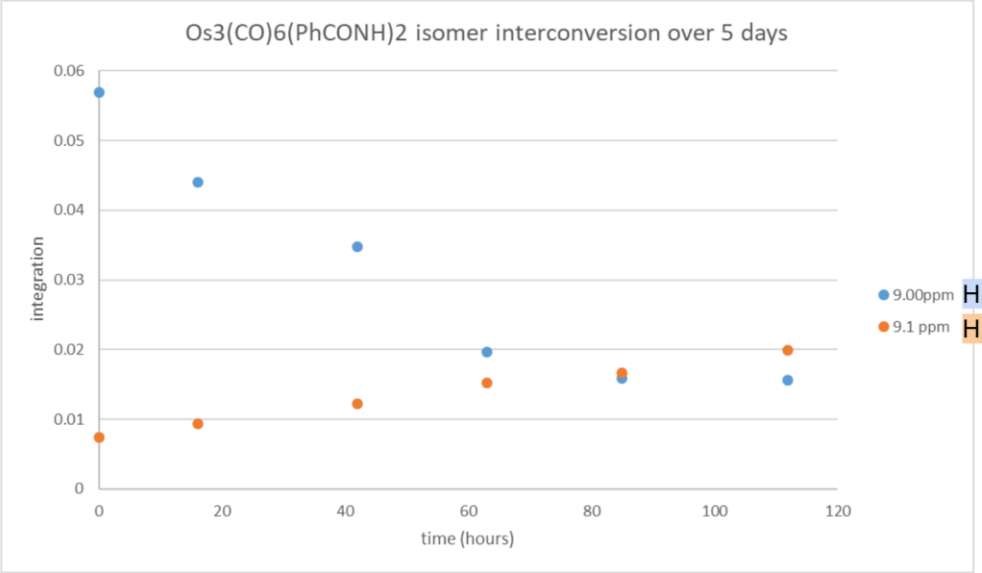

Graph 3: interconversion of $Os_2(CO)_6(PhCONH)_2$ from H,H to H,T (bw040) with an initial ratio of 88.5:11.5 (110°C) and final isomer ratio of 43.7:56.3 (RT).

Through analysis of data trends, the head-to-head decreases faster than the head-to-tail increases, but there is no significant decomposition found from total peak area analysis until after 6 days. The final H,H:H,T ratio after the 112 hours was 43.7:56.3. Thus, at high temperatures the H,H is favored, but at low temperatures, H,T is favored. This provides more information on the stability of these isomers, and is consistent with Marak's results who found isomer ratio at 110°C of 61:39 (kinetic product is H,H) and interconversion at RT resulting in final ratio of 43:57; concluding the H,T isomer as the thermodynamic product.[11]

Synthetic Approaches to $Os_2(CO)_6(NO_2\text{-}PhCONH)_2$

The reaction of bisethoxide and nitrobenzamide occurs in a 2:6 molar ratio, with an Os-Os bond breaking and resulting in 3 molar equivalents of $Os_2(CO)_6(Ph\text{-}NO_2CONH)_2$. This forms two possible isomers: head-to-head (H,H) and head-to-tail (H,T), as pictured below in figure 48.

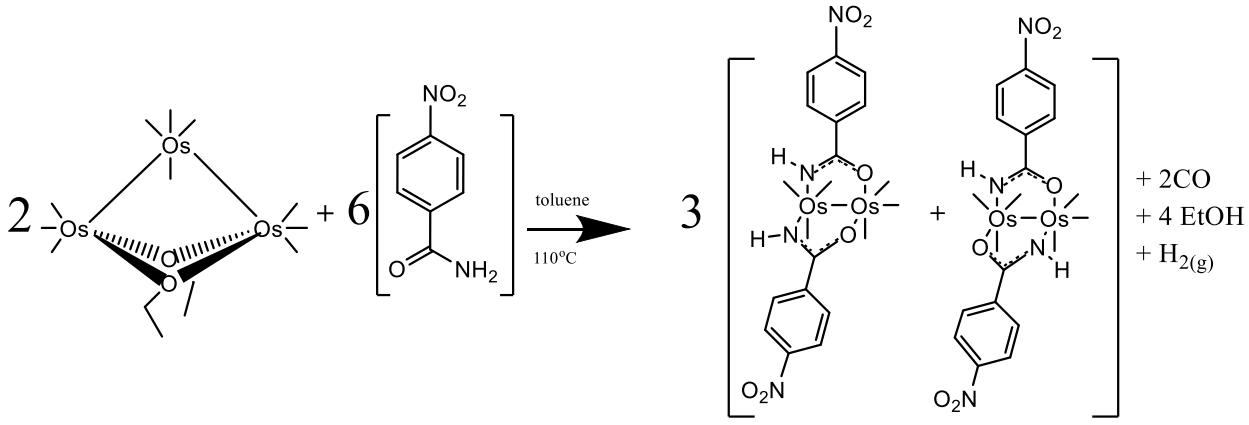

Figure 48: balanced scheme of benzamide and bisethoxide

The equilibrium isomer ratio of the $Os_2(CO)_6(Ph\text{-}NO_2CONH)_2$ isomers was previously obtained in the Pearsall lab by Abby Mullen.[23] Mullen isolated the isomers of nitrobenzamide through PrepTLC, and these two solutions were analyzed through ^{1}HNMR integrations in CD_2Cl_2, resulting in equilibrium at 110°C H,H: H,T ratio of 47:53. However, Mullen's NMRs show impurities from toluene and a low signal to noise ratio, and so there may be some error in the ratio which should be noted. Reaction was initially attempted following the Mullen procedure, but was unsuccessful at isolating the product; this was likely due to wet solvent. Thus, work was done to modify the experimental conditions.

Synthesis of $Os_2(CO)_6(NO_2\text{-}PhCONH)_2$ and isolation of isomers

Preparative TLC has proven by Marak to be a successful technique to isolate the $Os_2(CO)_6(PhCONH)_2$ isomers.[11] Although it was unsuccessful in separating the

benzamide product discussed on page 50. this was likely due to poor technique, so the aim of this work was to attempt the procedure again with the nitrobenzamide isomers to confirm identification with NMR.

50mg bisethoxide (0.0506mmol) and 25mg nitro-benzamide (0.1503mmol) was added to 25mL of freshly distilled toluene. The reaction was monitored with IR and spot TLC in a 30:70 solvent system; after 360 minutes, the reaction was complete as indicated by no further change in IR. The bisethoxide starting material can be contrasted with the crude coordinated amide product, figure 35.

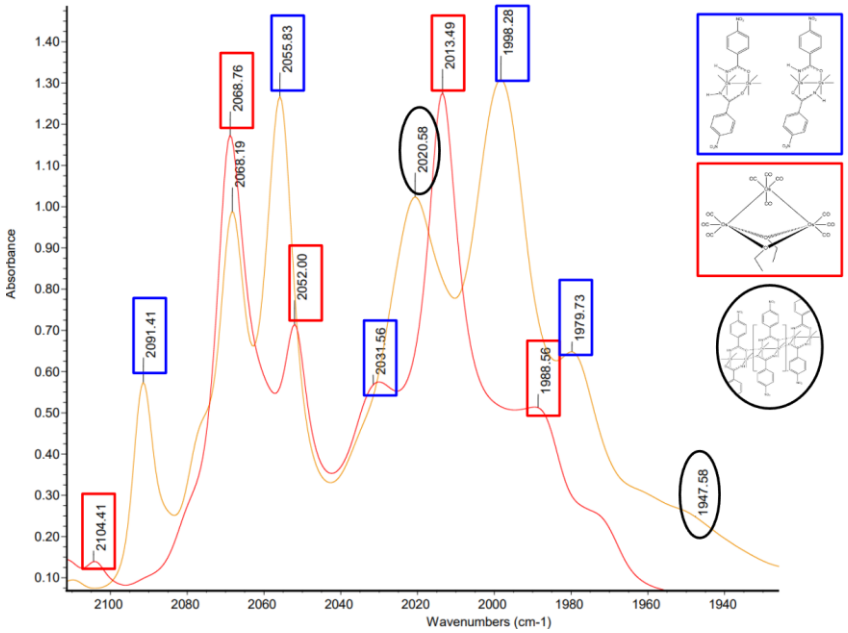

Figure 35: crude reaction mixture of $Os_2(CO)_6(Ph\text{-}NO_2CONH)_2$ in dichloromethane at 360min (purple spectrum) compared to bisethoxide starting material in toluene (red spectrum) with polymer impurity at 2020 and 1947cm^{-1}; $Os_2(CO)_6(PhCONH)_2$ product (blue rectangle), starting material (red rectangle), polymer (black circle) (bw032)

The shift in wavenumber as well as the change in pattern reflects the different carbonyl arrangement in the two clusters. In previous attempts, reaction to the polymer occurred as it had with the benzamide. Thus, a point was studied in which minimal

polymer formation occurred, but max product was obtained. At 360 minutes into the reaction, some starting material remained, but the small polymer formation indicated the point with maximum product formation had been slightly passed. Spot TLC also confirmed this, with a slight color at the baseline, isomer spots, and a bisethoxide spot (Rf=0.770) figure 36.

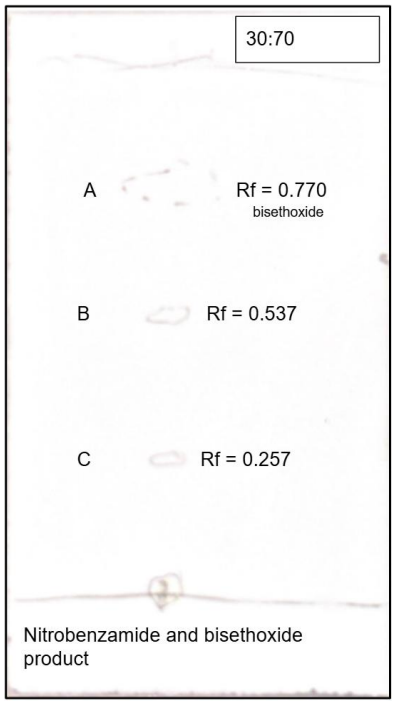

Figure 36: spot TLC of crude $Os_2(CO)_6(Ph\text{-}NO_2CONH)_2$ product at 360 minutes in 30 ethyl acetate:70 hexanes solvent system. Spot C: H,H isomer, spot B: H,T isomer (bw032)

The head-to-head and head-to-tail isomers have significantly different polarities, and are indistinguishable in IR but appear at different Rf values on TLC. They are separated well in this 30:70 solvent system with Rf values of 0.257:0.537 respectively. The separation of bands with PrepTLC occurred successfully, and infrared spectra and NMR of product B and C was obtained in d-DMSO with 1024 scans. The spectra were compared to a reference spectrum of benzamide in d-DMSO; although a different

molecule, the reference is valid as hydrogens of interest are in similar environments in both amide spectra. The aromatic peaks of benzamide in d-DMSO were seen at 7.2-7.8ppm, and the NH peaks at 7.25 and 7.94 ppm, figure 49.

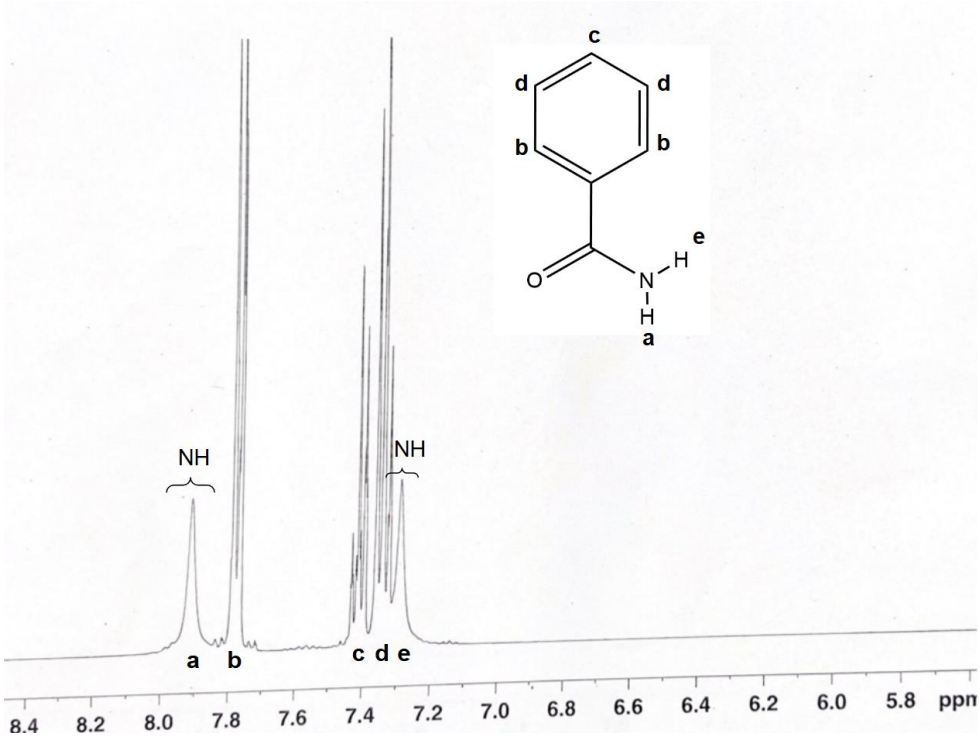

Figure 49: ^1H NMR of benzamide in d-DMSO (control).

This control of benzamide in d-DMSO shows two NH signals at 7.25 and 7.94ppm. This is likely as there is resonance between the oxygen and nitrogen, hydrogen bonding interactions between the hydrogen on the ring and the oxygen, as well as between H_a and the oxygen.

Product B showed a relatively pure $Os_2(CO)_6(Ph\text{-}NO_2CONH_2)$ product in IR, and NMR showed these aromatic C-H signals in the same region, with an additional singlet at 9.5ppm which was not seen in the reference, and so the H,T isomer signal could be identified, figure 37.

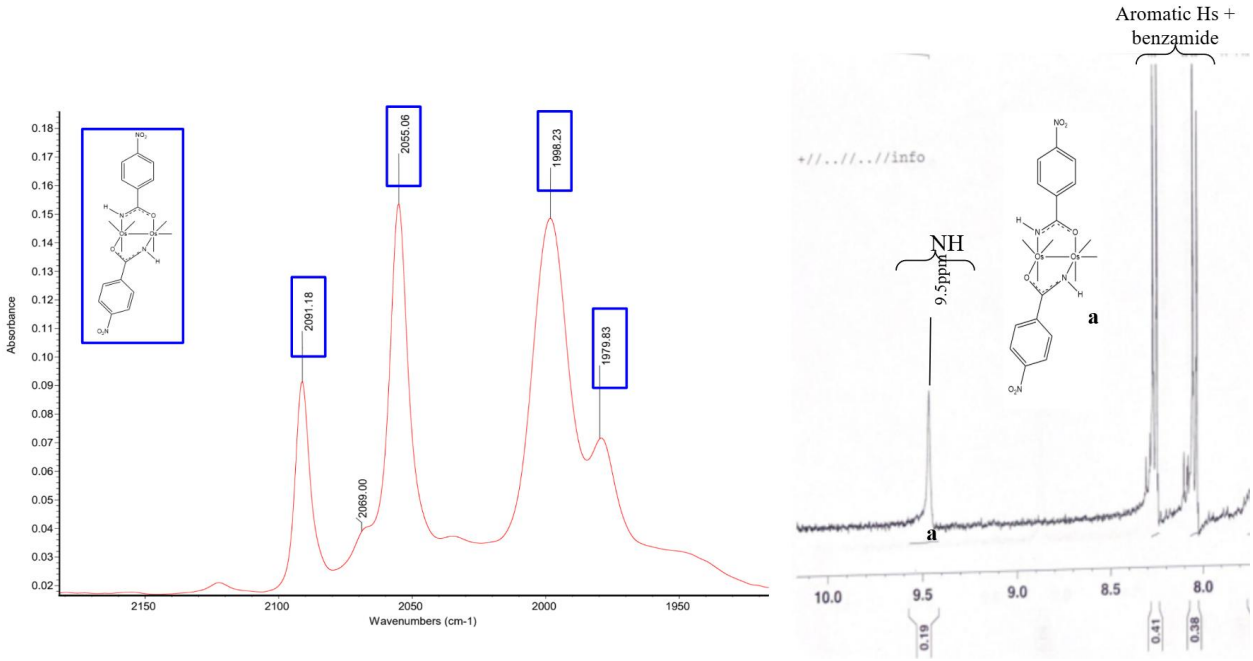

Figure 37: IR spectrum of Product B $Os_2(CO)_6(Ph\text{-}NO_2CONH)_2$ carbonyls (blue rectangle) - (less polar) head-to-tail isomer in 6mL of CH_2Cl_2

^1H NMR of Product B $Os_2(CO)_6(Ph\text{-}NO_2CONH)_2$ from Prep TLC separation in d-DMSO (bw032).

IR of product C, the H,H isomer, showed $Os_2(CO)_6(Ph\text{-}NO_2CONH_2)$ with some impurities. The NMR is similar to that of B - the benzene ring peaks are shifted more downfield as the overall molecule is more polar than the H,T isomer, but the NH signal has a lower chemical shift, 9.18, figure 38.

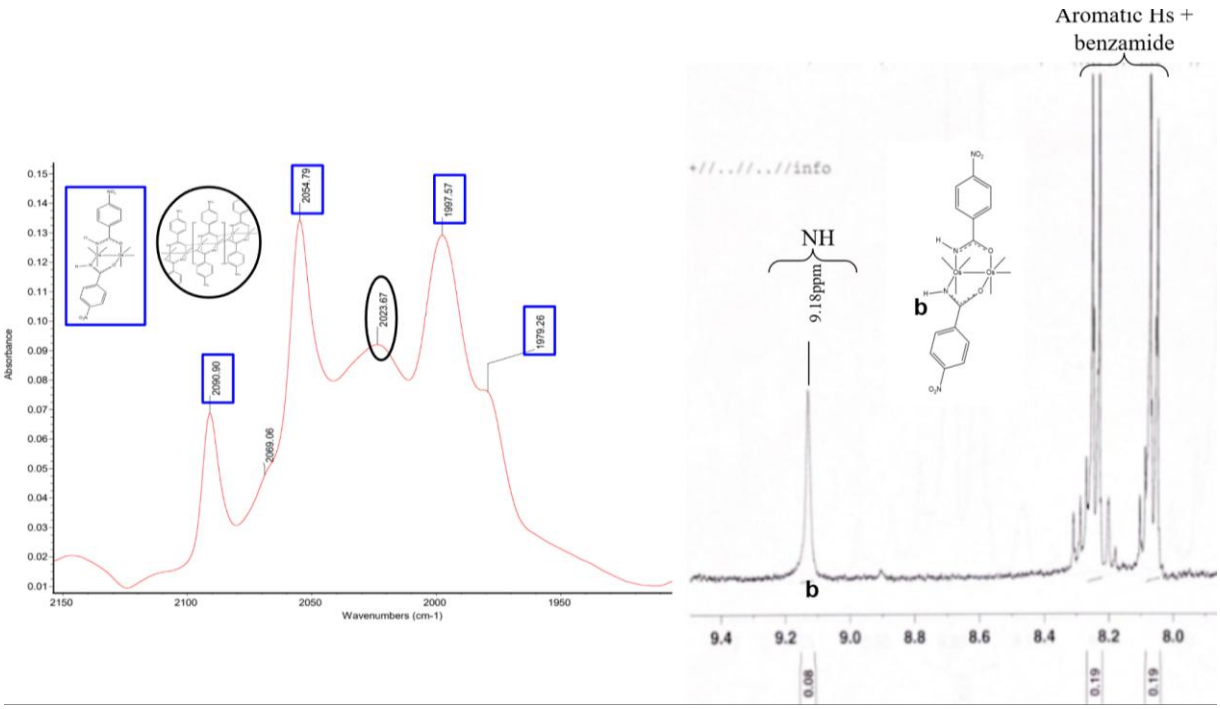

Figure 38: IR spectrum of Product C $Os_2(CO)_6(Ph\text{-}NO_2CONH)_2$ product C carbonyls - (more polar) head-to-head isomer (blue rectangle) in 3mL of CH_2Cl_2 with small starting material shoulder at 2069 and polymer formation at 2023.67 (black circle) ^1H NMR of Product C $Os_2(CO)_6(Ph\text{-}NO_2CONH)_2$ from Prep TLC separation in d-DMSO (bw032).

This difference in chemical shift is likely as the coordinated nitrogen in the H,T is opposite an oxygen, overall increasing the polarity of the hydrogen when compared to the H,H where the coordinated nitrogen is opposite another nitrogen. Thus, there is a significant difference in chemical shift in the two isomers to distinguish them, and so it was determined that separation through prep TLC does not need to be done in future experiments, and, instead, the integrations can be compared to follow the isomer ratio of the nitrobenzamide product over time.

Synthesis of $Os_2(CO)_6(NO_2\text{-}PhCONH)_2$ and isomer interconversion

Nitrobenzamide isomer interconversion had not been studied in the Pearsall lab previously, and so it was of interest to study the trends of this behavior in comparison to acetamide and benzamide. Additionally, since the nitrobenzamide isomers have distinct chemical shifts, separation and purification with PrepTLC is not necessary for accurate analysis with NMR. The integration of each NH peak provides quantitative information on the relative amount of each isomer present in the mixture. This work aimed to compare results to benzamide trials on page 61, and find patterns with Costa's work on acetamide and Marak's on benzamide.[11,12]

50mg $Os_3(CO)_{10}(OEt)_2$ (0.0506mmol) and 25.3mg nitrobenzamide (0.152mmol) were refluxed in 25mL of toluene, and monitored with IR. After 390 minutes, the polymer started appearing as seen from the appearance of 2020 peak, and so the heat was pulled off of the reaction. IR and spot TLC of the crude reaction mixture in dichloromethane was taken, figure 41.

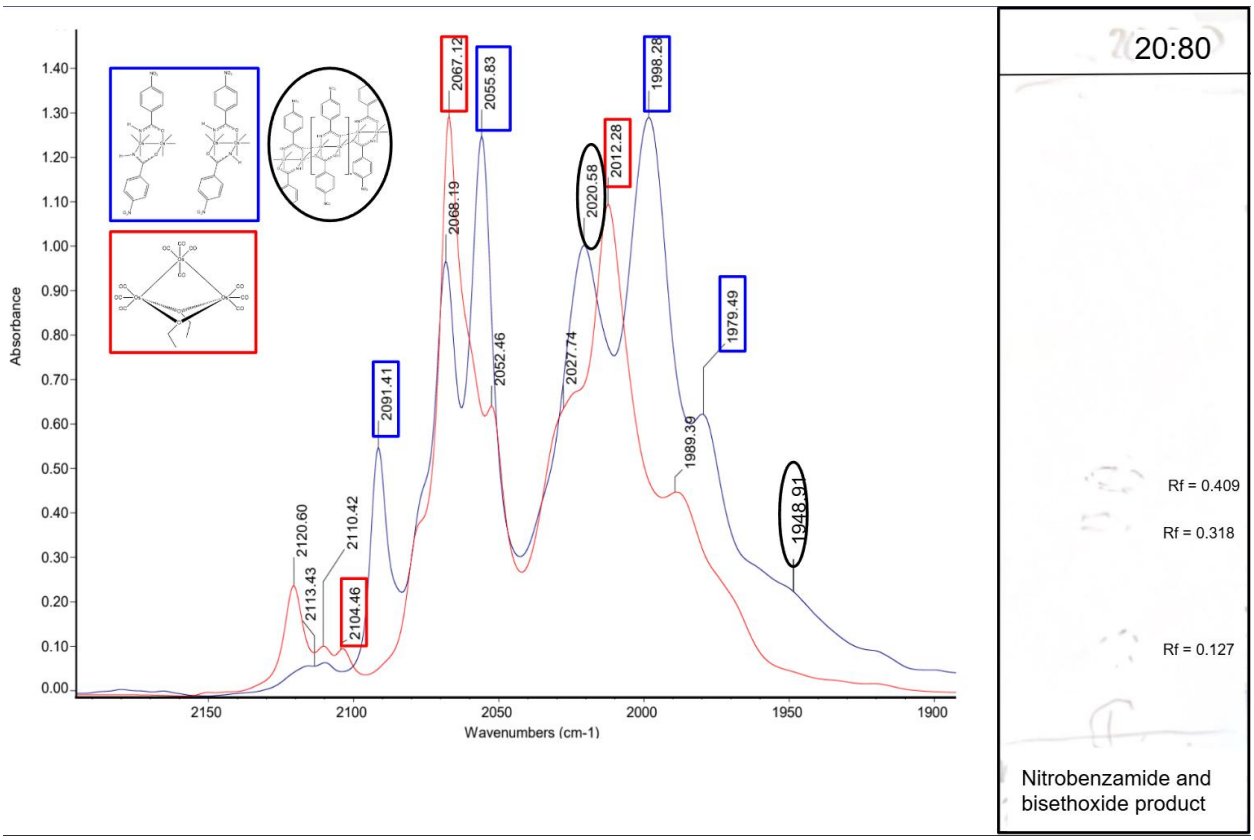

Figure 39: overlaid IR of bisethoxide starting material (red spectrum) and crude $Os_2(CO)_6(Ph\text{-}NO_2CONH)_2$ product (blue spectrum) at 390 minutes, highlighting the decrease of 2012 and 2067 starting material, and formation of polymer at 2020 and 1949cm^{-1}; $Os_2(CO)_6(PhCONH)_2$ product (blue rectangle), starting material (red rectangle), polymer (black circle)

Spot TLC is 20% ethyl acetate solvent system of final $Os_2(CO)_6(Ph\text{-}NO_2CONH)_2$ product (bw034).

The peaks at 2091, 2055, 1998, and 1979 and spot TLC confirm $Os_2(CO)_6(Ph\text{-}NO_2CONH)_2$ product, and so ^{1}HNMR was obtained in D-DMSO to see if the isomer ratios could be analyzed directly from the crude mixture. As identified from the previous experiment, the H,T amide appears at a higher chemical shift, around 9.5ppm, than the

H,H amide which appears around 9.1ppm. Most of the sample was dissolved in DMSO, but some solid remained.

The day zero ^{1}HNMR spectrum of the two isomers identified by coordinated NHs is below, figure 40.

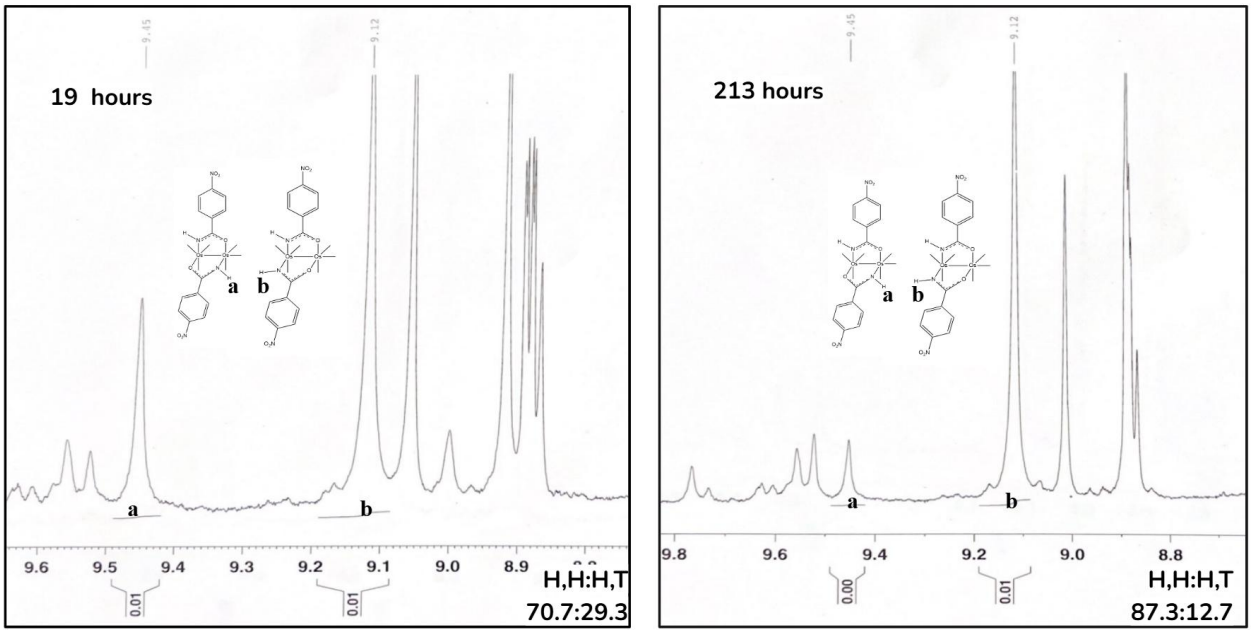

Figure 40: ^{1}HNMR of amide peaks of the two isomers in crude reaction mixture 19 hours on left, 213 hrs on right (bw034).

There were aromatic signals in the typical region, confirming the product was obtained. The exact integrations for the coordinated NH signals at time 19 hours are 0.01061 H,T and 0.0135 H,H. This shows the ratio of 70.7:29.3, favoring the head-to-head isomer. NMR was repeated each day, integrating each region consistently, and calibrated using the 3.33ppm water peak for each spectrum.

Another data point that was tracked was the total NH peak area, calculated by the sum of peak integrations. There was a significant decline after 213 hours, but before that the total peak area remained relatively consistent. Thus, 213 hours is the last reliable

isomer ratio, 87.3:12.7, and so it is valid to conclude that the isomers interconvert, favoring the head-to-head isomer over time, table 5.

This data of isomer integrations over time in table 4 are graphed, illustrated below, graph 4.

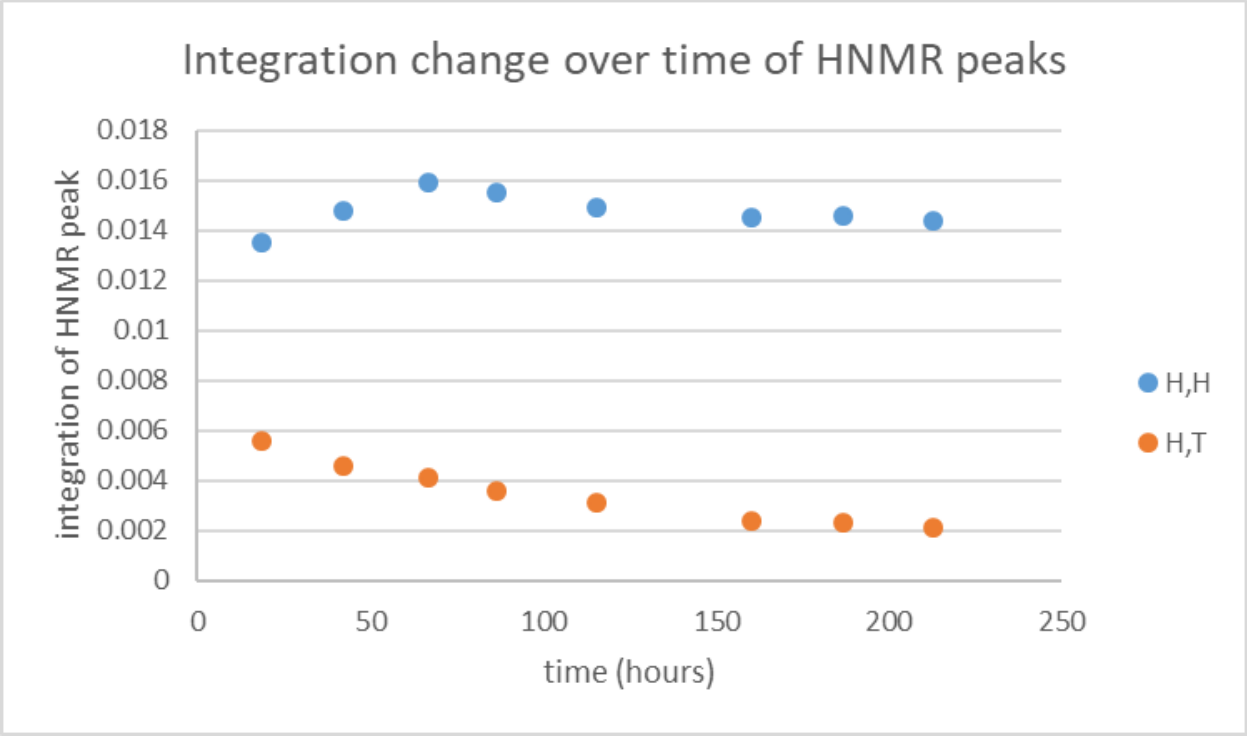

Graph 4: NMR integration over time of H,H and H,T signals in $Os_2(CO)_6(Ph\text{-}NO_2CONH)_2$ (bw034).

This proves that these isomers interconvert, but there is a steady decrease in head-to-tail isomer compared to the head-to-head, which remains stable throughout the last three points. NMR data indicates that head-to-tail decomposes faster than the head-to-head, again highlighting differences in stability of the isomers in DMSO. This is similar to the trend seen in the benzamide data, although favoring the H,H isomer. This is still being investigated as to why, but a hypothesis is the addition of the electron withdrawing NO_2 group in nitrobenzamide pulls electron density from the carbonyl, and

so coordinating in the H,H isomer creates a larger partial negative charge on the oxygens, stabilizing the molecule.

On day 0, NMR in d-DMSO was taken of the insoluble product initially left behind. This confirmed the less soluble isomer to be the H,T isomer, figure 44.

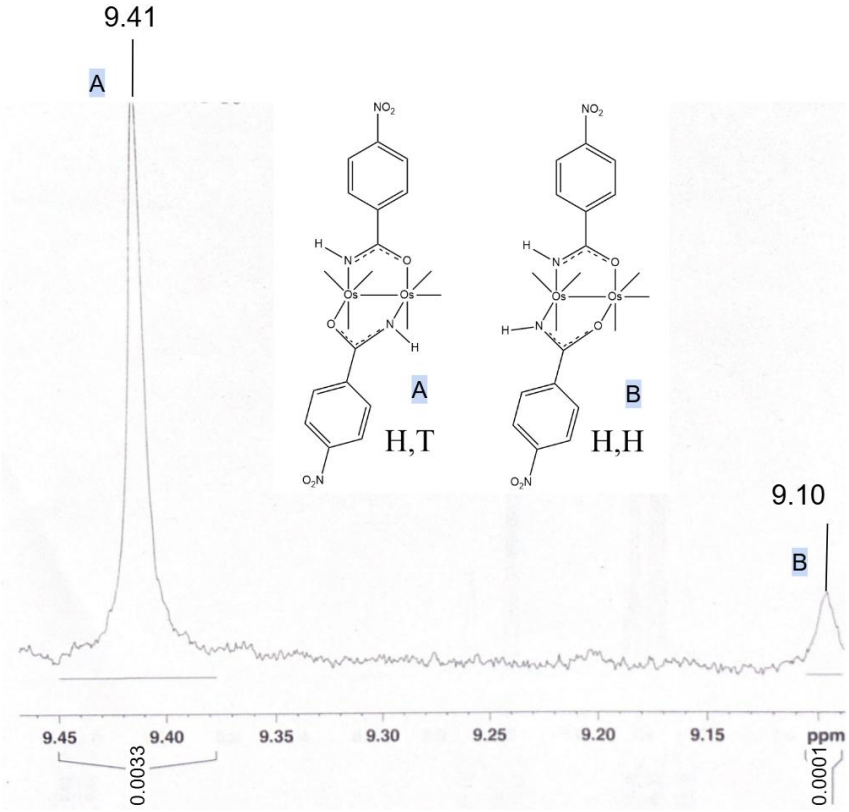

Figure 41: HNMR of insoluble product isolated from crude reaction mixture of $Os_2(CO)_6(Ph\text{-}NO_2CONH)_2$ (bw034).

This solubility is likely due to polarity. d-DMSO is a polar solvent, and the H,T isomer is nonpolar, and so it is likely this is why it does not dissolve in solution like the polar H,H isomer. Due to this, time 0 was not considered a valid ratio, and so it was not considered in the time trial outlined in graph 3.

<u>$Os_3(CO)_{12}I_2$ calibration curve</u>

It was of interest to produce a more recent calibration curve for the halide intermediate: $Os_3(CO)_{12}I_2$ which is formed from reaction with $Os_3(CO)_{12}$ and I_2 crystals in cyclohexane. Dichloromethane was added to solid $Os_3(CO)_{12}I_2$ to give a stock solution of 0.000862M. Parallel dilution was used to obtain five 10mL flasks with concentrations of 0.000862M, 0.000690M, 0.0005172M, 0.0003448M, 0.0001724M, 0.0000862M, figure 45.

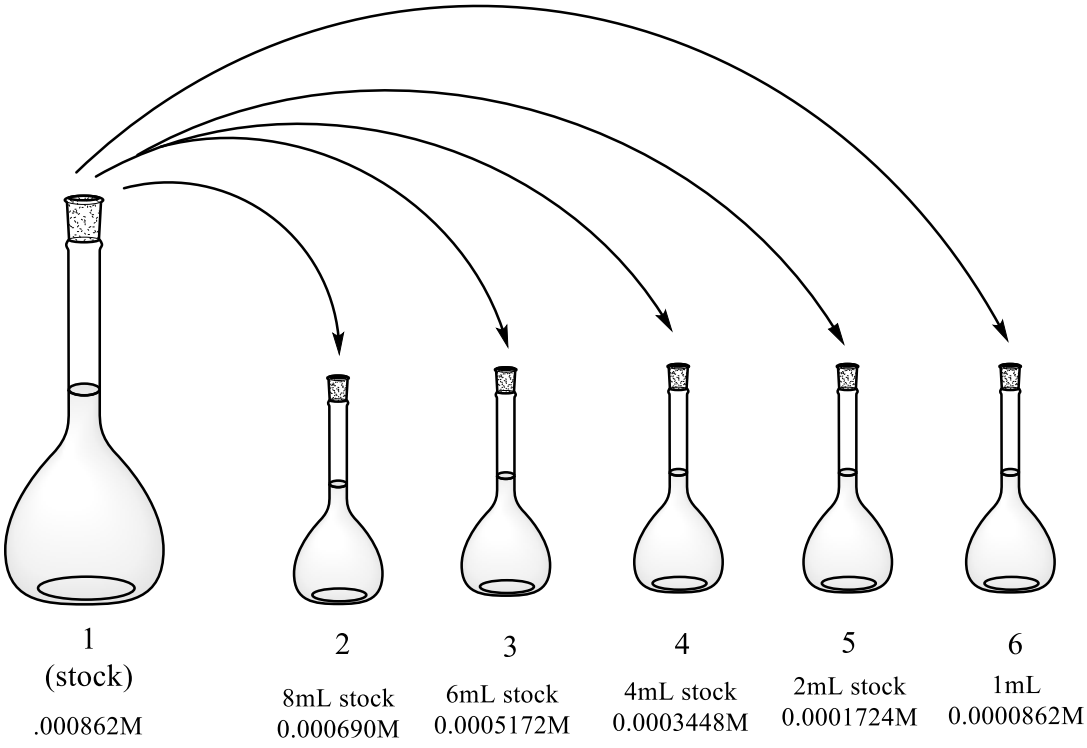

Figure 42: Parallel dilution of $Os_3(CO)_{12}I_2$

IR of each solution was taken with a dedicated calibration curve specific NaCl IR cell to analyze the distinguishing 2114 peak area and height in absorbance, table 6, to produce the calibration curve, graph 5.

Table 6: IR analysis of 2114cm^{-1} peak area and height

Flask	Molarity	Peak Area	Peak Height
1	0.000862	0.1405	0.0263

2	0.000690	0.1178	0.0225
3	0.0005172	0.0785	0.0160
4	0.0003448	0.0466	0.0107
5	0.0001724	0.0246	0.0060
6	0.0000862	too dilute	too dilute

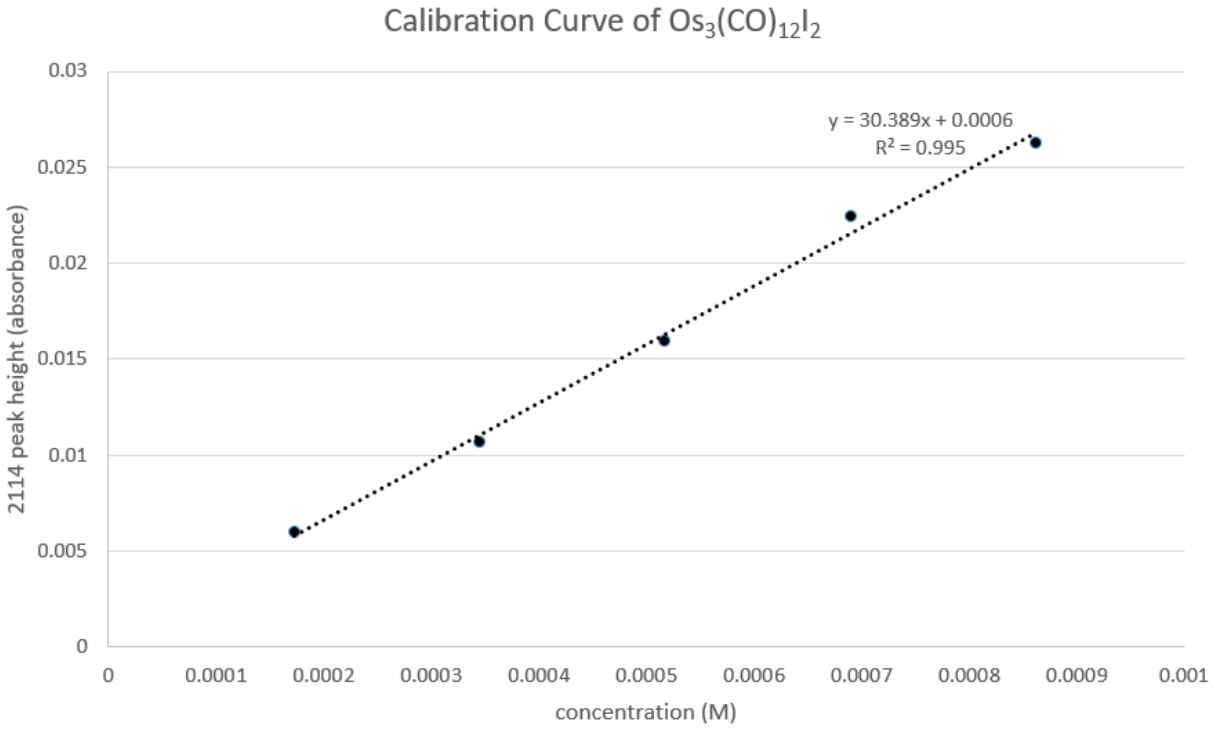

Graph 5: calibration curve of $Os_3(CO)_{12}I_2$ with linear trendline equation of y=30.389+0.0006 and a correlation coefficient $R^2 = 0.995$

Optimization of Microwave Reaction of $Os_3(CO)_{12}$ and I_2

It was standard in the Pearsall lab to synthesize bisethoxide utilizing halide intermediates. The formation of $Os_3(CO)_{10}(X)_2$ (X=Cl,Br,I) forms by the osmium-osmium bond breaking, two halide ligands attaching, and then the axial carbonyls breaking off to close the cluster. Analysis by Baum and Cavaliere reported the rate

constants of halide substitution reactions proved a general trend where Cl>Br>I.[16,17] However, the toxicity of storing and handling $Cl_{2(g)}$ resulted in the preferred intermediate of $Os_3(CO)_{10}I_2$ which is formed by microwave reaction of $Os_3(CO)_{12}$ and solid iodide in cyclohexane. Thus, work was done to establish if the conversion of the $Os_3(CO)_{12}$ to $Os_3(CO)_{10}I_2$ could be increased, also increasing bisethoxide starting material yield.

Previous microwave standard procedure for this iodine reaction utilized 300W, 275psi, 150°C, and so the control used was material generated under these conditions, figure 43.[22]

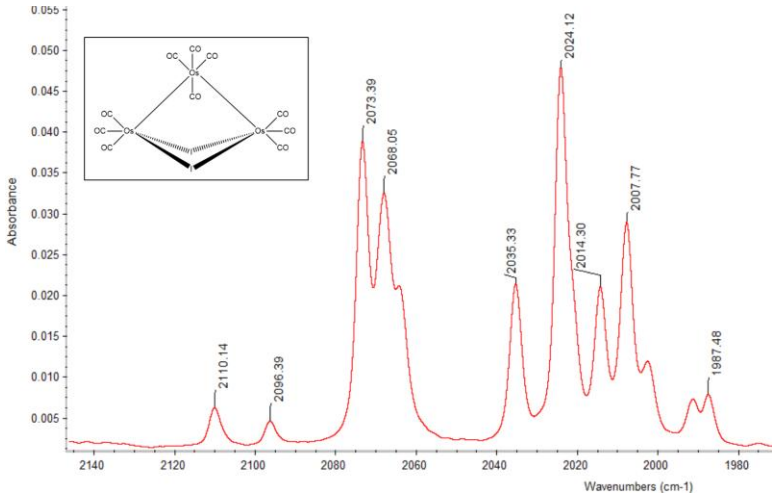

Figure 43: Paxtan Perry $Os_3(CO)_{12}I_2$ post microwave IR used as standard in this experiment: conditions = 150°C, 274 psi, and 300W

Temperature was varied, and IR spectra were taken post microwave. The 2110 and 2069 peaks of $Os_3(CO)_{10}(I)_2$ and $Os_3(CO)_{12}$, respectively, are characteristic. Thus the heights and relative ratios of the diiodide products were analyzed to identify highest conversion of product to starting material (2110:2069).

A higher ratio of 2110:2096 indicates a higher product yield, as there is a higher concentration of products to reactants. Ratios were analyzed throughout the different

temperatures, and so 160°C was determined the ideal temperature as it had the highest ratio out of tested temperatures, table 8.

Table 8: $Os_3(CO)_{10}(I)_2$ product post microwave 2110:2069 IR peak area with varying temperatures

Temperature (°C)	2110 area $Os_3(CO)_{10}I_2$ product	2069 area $Os_3(CO)_{12}$ starting material	Ratio of 2110:2069
150	0.270	0.460	1:1.703
155	0.371	1.210	1:3.26
160	2.174	10.549	1:4.85
165	1.820	4.746	1:2.608

It is important to note that, as seen in figure 43, the 2069 peak overlaps with the 2073, and so the found area may not be accurate. However, each temperature's IR was integrated consistently using the same baseline and range, and the ratios of these peaks are a reliable set of data for comparison. Additionally, although use of $Os_3(CO)_{10}I_2$ has been optimized, the conversion to bisethoxide is still lower than the Cl_2 approach.

Additionally, the percent yield of this reaction can be calculated using calibration curves previously developed in the Pearsall lab, graphs 6A, 6B.

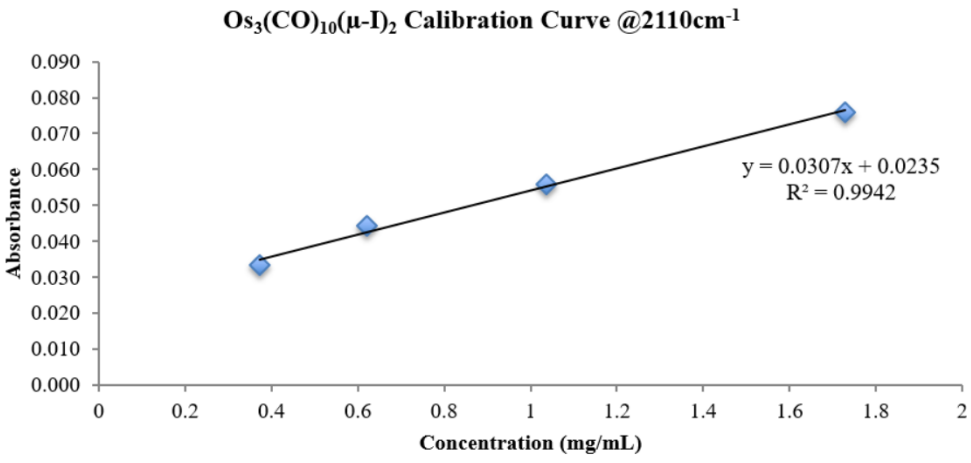

A

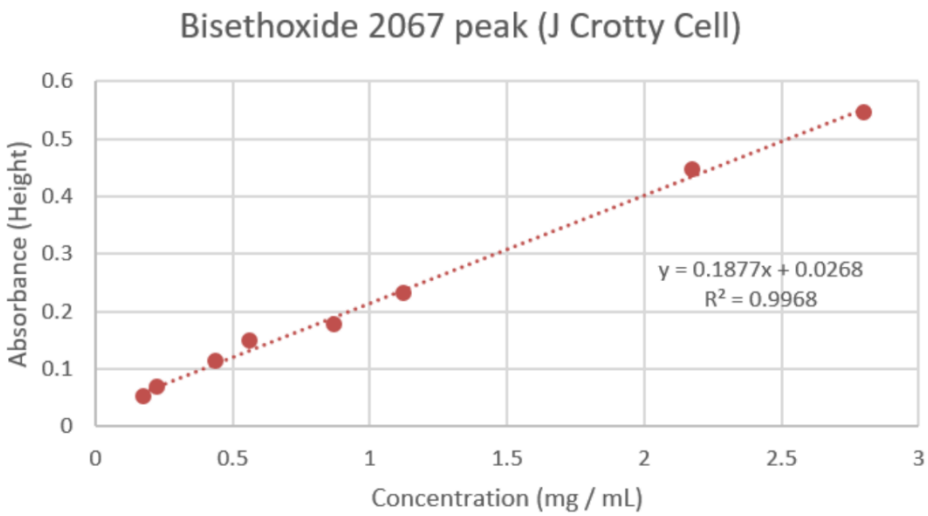

B

Graphs 6A 6B: calibration curves generated by previous researchers in Pearsall lab. Two peaks analyzed were reactant, iodide, 2110cm^{-1} (6A) and product, bisethoxide, 20167cm^{-1} (6B).

This was not performed for this experiment as a small amount of solid (not measured) was dissolved in dichloromethane for the IR spectra, and this means percent yield would only be representative of the unmeasured product in the vial, not the entire product formed in reaction.

Green Chlorination of $Os_3(CO)_{12}$ to form $Os_3(CO)_{12}Cl_2$

In previous work, chlorine intermediates converted to bisethoxide in higher yields than iodine or bromine.[16,17] The toxicity of chlorine gas was a limitation, and so a procedure was developed to generate chlorine gas in situ. This reaction was monitored through IR as the $Os_3(CO)_{12}$ starting material shows the characteristic four peaks of the cluster's carbonyl symmetry, figure 50.

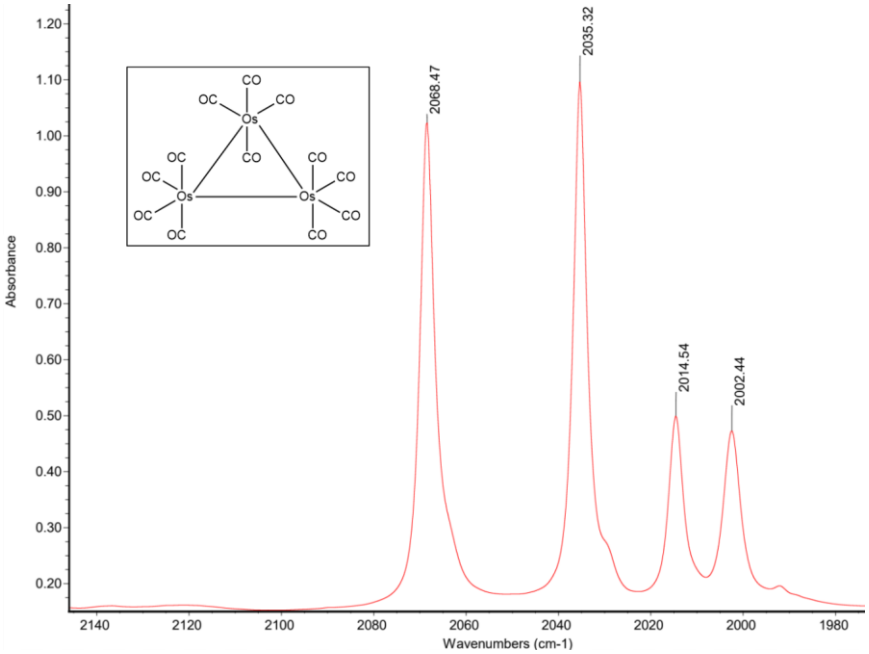

Figure 50: $Os_3(CO)_{12}$ infrared spectra in dichloromethane (bw030).

This is important to note as the chlorinated product differs in symmetry, and thus IR spectra.

Method 1: dichloromethane as a solvent

The first attempt utilized dichloromethane as a solvent at room temperature as outlined by Wright and Hallstorm.[19] After 1.8mL of NaOCl was added, IR confirmed complete conversion to $Os_3(CO)_{12}Cl_2$ with peaks at 2001, 2030, 2063, and 2120cm^{-1}, figure 44.

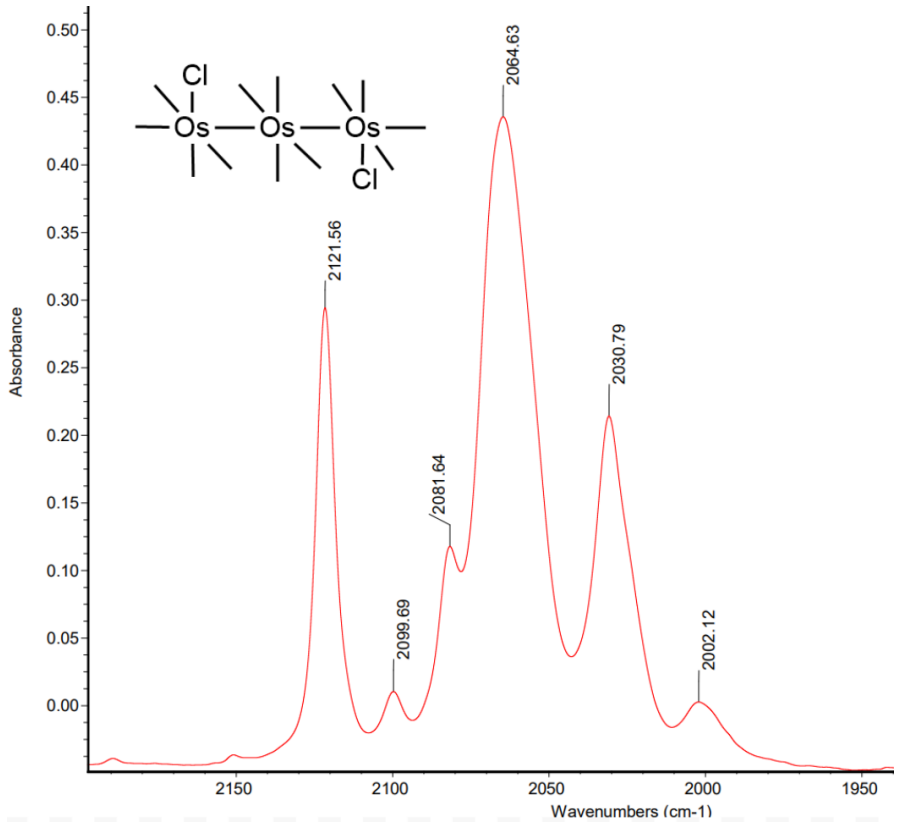

Figure 44: IR of $Os_3(CO)_{12}Cl_2$ product after liquid extraction in proving conversion with few impurities (bw018)

Although conversion was successful, this proved more difficult to separate as a pure product than the first procedure as $Os_3(CO)_{12}Cl_2$ is soluble in dichloromethane. Additionally, the reaction did not have a qualitative end point as it would if the product precipitated, so IR was taken continuously after each NaOCl addition, so a reaction in cyclohexane was preferred. However, there is a safety issue with HCl under reflux, and so this was taken into account when adapting the procedure moving forward.

Method 2: cyclohexane as a solvent

This method to attach chlorine ligands was built from Fukuyama et. al's work with a rapid in situ chlorination, but was adapted by first generating Cl_2 in a separate flask and then bubbling in wet chlorine gas.[18] This scheme is seen in figure 51 below.

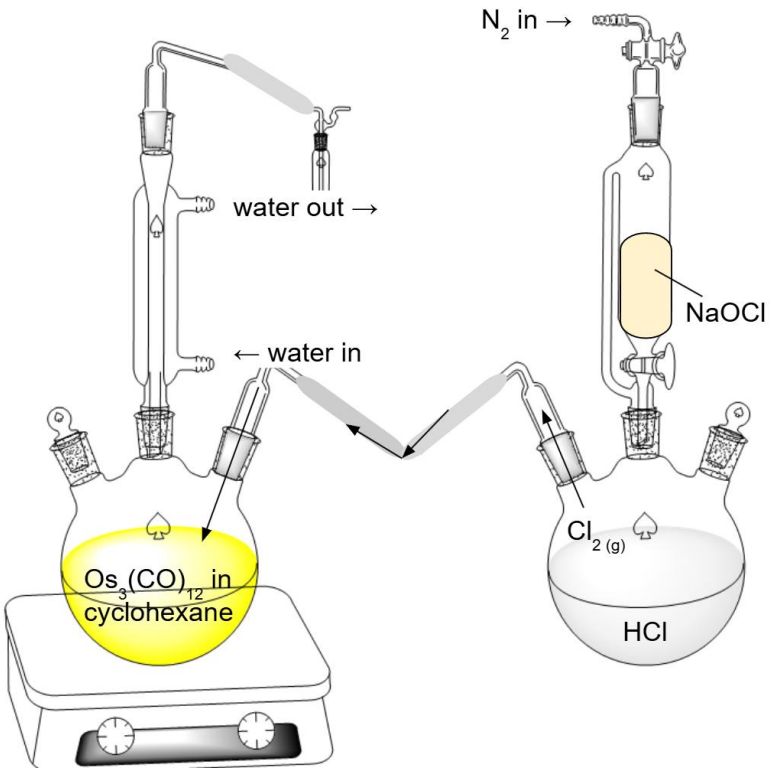

Figure 51: scheme of $Os_3(CO)_{12}$ chlorination.

This method proved successful as the product completely precipitated out of solution, identified by an IR of the solution showing only cyclohexane and no evidence of $Os_3(CO)_{12}$. The solid was removed using a pipet, left to dry, resulting in a high yield of around 90%, calculated by weight, with few impurities. This product was dissolved in dichloromethane to obtain IR, figure 45.

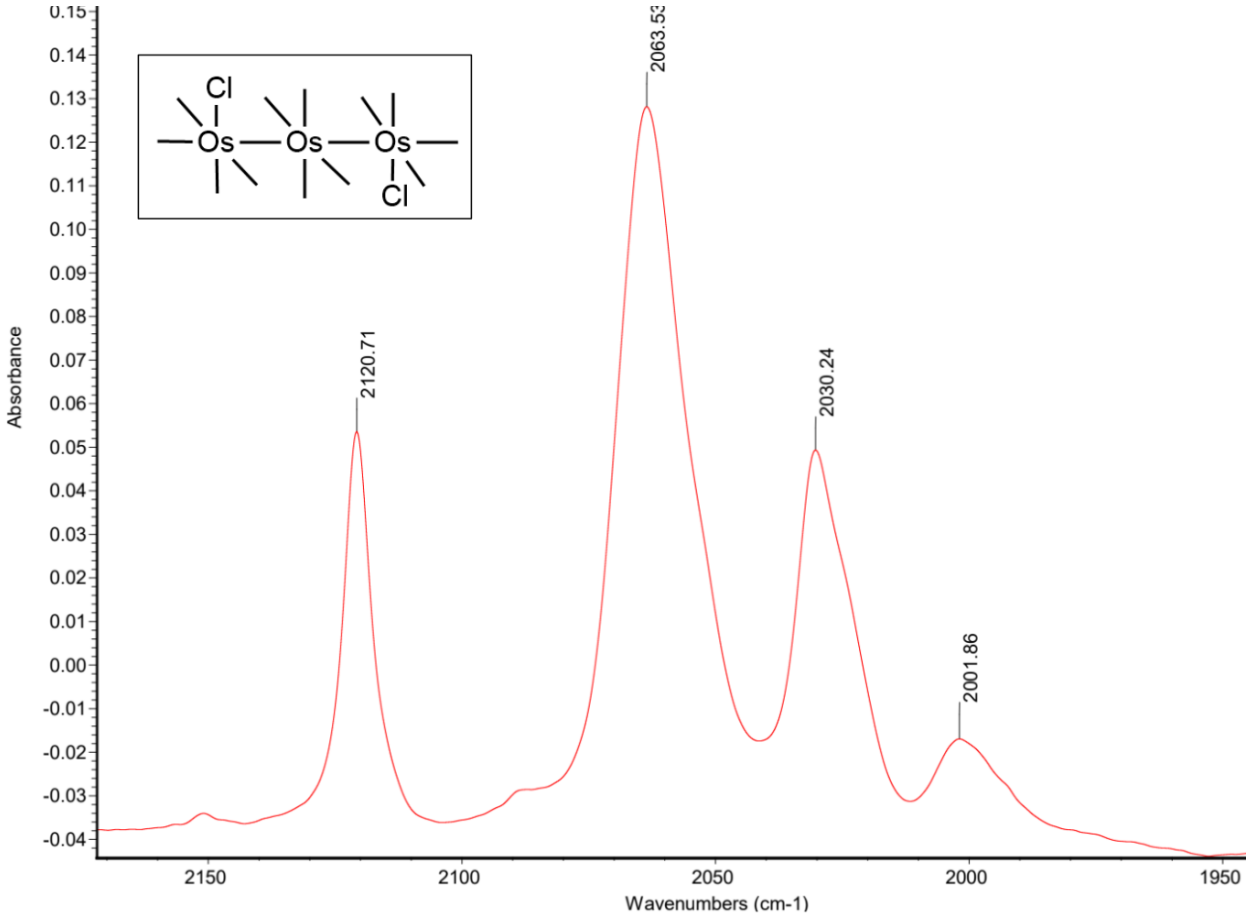

Figure 45: IR of isolated precipitate in CH_2Cl_2 proving complete conversion to $Os_3(CO)_{12}Cl_2$ (bw030).

This IR shows the four peaks: 2120, 2084, 2063, and 2029cm^{-1}, these wavenumbers and pattern represent the symmetry of this cluster differing from $Os_3(CO)_{12}$. The absence of any $Os_3(CO)_{12}$ peaks shows complete conversion. An IR of the solvent also proved complete transformation as it revealed only cyclohexane present.

Conclusions

From this work, it was determined that d-DMSO is a useful solvent for identifying isomer signals of $Os_2(CO)_6(R\text{-}CONH)_2$ (R=Ph, Ph-NO_2).

It was concluded the benzamide isomers interconverted with a final H,H:H,T ratio (112 hours at room temperature) of 43.7:56.3, favoring the H,T isomer. The nitrobenzamide isomers interconvert with a final H,H:H,T ratio (212 hours at room temperature) of 87.3:12.7, favoring the H,H isomer. This is consistent with results found by Mullen (nitrobenzamide) and Marak (benzamide). [11,23]

To observe a trend, this data was compared to Costa's work with the acetamide monomer: $Os_2(CO)_6(CH_3CONH)_2$.[12] Costa found the 110°C H,H:H,T ratio is 48:52, and the interconversion at RT resulted in a final ratio of 34:66, table 9.

Table 9: isomer interconversion summary

	Nitrobenzamide	**Benzamide**	**Acetamide: Sarah Costa**[12]
Favored isomer at 110°C	H,H	H,H	H,T
Favored isomer at RT	H,H	H,T	H,T

To hypothesize this observed difference, it must be noted that there is an addition of an electron withdrawing NO_2 group in nitrobenzamide. This pulls electron density from the carbonyl, making it more favorable to coordinate in the H,H configuration which allows for the two nitrogens opposite the oxygens to push electron density onto the oxygens, stabilizing the molecule, figure 52.

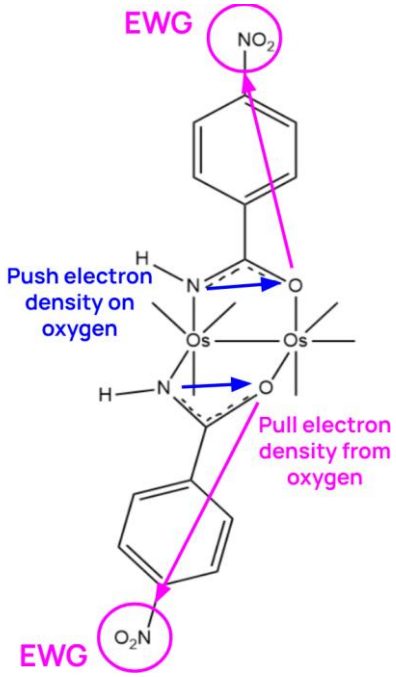

Figure 52: describing effect of NO_2 EWG on overall isomer stability of $Os_2(CO)_6(Ph\text{-}NO_2CONH)_2$

These ratios were determined by integration in NMR with d-DMSO solvent. The H,T and H,H NH signals of $Os_2(CO)_6(Ph\text{-}NO_2CONH)_2$ come around 9.5ppm and 9.2ppm, respectively. The H,T and H,H NH signals of $Os_2(CO)_6(PhCONH)_2$ come around 9.1ppm and 9.0ppm, respectively. Additionally, in d-DMSO, it was found that the nitrobenzamide's H,T isomer is less soluble, and so more work needs to be done on accuracy of the isomer ratios, but the interconversion results remain valid.

The H,T coordinated NH is more downfield than the H,H, although the molecule is more polar on TLC. This is as the coordinated hydrogen is opposite an oxygen, creating a partial positive on the nitrogen. The overall molecule, however, has a more symmetric pull than the H,H does, as the latter has a larger overall dipole, illustrated in figure 53.

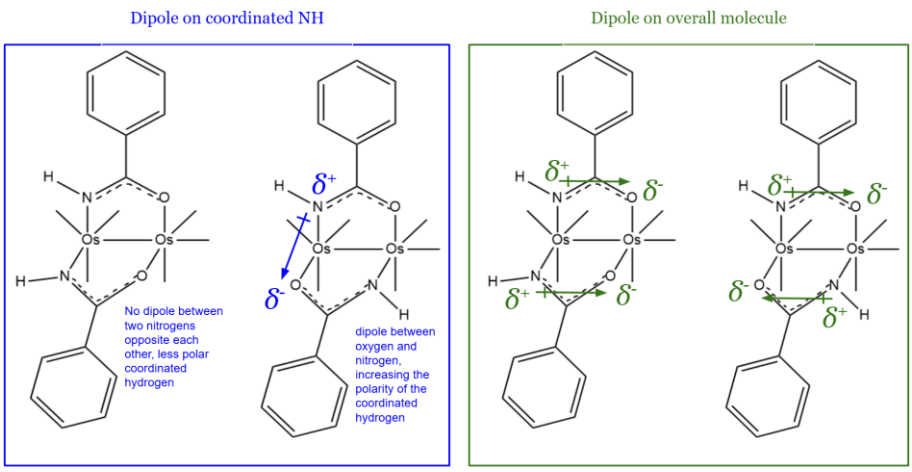

Figure 53: highlighting the differences in polarity when looking at the coordinated NH than the overall molecule. This is shown in benzamide, but the same logic holds through to nitrobenzamide

Separation from prepTLC was not entirely successful in this study, and further work could be done with column chromatography and different solvent systems to increase success of this technique. However, it is not necessary for interconversion studies as both isomers appear at distinctly different chemical shifts in NMR.

In both benzamide and nitrobenzamide, the polymer can be formed through extended reaction time, especially with an excess of the amide or wet solvent. This can be identified through IR as an intense peak will begin to appear around 2020-2030 cm^{-1}, and so it is critical to monitor these reactions in short intervals of time. The polymer proves difficult to reverse once the starting material has converted fully, but, if identified early enough, short cycles of 1. Refluxing reaction mixture to convert starting material to polymer (~10min) and 2. Addition of carbon monoxide gas at room temperature to convert polymer to monomer (~15min) is a successful method to reverse the polymerization. The $CO_{(g)}$ can remain on for as long as needed, as it does not convert the

monomers back to starting material. This polymer formation can be seen, in both benzamide and nitrobenzamide, from IR peaks appearing around 2020 and 1950cm^{-1}.

NMR analysis on reaction mixtures containing mainly polymer, identified by IR spectra, revealed a strong signal at 5.7ppm. This signal is very weak in NMR spectra of the monomers, and there was no change in the 5.7ppm integration over time, which would be to be expected of the polymer, table 10.

Table 10: Summary table of all work

	Nitrobenzamide	Benzamide	Polymer (nitrobenzamide and benzamide have same properties)
NMR signals of interest in d-DMSO H,H H,T	9.2ppm 9.5ppm	9.0ppm 9.1ppm	5.7ppm
Initial ratio (110^{o}C) H,H:H,T	70.7:29.3	88.5:11.5	x
Final ratio (RT) H,H:H,T	87.3:12.7	43.7:56.3	x
Favored isomer at 110^{o}C	H,H	H,H	x
Favored isomer at room temperature	H,H	H,T	x
Reaction conditions	110^{o}C Dry toluene 360 minutes Molar equivalence	110^{o}C Dry toluene 240 minutes Molar equivalence	110^{o}C Initial formation 15 minutes into reflux with wet solvent

Polymer formation + reversal	Small polymer formation at 360 minutes Reversal not attempted, but likely can be achieved similarly to benzamide	Formation 15 minutes into reflux with wet solvent 240 minutes with molar excess benzamide Reversible with rounds of $CO_{(g)}$ if begun once IR peak is first seen	
IR peaks of interest in toluene	2091, 2056, 2998, 1979cm^{-1}	2088, 2051, 1994 1976cm^{-1}	2020, 1950cm^{-1}

References

(1) Cowan, J. A. Transition Metals as Probes of Metal Cofactors in Nucleic Acid Biochemistry. *Comments on Inorganic Chemistry* **1992**, *13* (5), 293–312. https://doi.org/10.1080/02603599208048465.

(2) Kennelly, P. J. The Biochemical Roles of Transition Metals. In *Harper's Illustrated Biochemistry, 31e*; Rodwell, V. W., Bender, D. A., Botham, K. M., Kennelly, P. J., Weil, P. A., Eds.; McGraw-Hill Education: New York, NY, 2018.

(3) Housecroft, C. E.; Sharpe, A. G. Physical Properties: Effects of the Lanthanoid Contraction. In *Inorganic Chemistry*; Pearson Education Inc, 2018; pp 806–809.

(4) Pyper, K. J.; Jung, J. Y.; Newton, B. S.; Nesterov, V. N.; Powell, G. L. Reactions of Os3(CO)12 with Carboxylic Acids in a Microwave Reactor; Synthesis of Os2(Benzoate)2(CO)6, a Dinuclear Osmium(I) Compound with Aromatic Carboxylate Ligands. *Journal of Organometallic Chemistry* **2013**, *723*, 103–107. https://doi.org/10.1016/j.jorganchem.2012.09.014.

(5) Sommerhalter, R. New Synthetic Approaches to Triosmium Decacarbonyl Bisethoxide and the Systematic Design of Linked Triosmium Clusters via Bridging Diols, Drew University, 2016.

(6) Shah, A.; Crotty, J. Drew University, 2010.

(7) Fortna, C. Kinetics and Mechanism of Carbonyl Substitution of Os3(CO)10(μ-I)2 by P(OR)3, Drew University, 2022.

(8) Barnum, T. Synthesis and Theoretical Analysis of Dibridged Triosmium Carbonyl Clusters, Drew University, 2013.

(9) Schmitt, L. Steric Effects on the Reactions of Triosmium Dodecacarbonyl Bisethoxide and Carboxylic Acids, Drew University, 2013.

(10) Crooks, G. R.; Johnson, B. F. G.; Lewis, J.; Williams, I. G.; Gamlen, G. Chemistry of Polynuclear Compounds. Part XVII. Some Carboxylate Complexes of Ruthenium and Osmium Carbonyls. *J. Chem. Soc., A* **1969**, 2761. https://doi.org/10.1039/j19690002761.

(11) Marak, K. Some Reactions of Triosmium Decacarbonyl Bisethoxide, Os3(CO)10(M2 -OEt)2, with Amides, Drew University, 2017.

(12) Costa, S. Reactivity of Os2(CO)6(RCONH)2: Mechanisms and Thermodynamic Properties, Drew University, 2019.

(13) Burya, S. J.; Palmer, A. M.; Gallucci, J. C.; Turro, C. Photoinduced Ligand Exchange and Covalent DNA Binding by Two New Dirhodium Bis-Amidato Complexes. *Inorg. Chem.* **2012**, *51* (21), 11882–11890. https://doi.org/10.1021/ic3017886.

(14) Neumann, F.; Suess-Fink, G. Binuclear Ruthenium Clusters with Nitrogen and Oxygen-Containing Chelate Bridges: Conversion of M2-H2-Pyrazolate Ligands into M1-H1-Pyrazole Ligands by Reactions with Carboxylic Acids. In *Journal of Organometallic Chemistry*; Elsevier, 1989; Vol. 367.

(15) Parker, M. Reactions of and Synthetic Approaches to Os3(CO)10(OEt)2, and the Kinetics of Osmium Carbonyl Clusters Using Triphenyl Phosphite, Drew University, 2007.

(16) Baum, B. An Investigation of the Kinetics of the Disubstitution Reaction of Triosmium Complexes of Tyle Os3(CO)10(X)2 with Trimethyl Phosphite, Drew University, 2004.

(17) Cavaliere, V. Substitution Kinetics of Dihalo-Bridged Triosmium Complexes, Drew University, 2006.

(18) Fukuyama, T.; Tokizane, M.; Matsui, A.; Ryu, I. A Greener Process for Flow C–H Chlorination of Cyclic Alkanes Using in Situ Generation and on-Site Consumption of Chlorine Gas. *React. Chem. Eng.* **2016**, *1* (6), 613–615. https://doi.org/10.1039/C6RE00159A.

(19) Wright, S. W.; Hallstrom, K. N. A Convenient Preparation of Heteroaryl Sulfonamides and Sulfonyl Fluorides from Heteroaryl Thiols. *J. Org. Chem.* **2006**, *71* (3), 1080–1084. https://doi.org/10.1021/jo052164+.

(20) Pyper, K. J.; Kempe, D. K.; Jung, J. Y.; Loh, L.-H. J.; Gwini, N.; Lang, B. D.; Newton, B. S.; Sims, J. M.; Nesterov, V. N.; Powell, G. L. Microwave Promoted Oxidative Addition Reactions of Os3(CO)12: Efficient Syntheses of Triosmium Clusters of the Type Os3(μ-X)2(CO)10 and Os3(μ-H)(μ-OR)(CO)10. *J Clust Sci* **2013**, *24* (3), 619–634. https://doi.org/10.1007/s10876-012-0532-5.

(21) Johnson, B. F. G.; Lewis, J.; Pippard, D. A. The Preparation, Characterisation, and Some Reactions of [Os3(CO)11-(NCMe)]. *J. Chem. Soc., Dalton Trans.* **1981**, No. 2, 407. https://doi.org/10.1039/dt9810000407.

(22) Perry, P. The Synthesis and Analysis of Triosmium Carbonyl Clusters with Potential Biological Activity, Drew University, 2022.

(23) Mullen, A. Ethoxide Substitution Reactions of Os3(CO)10(OEt)2 with Diols and Amides, Drew University, 2019.

Appendix

Table 1: reaction summaries of bisethoxide and bidentate ligands (A) and further information on benzamide isomer interconversion post TLC seperation (B) as studied by Katie Marak in 2017.

1A:

Bidentate ligand	Solvent and temperature	Ratio (H,H:H,T)	Interconversion over one month
CH_3CONH_2	Toluene 110°C	52:48	D_2O exchange is slow and H,T is exchanging at faster rate than H,H
$PhCONH_2$	Toluene 110°C	39:61	Isomers interconvert in solution

1B:

	Solution A		Solution B	
	H,H	**H,T**	**H,H**	**H,T**
Initial (110°C)	3	97	95	5
Week 3 (RT)	12	88	43	57

Table 2: $CO_{(g)}$ added to crude benzamide reaction mixture

Time (min)	$CO_{(g)}$
0-25	on
25-35	off
35-45	on
45-55	off
55-65	on
65-75	off
75-85	on

Table 3: absorbance of IR peaks of crude reaction mixture as $CO_{(g)}$ is added (at RT) and removed (at 110°C)

		Approximate absorbance of peaks			
Time (min)	**Conditions**	**2069 (starting material)**	**2087 (product)**	**2050 (product)**	**2019 (polymer)**
0-25	$+CO_{(g)}$ *~26°C*	0.45	0.05	0.17	0.20 (slight shoulder)
25-35	Under $N_{2(g)}$ *~110°C*	0.32	0.05	0.13	0.47 (intense peak)
35-45	$+CO_{(g)}$ *~26°C*	0.41	0.06	0.15	0.30 (shoulder)
45-55	Under $N_{2(g)}$ *~110°C*	0.31	0.05	0.13	0.65 (intense peak)
55-65	$+CO_{(g)}$ *~26°C*	0.35	0.30	0.58	0.20 (slight shoulder)
65-75	Under $N_{2(g)}$ *~110°C*	0.50	0.15	0.30	0.52 (intense peak)
75-85	$+CO_{(g)}$ *~26°C*	0.30	0.25	0.48	0.12 (slight shoulder)

Table 4: H,T and H,H $Os_2(CO)_6(PhCONH)_2$ isomer NMR integrations over 112 hours

Time (hours)	**H,T integration (9.1ppm)**	**H,H integration (9.0ppm)**	**H,H:H,T**
0	0.0569	0.0074	88.5:11.5
16	0.044	0.0093	82.6:17.4
42	0.0347	0.0122	74.1:25.9
63	0.0197	0.0152	56.5:43.5

85	0.0159	0.0166	49:51
112	0.0156	0.0199	43.7:56.3

Table 5: HNMR data collected over nine days of crude nitrobenzamide product

Time (hours)	H,H integration	H,T integration	H,H:H,T	Total peak area
19	0.0135	0.0056	70.7:29.3	0.0191
42	0.0148	0.0046	76.3:25.7	0.0194
67	0.0159	0.0041	79.5:20.5	0.0200
86	0.0155	0.0036	81.2:18.8	0.0191
116	0.0149	0.0031	82.8:17.2	0.0180
160	0.0145	0.0024	85.8:14.2	0.0169
187	0.0146	0.0023	86.4:13.6	0.0169
213	0.0144	0.0021	87.3:12.7	0.0165

Table 6: IR analysis of 2114cm^{-1} peak area and height

Flask	Molarity	Peak Area	Peak Height
1	0.000862	0.1405	0.0263
2	0.000690	0.1178	0.0225
3	0.0005172	0.0785	0.0160
4	0.0003448	0.0466	0.0107
5	0.0001724	0.0246	0.0060
6	0.0000862	too dilute	too dilute

Table 7: amount of reactants added each temperature for $Os_3(CO)_{10}I_2$ microwave synthesis

Temperature	$Os_3(CO)_{12}$ added	I_2 added
155	51.7mg (0.0570mmol)	14.6mg (0.0575mmol)
160	51.4mg (0.0567mmol)	14.2mg (0.0560mmol)
165	51.9mg (0.0572mmol)	14.7mg (0.0579mmol)

Table 8: $Os_3(CO)_{10}(I)_2$ product post microwave 2110:2069 IR peak area with varying temperatures

Temperature (°C)	**2110 area $Os_3(CO)_{10}I_2$ product**	**2069 area $Os_3(CO)_{12}$ starting material**	**Ratio of 2110:2069**
150	0.270	0.460	1:1.703
155	0.371	1.210	1:3.26
160	2.174	10.549	1:4.85
165	1.820	4.746	1:2.608

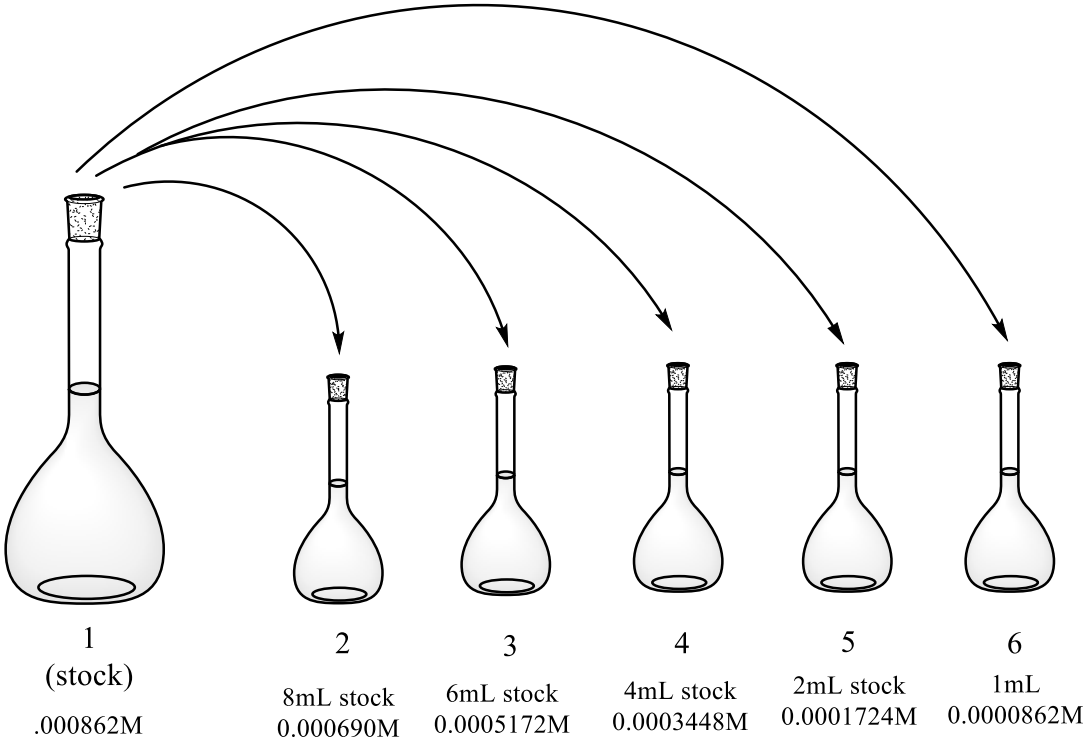

Figure 42: Parallel dilution of $Os_3(CO)_{12}I_2$

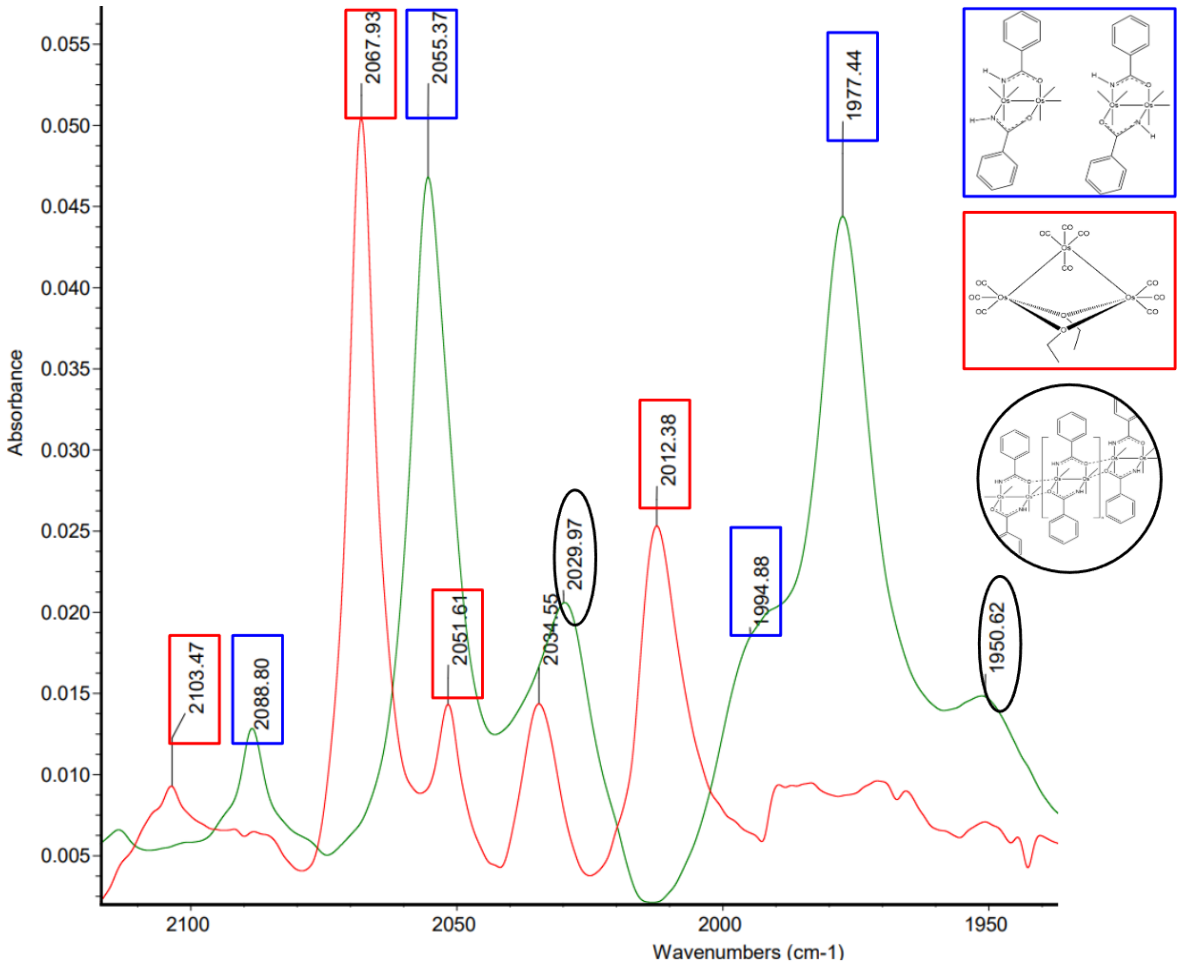

Figure 24: green spectrum = mixture of $Os_2(CO)_6(PhCONH)_2$ product (blue rectangle) in CH_2Cl_2 with slight polymer impurity (black circle) at 2029cm^{-1} (bw021) compared to red spectrum = bisethoxide starting material (red squares).

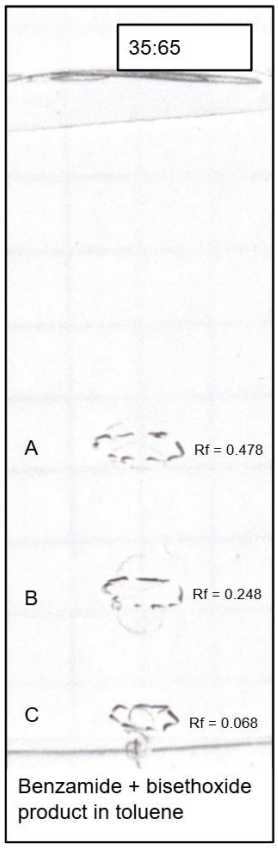

Figure 25: spot TLC in 35% ethyl acetate solvent system of $Os_2(CO)_6(PhCONH)_2$ in toluene (bw021)

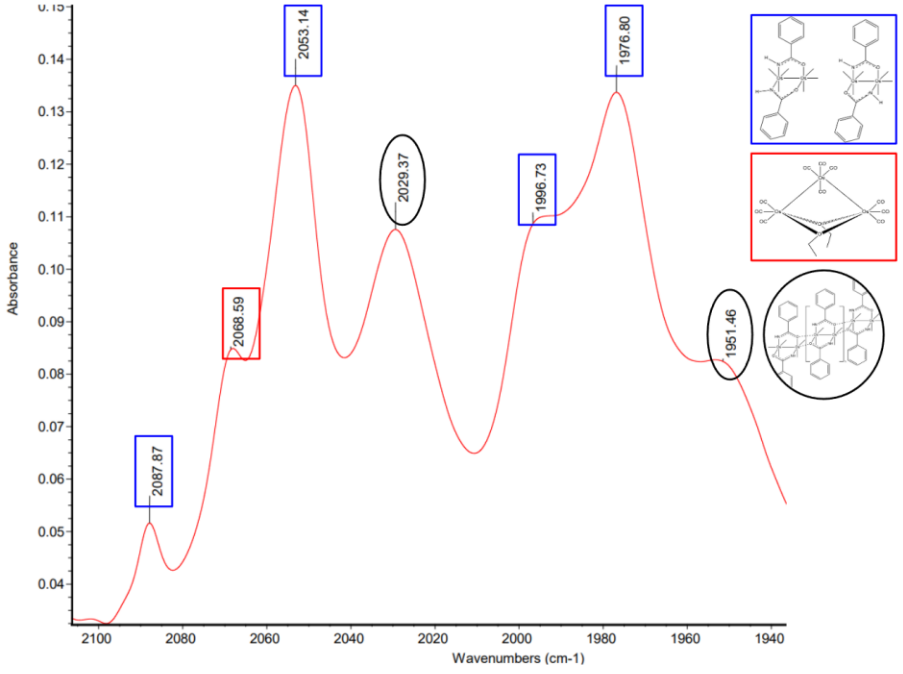

Figure 26: product A from prepTLC in $CHCl_2$, revealing polymer (black circle), starting material (red rectangle) and $Os_2(CO)_6(PhCONH)_2$ (blue rectangle) (bwo21)

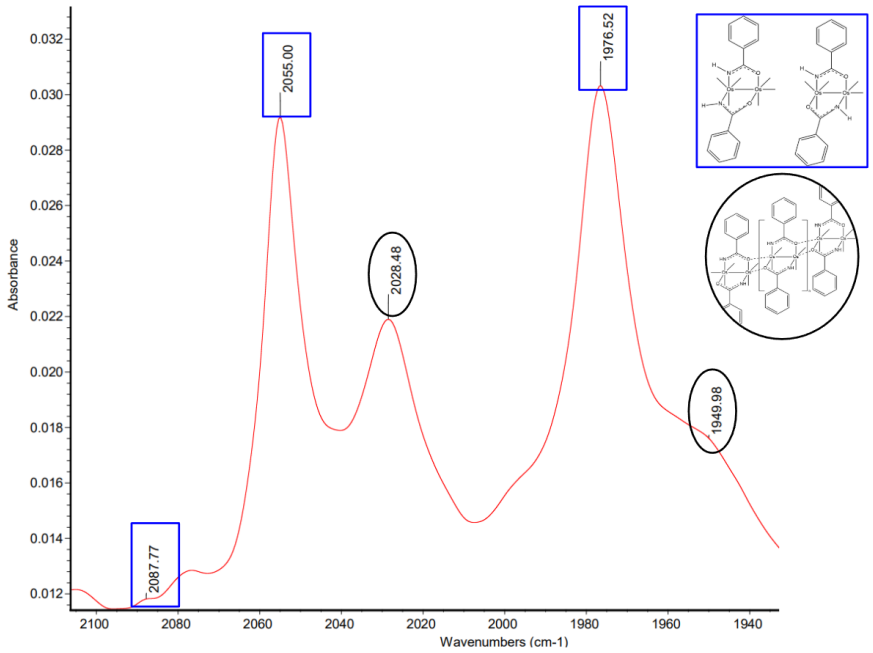

Figure 27: product B from prepTLC in $CHCl_2$, revealing polymer (black circle) and $Os_2(CO)_6(PhCONH)_2$ (blue rectangle) (bwo21)

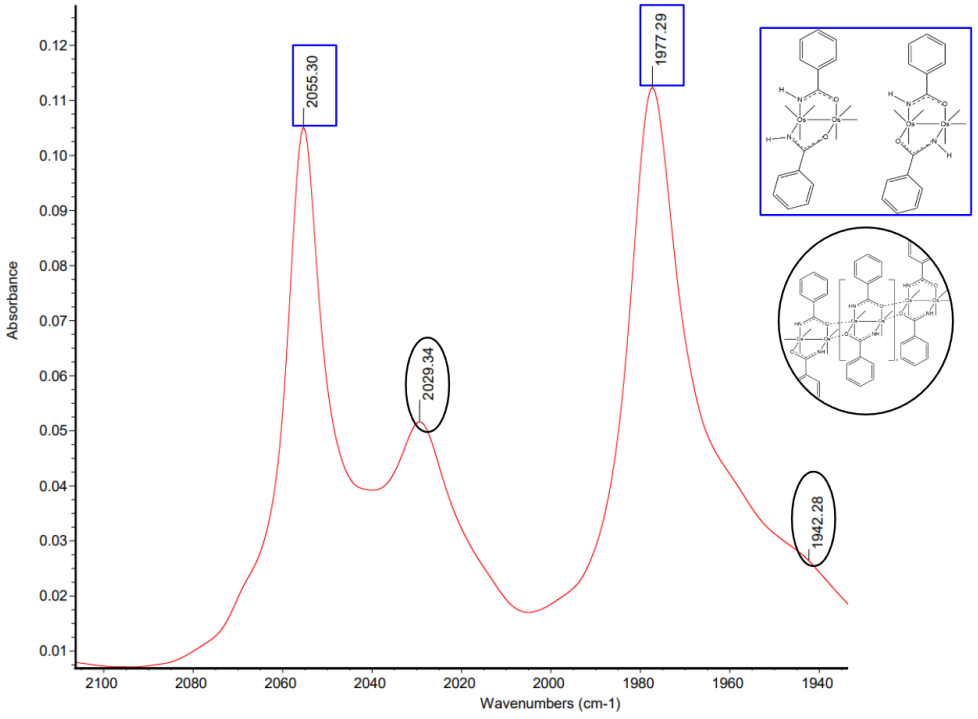

Figure 28: product C from prepTLC in $CHCl_2$, revealing polymer (black circle) and $Os_2(CO)_6(PhCONH)_2$ (blue rectangle) (bw021)

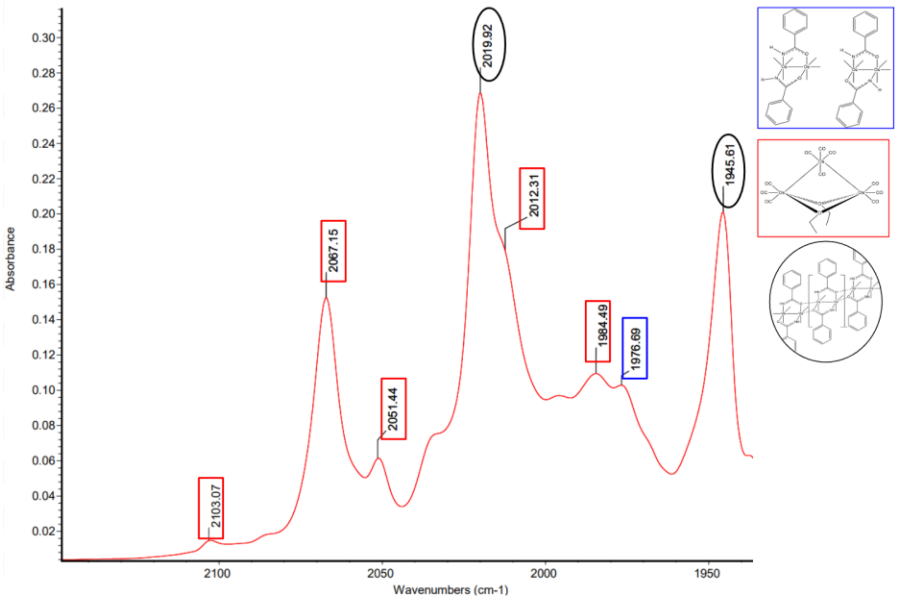

Figure 29: IR of benzamide polymer formation (black circle) catalyzed by water at 80 minutes; $Os_2(CO)_6(PhCONH)_2$ product (blue rectangle), starting material (red rectangle) (bw038)

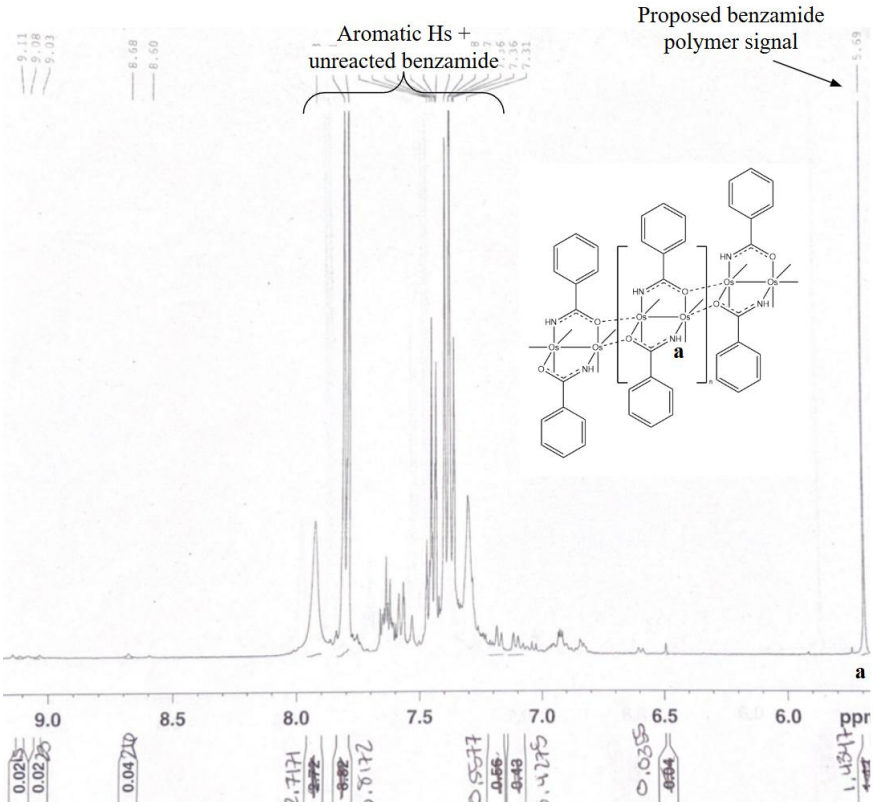

Figure 30: HNMR of benzamide polymer in DMSO (bw038)

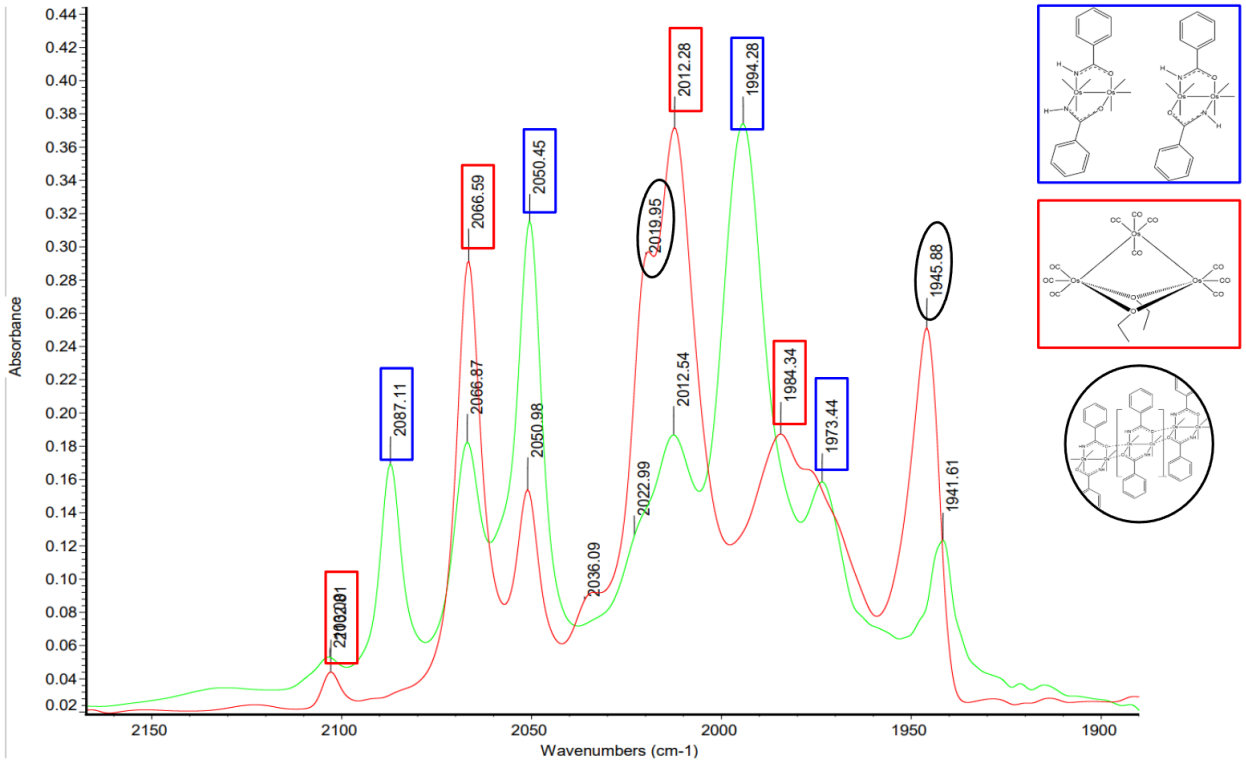

Figure 31: polymer formation (red spectrum) and $Os_2(CO)_6(PhCONH)_2$ monomer after six rounds with carbon monoxide (green spectrum); $Os_2(CO)_6(PhCONH)_2$ product (blue rectangle), starting material (red rectangle), polymer (black circle) (bw040)

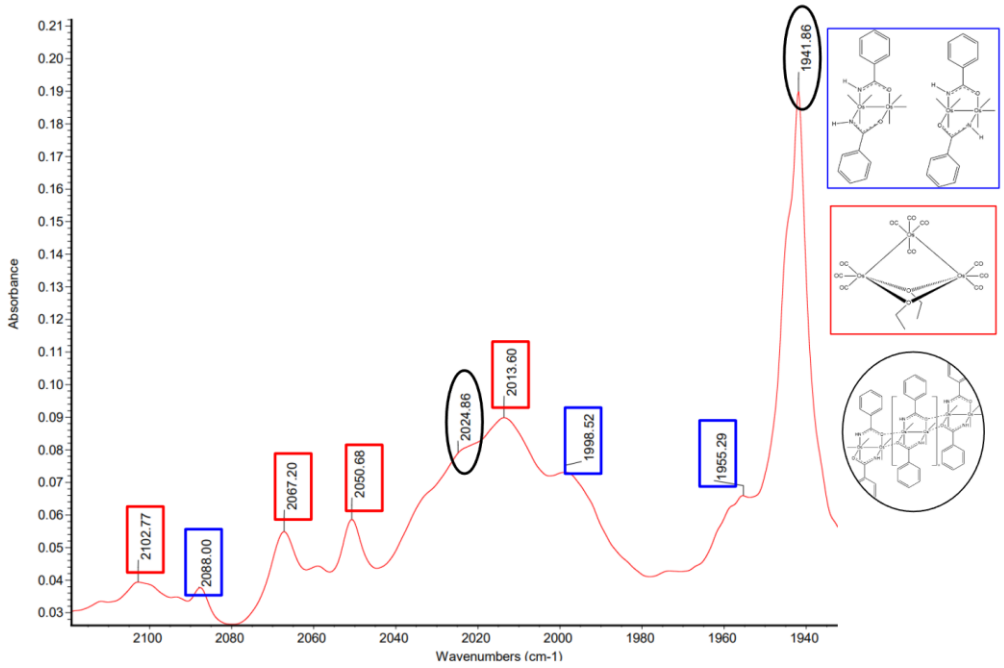

Figure 33: $Os_2(CO)_6(PhCONH)_2$ monomer in toluene after 5 rounds of $CO_{(g)}$ - $Os_2(CO)_6(PhCONH)_2$ product (blue rectangle), starting material (red rectangle), polymer (black circle) (bw044)

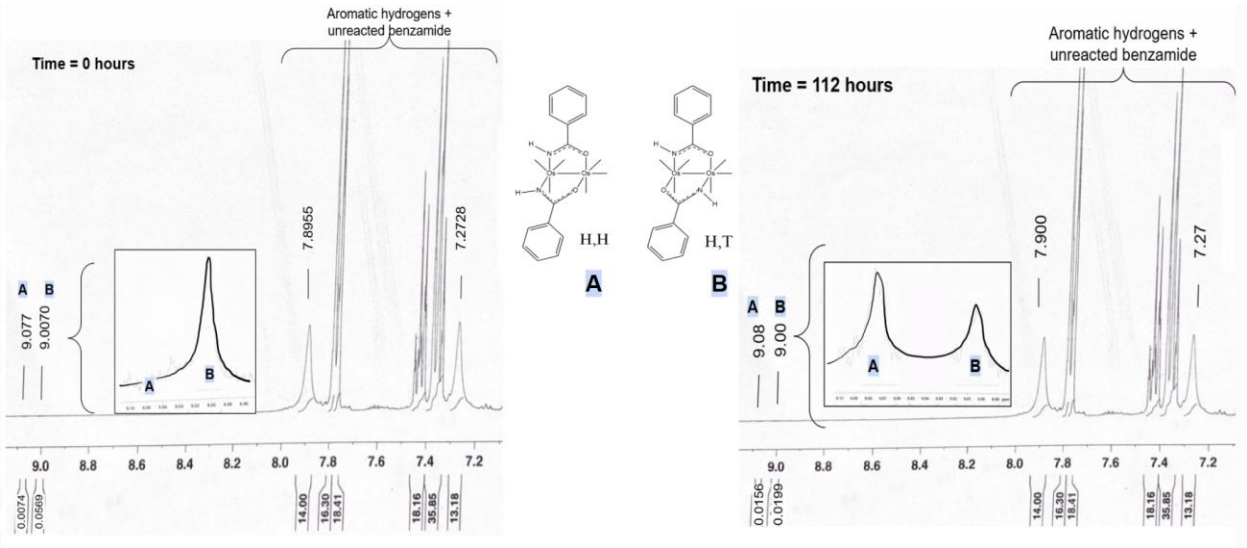

Figure 34: HNMR in DMSO of crude reaction mixture $Os_2(CO)_6(PhCONH)_2$ time 0 vs time 112 hours (bw044).

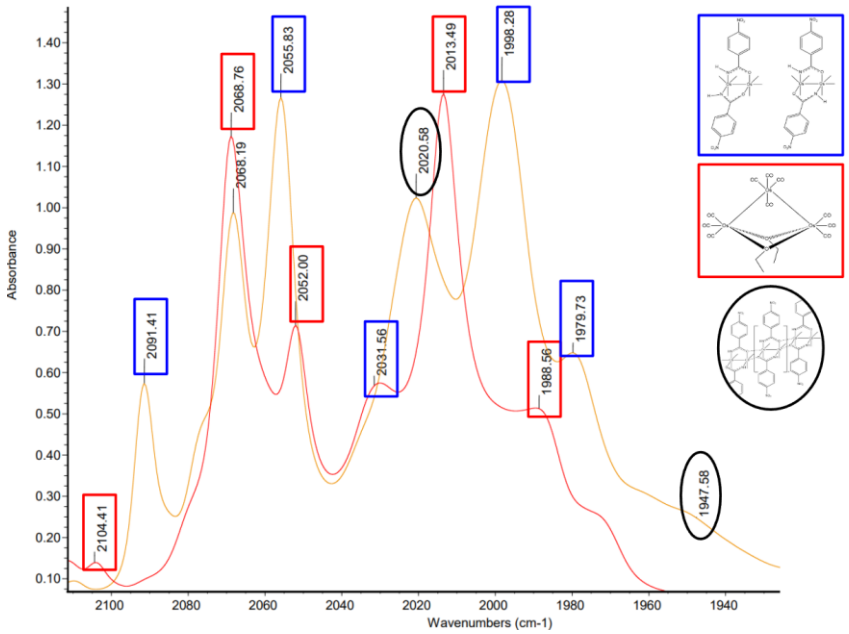

Figure 35: crude reaction mixture of $Os_2(CO)_6(Ph\text{-}NO_2CONH)_2$ in dichloromethane at 360min (purple spectrum) compared to bisethoxide starting material in toluene (red spectrum) with polymer impurity at 2020 and 1947cm^{-1}; $Os_2(CO)_6(PhCONH)_2$ product (blue rectangle), starting material (red rectangle), polymer (black circle) (bw032)

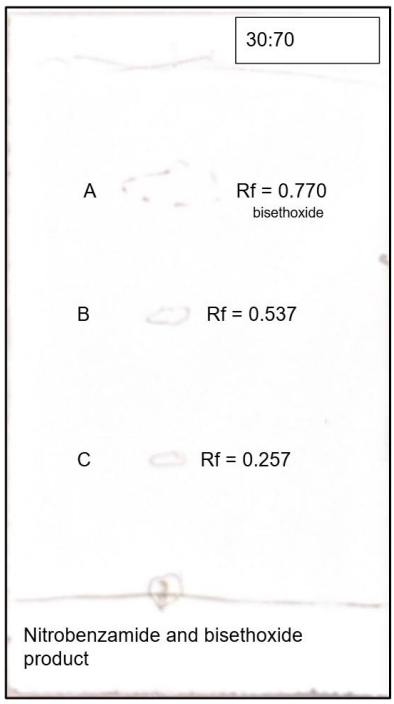

Figure 36: spot TLC of crude $Os_2(CO)_6(Ph\text{-}NO_2CONH)_2$ product at 360 minutes in 30 ethyl acetate:70 hexanes solvent system. Spot C: H,H isomer, spot B: H,T isomer (bw032)

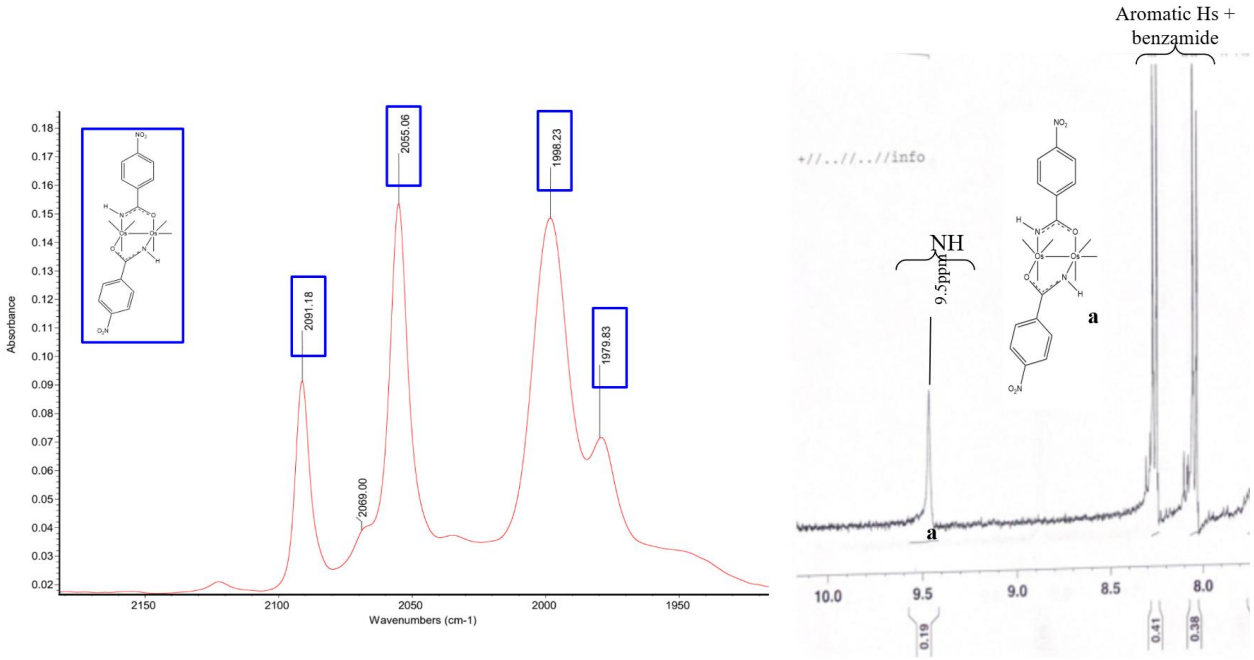

Figure 37: IR spectrum of Product B $Os_2(CO)_6(Ph\text{-}NO_2CONH)_2$ carbonyls (blue rectangle) - (less polar) head-to-tail isomer in 6mL of CH_2Cl_2

^1H NMR of Product B $Os_2(CO)_6(Ph\text{-}NO_2CONH)_2$ from Prep TLC separation in d-DMSO (bw032).

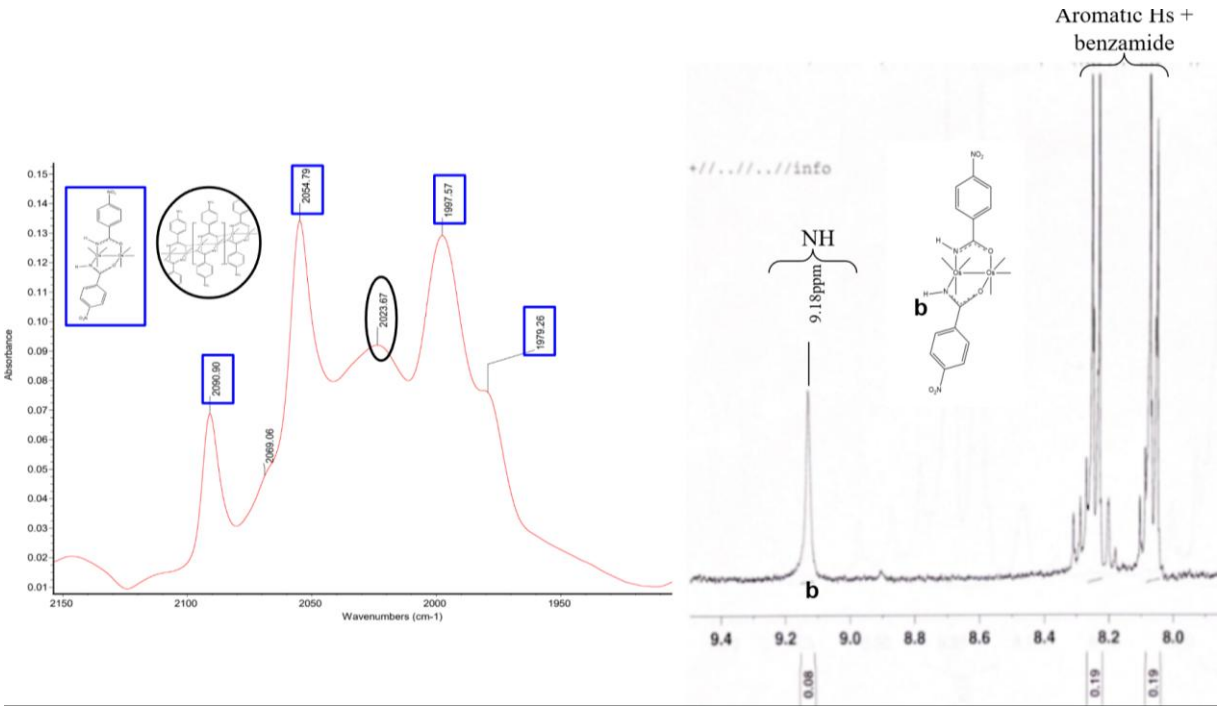

Figure 38: IR spectrum of Product C $Os_2(CO)_6(Ph\text{-}NO_2CONH)_2$ product C carbonyls - (more polar) head-to-head isomer (blue rectangle) in 3mL of CH_2Cl_2 with small starting material shoulder at 2069 and polymer formation at 2023.67 (black circle)

^1H NMR of Product C $Os_2(CO)_6(Ph\text{-}NO_2CONH)_2$ from Prep TLC separation in d-DMSO (bw032).

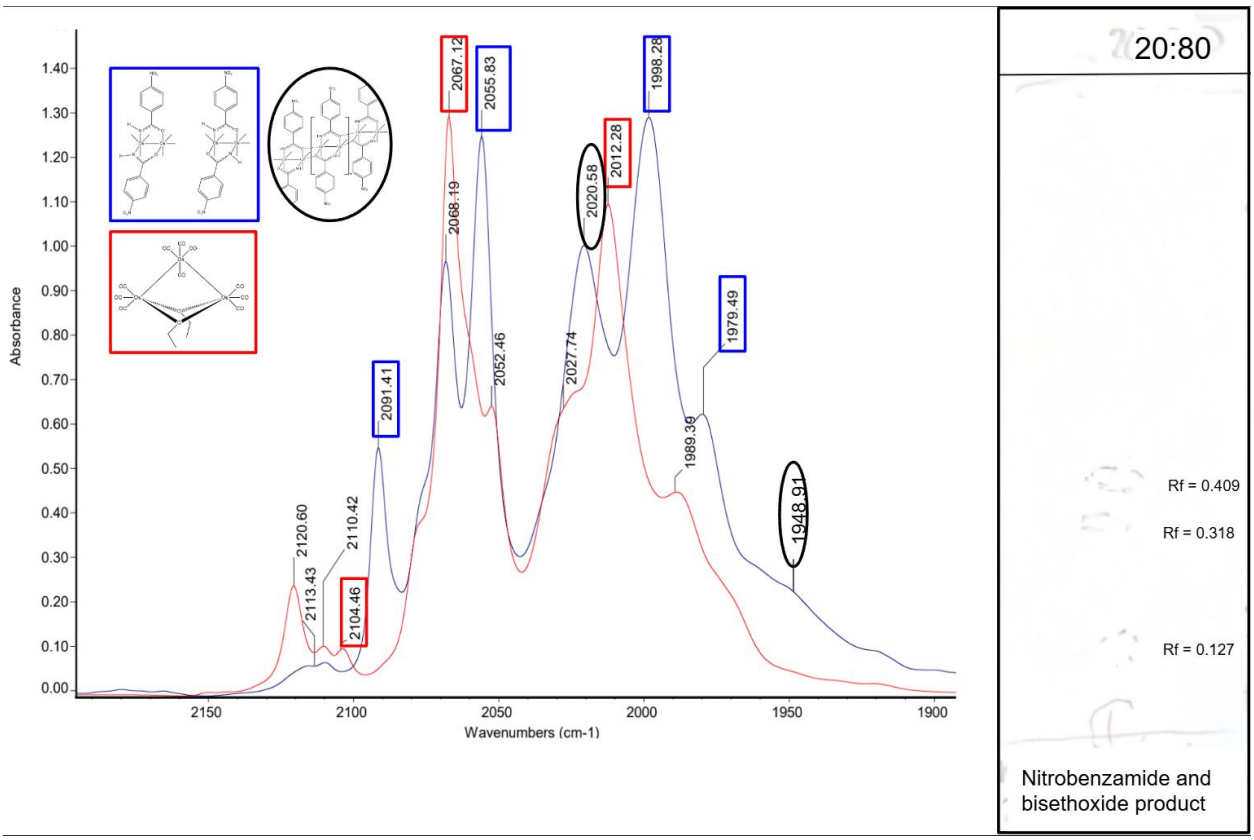

Figure 39: overlaid IR of bisethoxide starting material (red spectrum) and crude $Os_2(CO)_6(Ph\text{-}NO_2CONH)_2$ product (blue spectrum) at 390 minutes, highlighting the decrease of 2012 and 2067 starting material, and formation of polymer at 2020 and 1949cm^{-1}; $Os_2(CO)_6(PhCONH)_2$ product (blue rectangle), starting material (red rectangle), polymer (black circle)

Spot TLC is 20% ethyl acetate solvent system of final $Os_2(CO)_6(Ph\text{-}NO_2CONH)_2$ product (bw034).

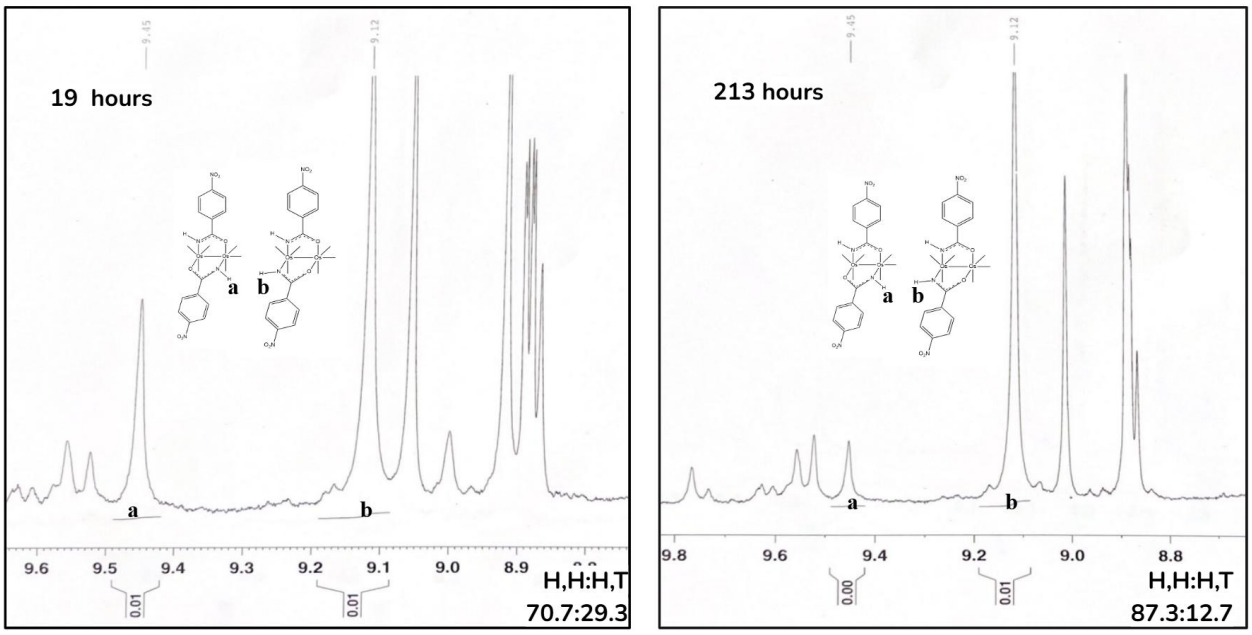

Figure 40: ^{1}HNMR of amide peaks of the two isomers in crude reaction mixture 19 hours on left, 213 hrs on right (bw034).

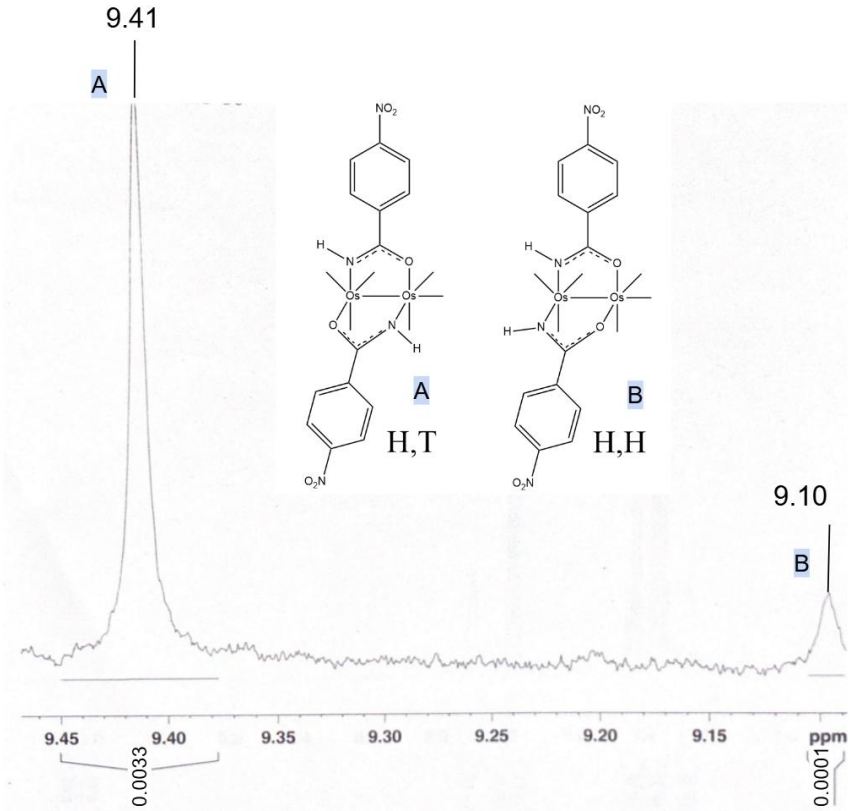

Figure 41: HNMR of insoluble product isolated from crude reaction mixture of $Os_2(CO)_6(Ph\text{-}NO_2CONH)_2$ (bw034).

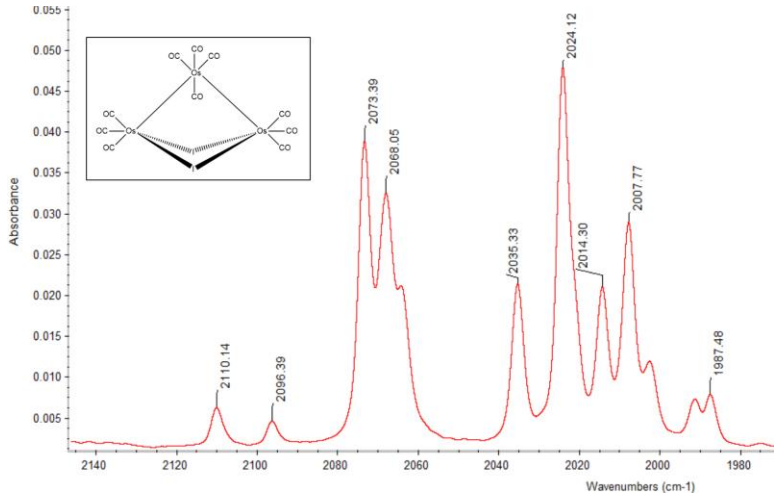

Figure 43: Paxtan Perry $Os_3(CO)_{12}I_2$ post microwave IR used as standard in this experiment: conditions = 150°C, 274 psi, and 300W

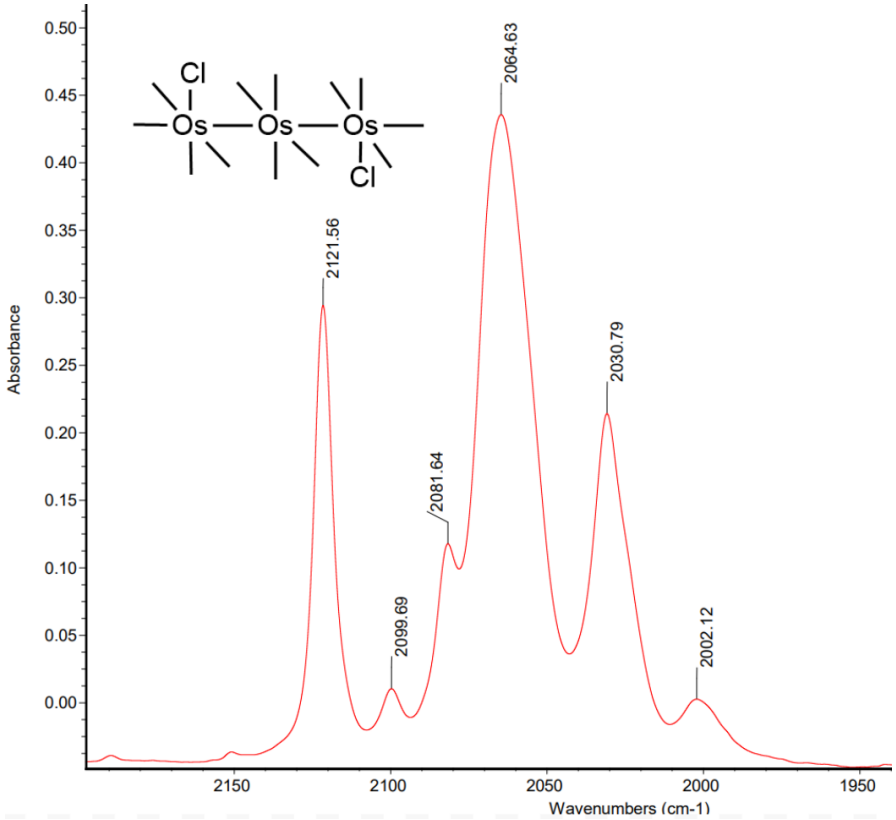

Figure 44: IR of $Os_3(CO)_{12}Cl_2$ product after liquid extraction in proving conversion with few impurities (bw018)

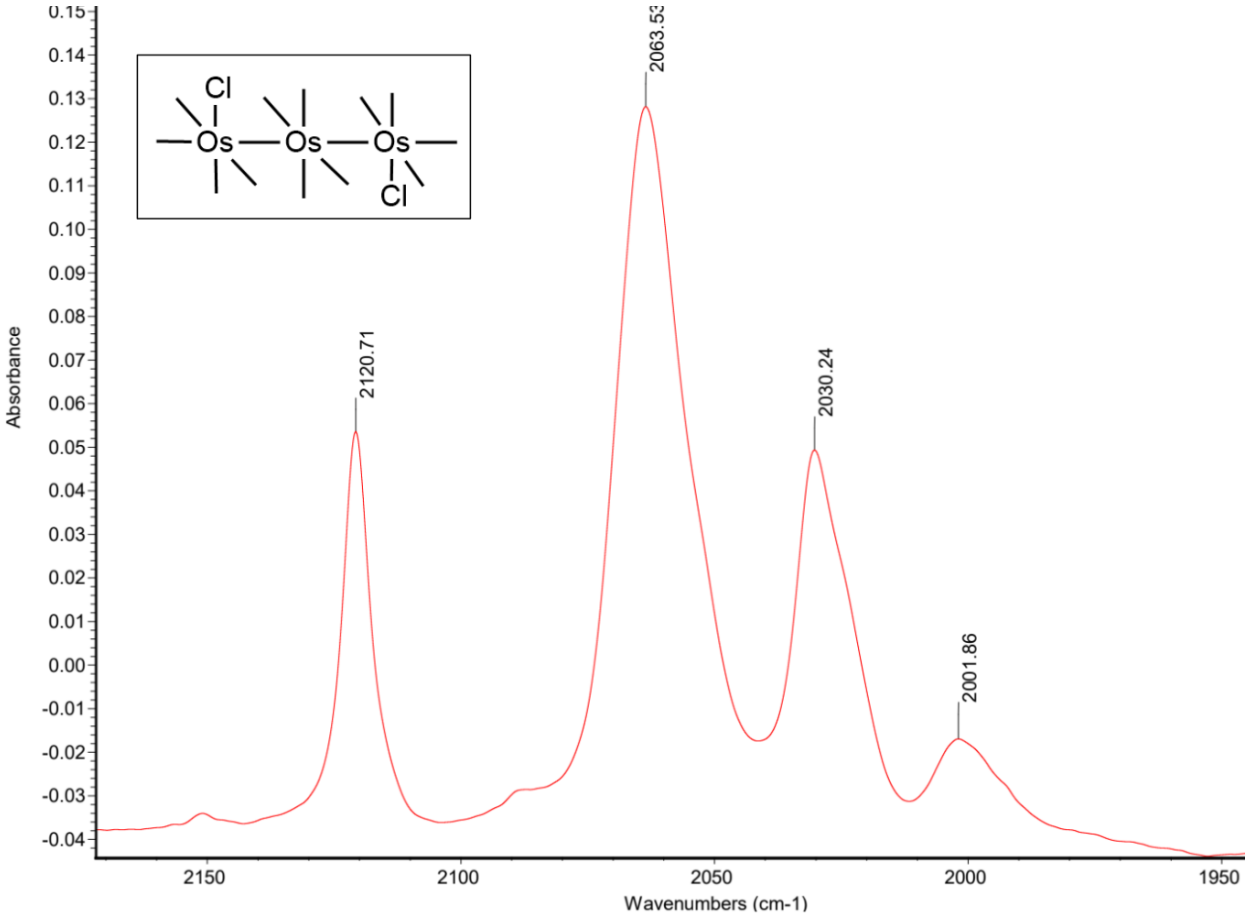

Figure 45: IR of isolated precipitate in CH_2Cl_2 proving complete conversion to $Os_3(CO)_{12}Cl_2$ (bw030).

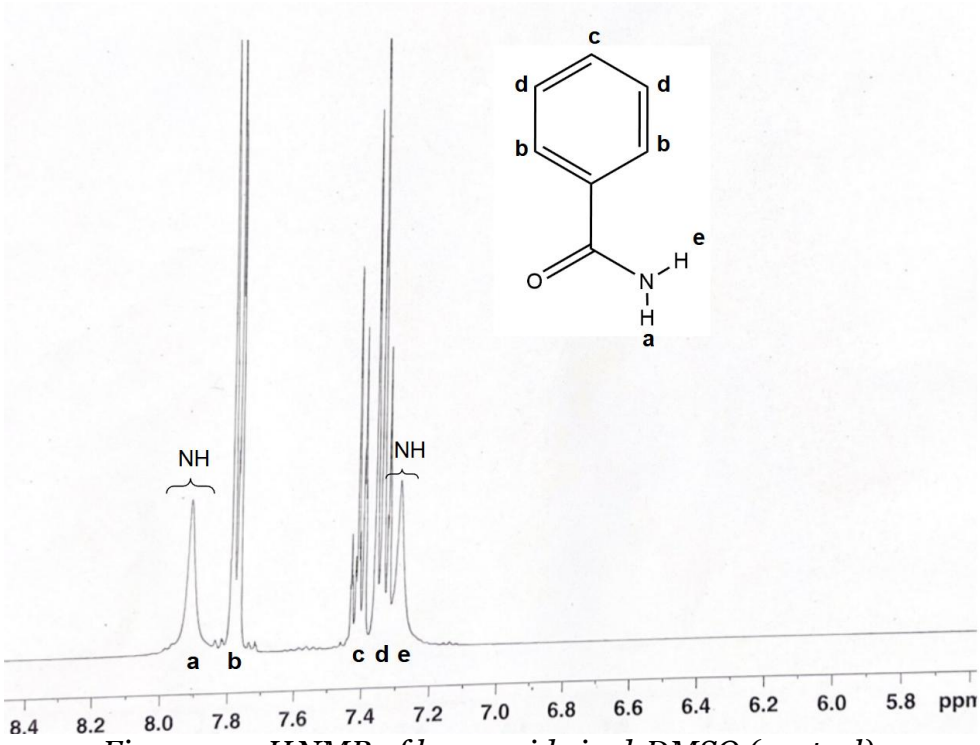

Figure 49: ^{1}HNMR of benzamide in d-DMSO (control).

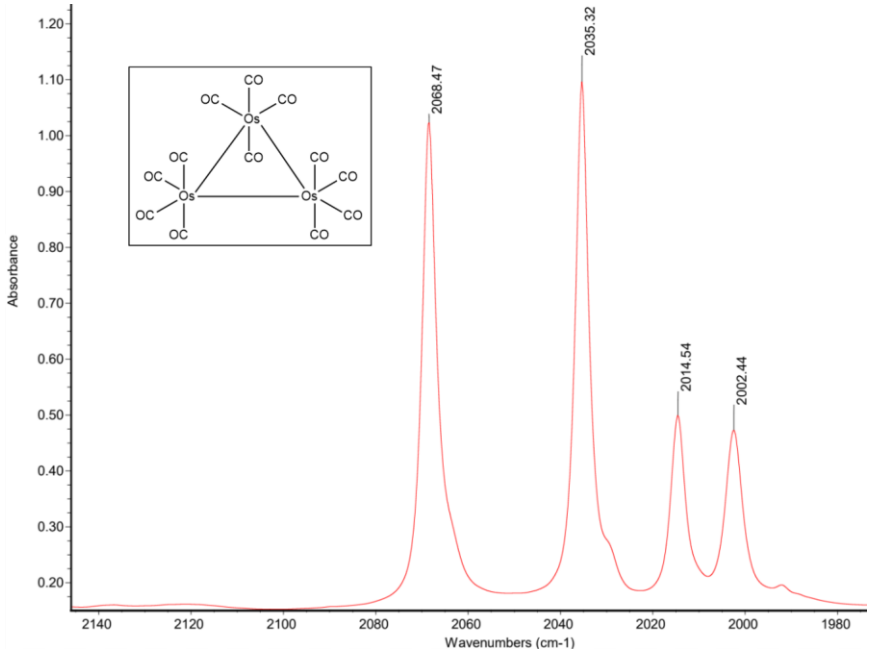

Figure 50: $Os_3(CO)_{12}$ infrared spectra in dichloromethane (bw030).

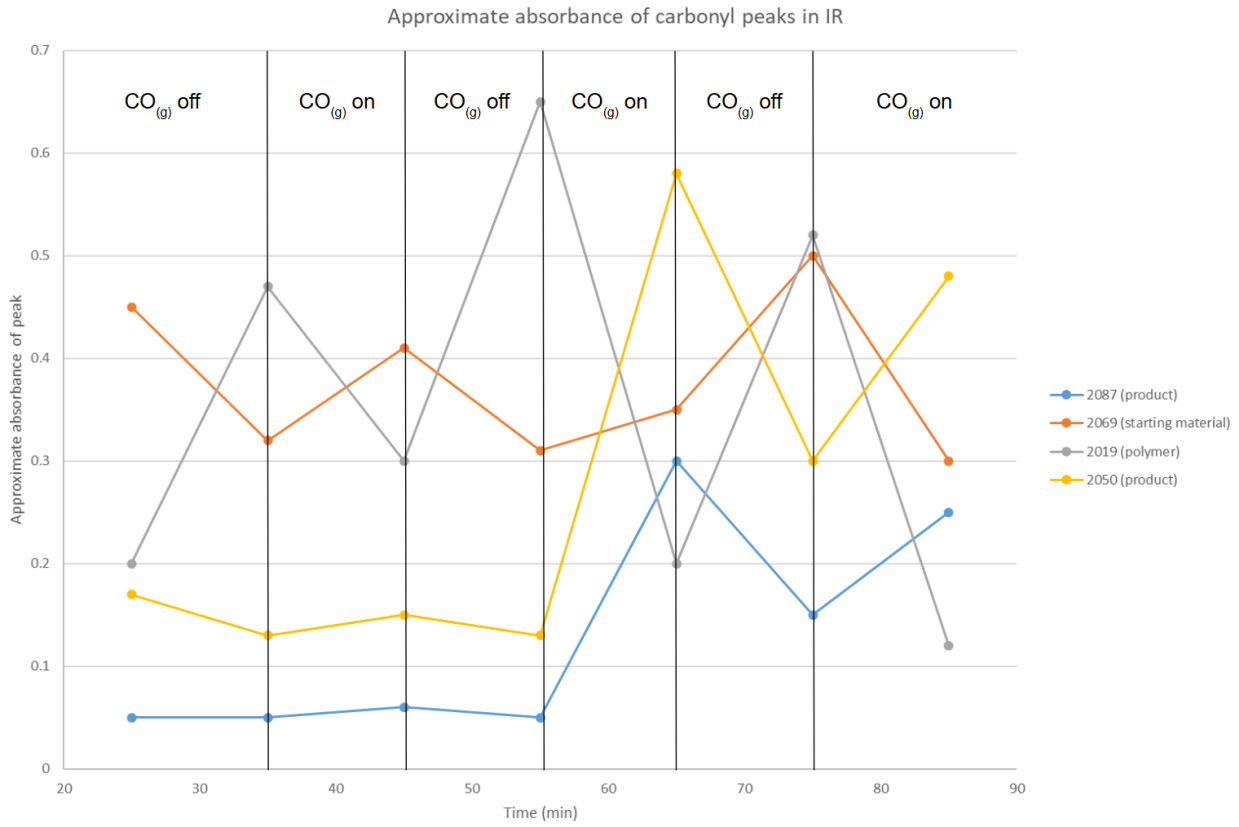

Graph 2: absorbance of IR peaks of crude reaction mixture as $CO_{(g)}$ is added at RT and removed at 110°C (blue = 2087 product peak; yellow = 2055 product peak; orange = 2069 bisethoxide peak; grey = 2019 polymer peak)

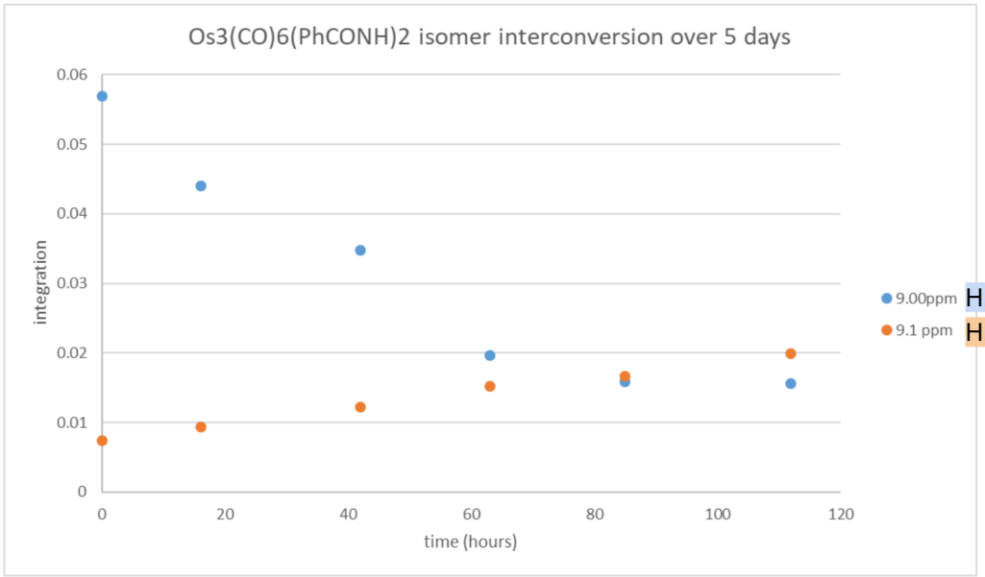

Graph 3: interconversion of $Os_2(CO)_6(PhCONH)_2$ from H,H to H,T (bw040) with an initial ratio of 88.5:11.5 (110°C) and final isomer ratio of 43.7:56.3 (RT).

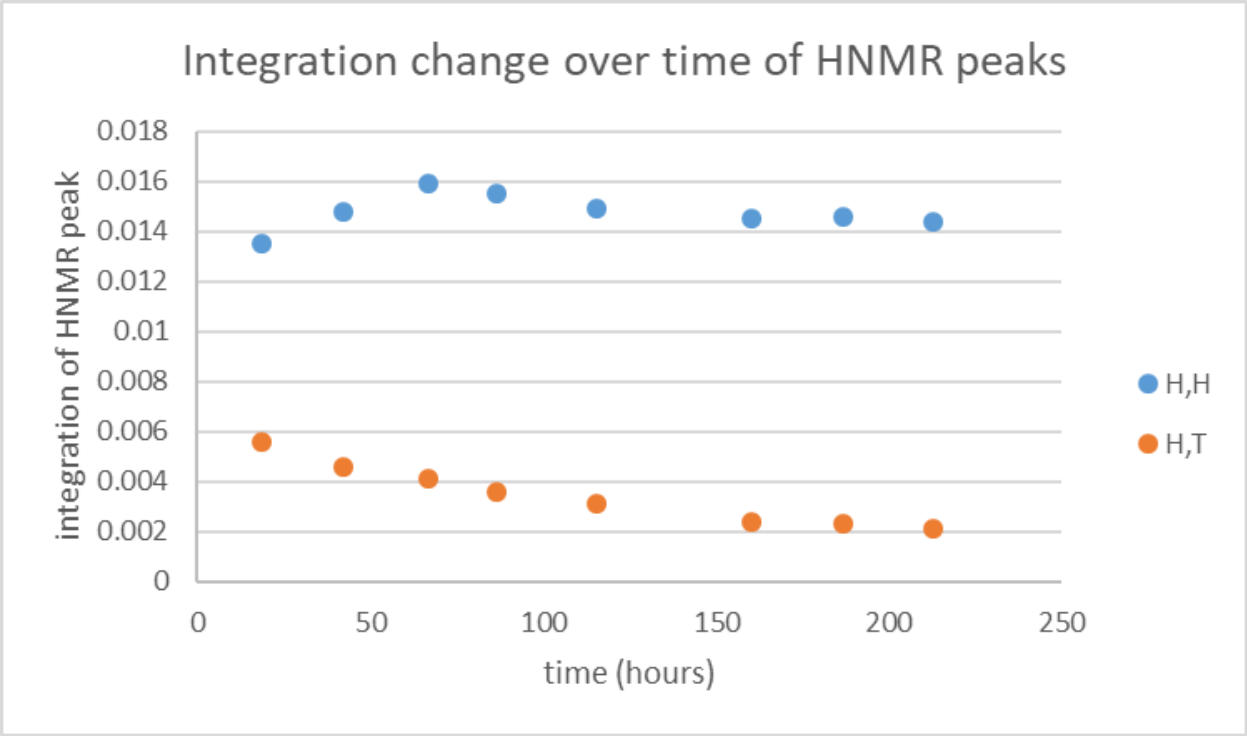

Graph 4: NMR integration over time of H,H and H,T signals in $Os_2(CO)_6(Ph\text{-}NO_2CONH)_2$ (bw034).

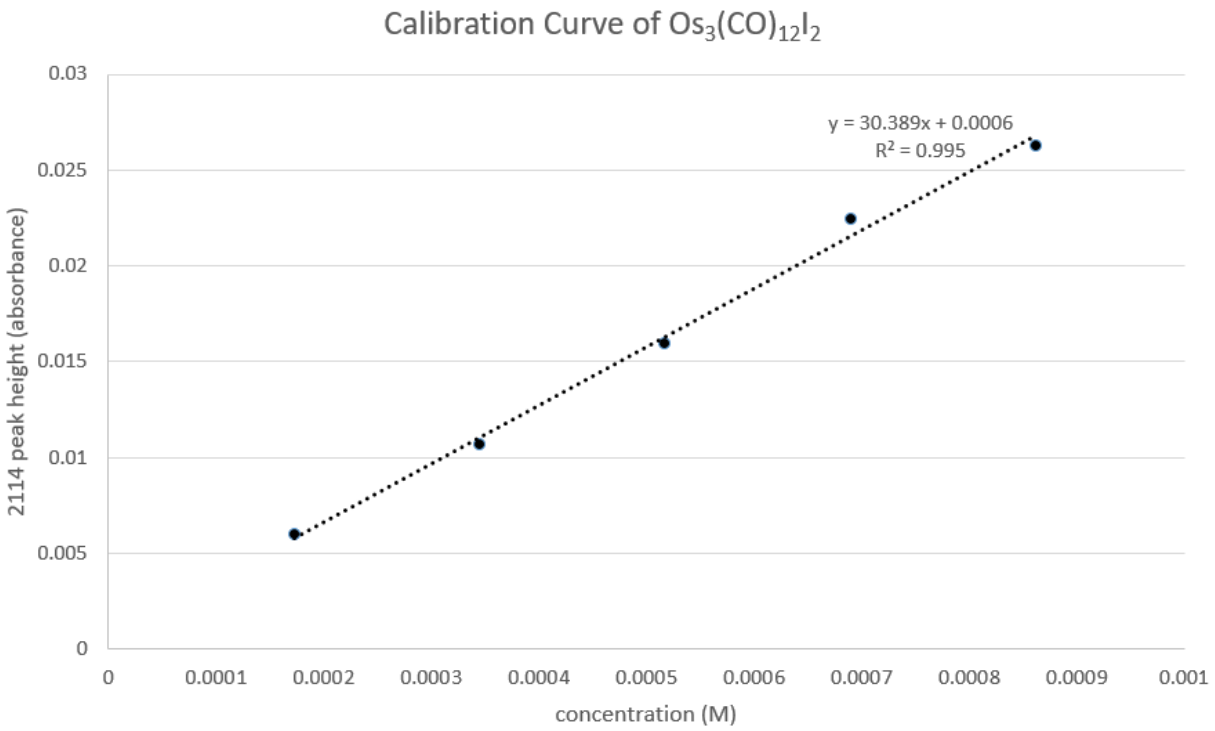

Graph 5: calibration curve of $Os_3(CO)_{12}I_2$ with linear trendline equation of $y=30.389+0.0006$ and a correlation coefficient $R^2 = 0.995$